Oxidative DNA damage by 1-hydroxyphenazine, virulence factor of *Pseudomonas aeruginosa*: Towards a Molecular understanding of the bacterial virulence factor 1-hydroxyphenazine

A Dissertation

Presented to

The Faculty of the Graduate School

University of Missouri-Columbia

In Partial Fulfillment

Of the Requirements for the Degree

Doctor of Philosophy

By

Sarmistha Sinha

Dissertation Supervisor: Dr. Kent S. Gates

May 2008

The undersigned, appointed by the dean of the Graduate School, have examined the dissertation entitled

Oxidative DNA damage by 1-hydroxyphenazine, virulence factor of *Pseudomonas aeruginosa*: Towards a Molecular understanding of the bacterial virulence factor 1-hydroxyphenazine

presented by Sarmistha Sinha,

a candidate for the degree of [doctor of philosophy],

and hereby certify that, in their opinion, it is worthy of acceptance.

Dr. Kent S. Gates

Dr. Susan Z. Lever

Dr. Timothy E. Glass

Dr. John J. Tanner

Dr. Jay J. Thelen

ACKNOWLEDGEMENTS

During my graduate career in University of Missouri-Columbia, I have had the opportunity to meet with many people, who has influenced, guided and helped me. So, I take this opportunity to thank them. At first, I would like to thank to my advisor Dr. Kent S. Gates for his excellent guidance and encouragement. Apart from teaching me how to design and perform an experiment, he also taught me how to think about science. I thank him for helping me to grow as a scientist.

I would also like to thank to my committee members Dr. Timothy Glass, Dr. Susan Lever, Dr. John Tanner and Dr. Jay Thelen for their help. My thanks also go to the past and present Gates Group's members, for their help and for making the lab a comfortable place to work.

I would like to thank to my parents Mr. Jnan Bikash Sinha and Mrs. Mira Sinha for their extreme support, inspiration and encouragement to achieve my goals. I also thank to my sister Sharmila Sinha and my in-laws Mr. Dilip Deb and Mrs. Lakshmi Deb for their support.

Finally I would like to thank to my beloved husband Dr. Kaushik Deb, the most important person in my life for his extreme moral support and inspiration to complete my PhD.

TABLE OF CONTENTS

CHAPTER 3: DNA Strand Cleavage by the 1,2,4-benzotriazine 1,4-Dioxide Family of Antitumor Agents: Mechanistic Insight from the use of a classical hydroxyl radical scavenging agent

LIST OF TABLES

CHAPTER 3:

LIST OF FIGURES

CHAPTER 1:

CHAPTER 2:

CHAPTER 3:

CHAPTER 4:

CHAPTER 5:

LIST OF SCHEMES

CHAPTER 1:

CHAPTER 2:

CHAPTER 3:

CHAPTER 4:

CHAPTER 5:

ABSTRACT

1-Hydroxyphenazine is a secondary metabolite and virulence factor of *Pseudomonas aeruginosa*. This organism colonizes the airways of the patients of cystic fibrosis and causes progressive destruction of the airways. It is suggested that 1-hydroxyphenazine plays an important role in such tissue damage but mechanisms underlying the biological properties of 1-hydroxyphenazine are not well studied. We report chemical properties of 1-hydroxyphenazine which might help to explain its biological activities.

The work presented here provides first evidence that 1-hydroxyphenazine in presence of one electron reducing enzyme NADPH:cytochrome P450 reductase undergoes redox cycling by reaction with molecular oxygen and produces reactive oxygen species (ROS) for example, superoxide radical, hydrogen peroxide and hydroxyl radical and generation of ROS cause oxidative stress inside the cell. In addition to this, we show that 1-hydroxyphenazine oxidizes into cytotoxic *N*-oxides by reaction with hydrogen peroxide, oxygen and peroxynitrite and these *N*-oxides of 1-hydroxyphenazine also generate ROS in presence of NADPH:cytochrome P450 reductase via redox-cycling mechanism. Generation of ROS by both 1-hydroxyphenazine and its *N*-oxides might be the one of the causes of cytotoxicity of lung airways of cystic fibrosis patients. We used plasmid based DNA damage assay as a tool to elucidate the chemistry of oxidative stress caused by both 1-hydroxyphenazines and *N*-oxides of 1-hydroxyphenazine.

Tirapazamine is a hypoxia-selective promising antitumor agent which is currently undergoing phase III clinical trials. TPZ achieves its medicinal activity through its ability to damage DNA selectively in the oxygen poor or hypoxic cells inside the solid tumors.

TPZ undergoes one electron reductive activation in presence of one-electron reducing system to yield a radical intermediate. Under hypoxic conditions, this radical intermediate leads to oxidative DNA damage. The identity of the reactive intermediate of TPZ which is responsible for oxidative DNA damage under hypoxic condition remains a subject of ongoing research. We provide direct evidence that TPZ leads to oxidative DNA damage through hydroxyl radical mediated pathway. Interestingly, we found that 1-hydroxyphenazine 5,10-di-*N*-oxide induces redox-activated, hypoxia-selective oxidative DNA damage and its DNA damage efficiency is similar to TPZ.

Chapter 1: Production of reactive oxygen species by redox cycling of 1-hydroxyphenazine: Towards a Molecular understanding of the bacterial virulence factor 1-hydoxyphenazine

1.1. Introduction:

Phenazines are natural products which are originated from bacteria and are isolated as secondary metabolites from *Pseudomon*as, *Streptomyces,* and a few other genera of soil and marine habitants.[1,2] There are more than fifty phenazine pigments found in nature (**Figure 1**).[1,2]

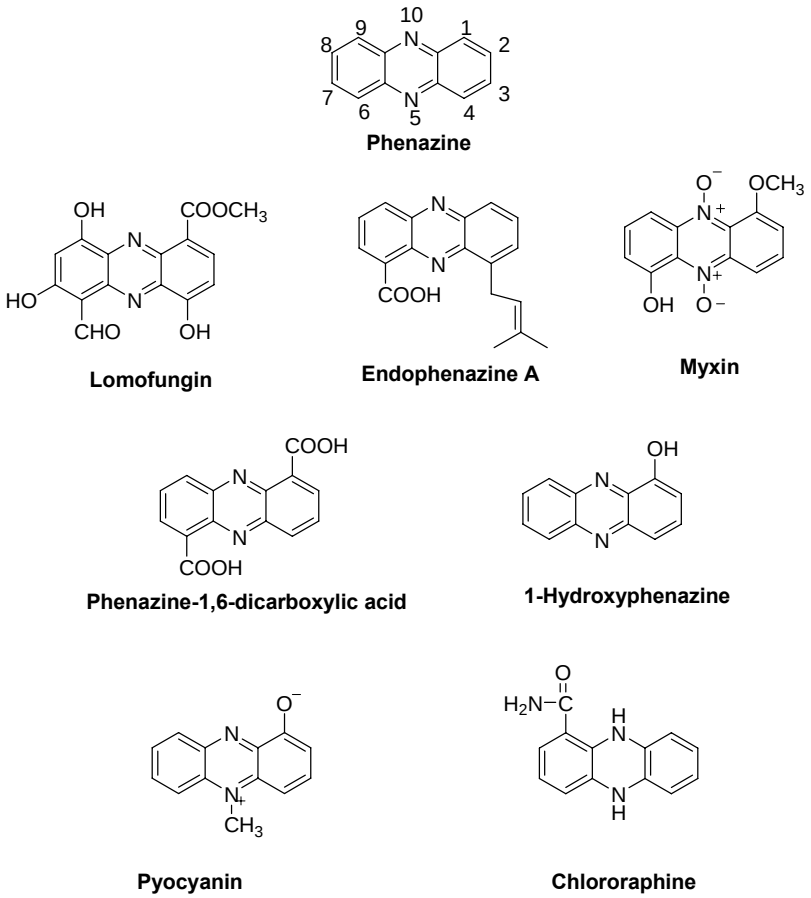

Figure 1: Phenazine pigments contain phenazine hetero cyclic ring system.[1,2,47]

Phenazines are colored compounds, for instance pyocyanin is blue, chlororaphine is green, iodinin is purple, and 2-hydroxyphenazine-1 carboxylic acid is orange.[1] The color of phenazines is due to the presence of a major peak in the visible region (400-600 nm).[1] Most phenazines are water soluble.[1] Phenazines possess antibiotic activity against a wide range of organisms including gram-positive and gram-negative bacteria, fungi, yeast and algae.[1,2] They also exhibit antitumor, antimalarial and antiparasitic properties.[1,3] Phenazines are known to be cytotoxic. The IC_{50} value of phenazines is with in the range 0.13-16 μM.[2] One of the reasons of phenazine-mediated cytotoxicity is their aptitude to interact with nucleic acids.[2,4-6] For example, it has been demonstrated that phenazines intercalate with double stranded DNA with a binding constant in the 10^4 to 10^6 M^{-1} range.[5] Moreover it has been found that phenazines inhibit DNA controlled RNA synthesis.[4] Phenazines like pyocyanin readily accept electrons. This property is responsible for the disruption of electron transport and respiratory flow in cell.[7] Moreover early studies suggest that some phenazines, for example 2-hydroxyphenazine, act as artificial electron carriers.[8,9] Some phenazines have been shown to behave as virulence factors of their producing organism.[1]

1.2. Biosynthesis of phenazine pigments:

The biosynthetic pathways leading to phenazines have been studied mostly in *P.aeruginosa* strain.[2] Based on early studies it is demonstrated that phenazine precursors are derived from shikimic acid pathway [1,2] and shikimic acid is converted to chorismic acid by known biotransformation pathway (**Scheme 1**).[1,2]

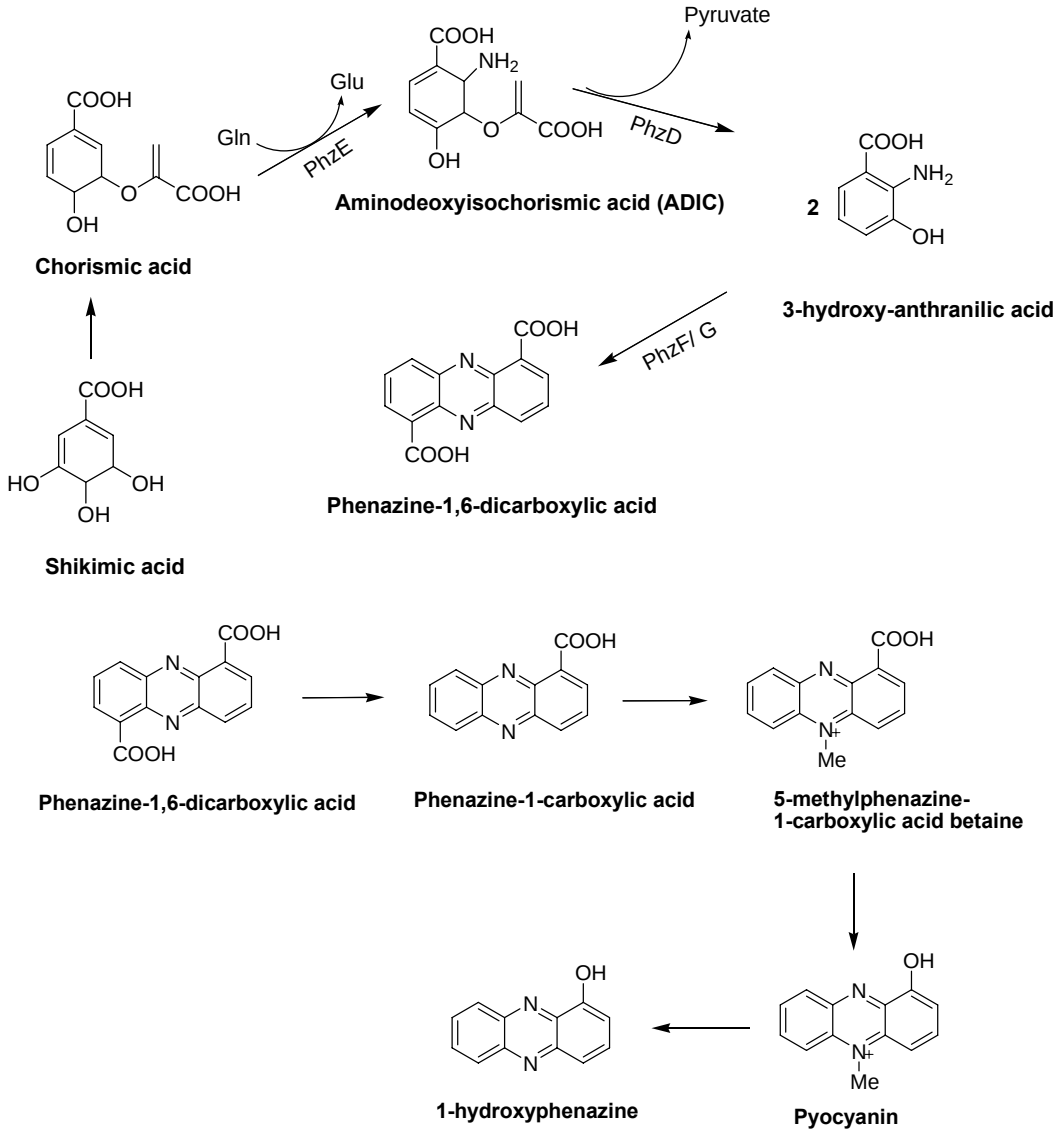

Scheme 1: A common pathway of phenazine biosynthesis in bacteria.[1,2]

Recently it has been studied that seven genes (*phz*ABCDEFG) are involved in production of phenazine-1-carboxylic acid in *P. fluorescens* strain 2-79.[1] Products obtained from genes phzc, phzD and phzE are similar to enzymes which are involved in shikimic acid and chorismic acid metabolism.[1] At first chorismic acid reacts with

glutamine to produce 2-amino-2-deoxyisochorismate (ADIC) in presence of phzE.[1,2] Then ADIC is converted into *trans* 2,3-dihydro-3-hydroxyanthranilic acid (DHHA) by phzD.[1,2] The two DHHA molecules are oxidized to produce corresponding ketone which undergoes self-condensation to produce phenazine-1,6-dicarboxylic acid.[1,2] PhzF is required for the formation of phenazine-1,6-dicarboxylic acid.[1] Phenazine 1-carboxylic acid is produced from phenazine-1,6-dicarboxylic acid after decarboxylation.[1,2] The other phenazines like pyocyanin and 1-hydroxyphenazine are obtained from either phenazine-1,6-dicarboxylic acid or phenazine 1-carboxylic acid by common biotransformation pathways.[1,2]

1.3. Phenazine pigments in *Psedomonas aeruginosa*-Biological activity:

Psedomonas aeruginosa is a gram-negative, aerobic bacteria.[10] This organism can also grow without oxygen if NO_3/NO_2^- or arginine is available in the system.[10-12] *P.aeruginosa* can be isolated from soil, marshes, coastal marine habitants, plants and mammalian tissue.[10]

1.3.1. *Pseudomonas aeruginosa* and its role in respiratory infections:

Early studies suggest that *P.aeruginosa* is an opportunistic pathogen that causes a wide range of respiratory infections.[13,14] One extreme example is *P.aeruginosa* associated acute pneumonia which occurs due to the colonization of *P.aeruginosa* in the respiratory tract of the patients having damaged airways from mechanical ventilation, burn patients, or patients suffering from malignancis or HIV infection.[14] Another serious example is the chronic respiratory infection by *P.aeruginosa* in the respiratory tract of cystic fibrosis

patients.[13,14] Cystic fibrosis (CF) is a genetic disease which is caused by the mutation of a gene called cystic fibrosis transmembrane conductance regulator (CFTR) gene.[15] This gene makes a protein which regulates the transportation of salt and water into the cells in our body.[15] In CF patients, the gene doesn't work properly resulting in enhanced absorption of Na^+, Cl^- and water that, in turn, leads to production and accumulation of thick, sticky mucus at the apical surface[13,15,16]which causes disruption of the functions of several organs of human body.[17] The atmosphere which is created in the lung of CF patients due to accumulation of thick mucus is susceptible to *P.aeruginosa* and as a result this organism colonizes lung airways of CF patients by biofilm formation[13] and modulates functions of host immune system and causes progressive lung tissue damage which leads to chronic respiratory infection in CF patients.[13]

1.3.2. Role of phenazines: bacterial virulence factors produced and secreted by *P.aeruginosa*:

The definition of virulence is the ability of a microbe to cause deleterious effects and diseases in host cell.[18,19] Virulence factors are proteins or small molecules which are produced by the bacteria during pathogenesis in the host cell.[18,19] Virulence factors help bacteria to thrive in the host cell by modulating the cellular functions of host which causes adverse effects in host cells.[18,19] *P.aeruginosa* produces and secrets numerous virulence factors which alter the functions of lung epithelial cell and also causes progressive lung tissue destruction.[13,14]

Phenazines are one of the important virulence factors produced and secreted by *P.aeruginosa.*[1,2,13,14] Phenazines exhibit wide range of antibiotic activity[1,2] and

consequently inhibit the growth of other organisms in the host cell. This helps the phenazine producing organism to get sufficient nutrition from host cell due to less competition and as a result phenazine producing bacteria survive longer in the host organism.[1,2] Therefore, bacteria that produce phenazines as a secondary metabolites persist longer in the host organism by suppressing other microorganisms.[1,2] Most strains of *P.aeruginosa* produce phenazines like pyocyanin, 1-hydroxyphenazine and phenazine 1-carboxylic acid as secondary metabolites.[1,2,13,14]

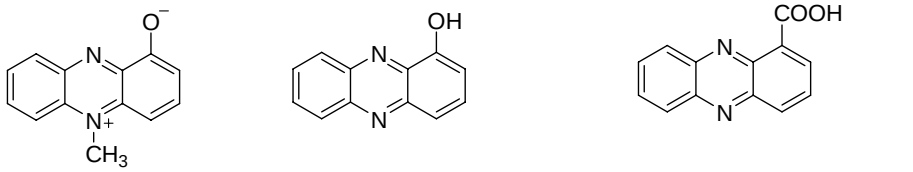

pyocyanin **1-hydroxyphenazine** **phenazine-1-carboxylic acid**

Figure 2: Phenazines produced in *P.aeruginosa*.[1,2]

P.aeruginosa produces and secrets phenazines in the lung airways of cystic fibrosis patients.[1,2,13,14] The phenazine molecules not only assist bacteria to persist longer in CF lung by suppressing growth of other organisms, these molecules also cause deleterious effects in the host organism.[1,2,13,14] In this section, we discuss the virulence, or in other words detrimental effects, of phenazines produced and secreted by *P.aeruginosa* in lung airways of cystic fibrosis patients.

Pyocyanin: A large amount of pyocyanin is recovered from the sputum of *P.aeruginosa* infected cystic fibrosis patients.[16] Pyocyanin is the most extensively studied phenazine which causes different types of virulence in host cell. For example, pyocyanin enhances oxidative metabolism of neutrophils,[20] alters lymphocyte function,[21-23] reduces

ciliary beat frequency.[24,25] Moreover pyocyanin is found to cause lung tissue damage in *P.aeruginosa* infected CF patients.[1,26,16] Early studies suggest that pyocyanin also modulates glutathione or GSH redox cycling in lung epithelial and endothelial cells.[16] Additionally, it is known that pyocyanin undergoes redox cycling by accepting electrons nonenzymatically either from NADH or NADPH and produces reactive oxygen species (ROS) like superoxide radical and H_2O_2 (**Scheme 2**).[27,28,29,31-36,16,37]

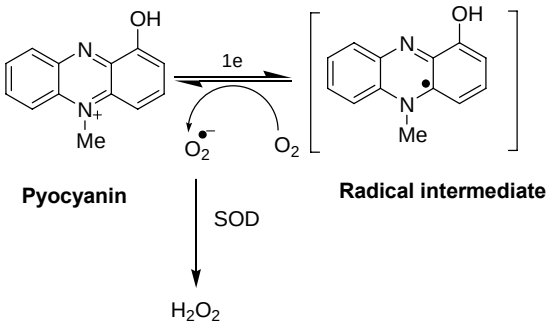

Scheme 2: Proposed mechanism of production of ROS by pyocyanin.

Generation of ROS causes oxidative stress inside the host cell. Oxidative stress is a condition where the concentration of ROS is increased compare to normal and consequently antioxidant labels are decreased with respect to normal. Oxidative stress is created due to generation of reactive oxygen species (ROS) like H_2O_2, superoxide radicals and hydroxyl radicals from endogenous or exogenous source. ROS cause DNA damage and disturb physiologically important functions of proteins, lipids, enzymes and also interfere in cellular function. Overall the effects of oxidative stress lead to cytotoxicity in cell[38-40] which in turn leads to development of variety of diseases and accelerated aging.[38-41]

In addition to causing harmful effects in host cell pyocyanin has also been suggested to exhibit antifungal and antibiotic activity.[28,29] Generation of toxic ROS has been proposed as the basis of these compound's antibiotic activity and also one of the causes of tissue destruction in CF lung.[36,16]

Phenazine 1-carboxylic acid (PCA): PCA increases IL-8 release and ICAM-1 expression, decreases RANTES. It also increases extra cellular oxidants.[42]

Virulence factor 1-hydroxyphenazine: Pyocyanin slowly decomposes to yield the metabolite 1-hydroxyphenazine[1,2] which also have been found to cause deleterious effects in CF patients. Early studies suggest that 1-hydroxyphenazine down regulates the ciliary beat frequency of respiratory epithelial cells[24] and reduces tracheal mucus velocity.[25] 1-Hydroxyphenazine also increases the rate of release of lysozymes by activated neutrophils.[20] It is also suggested that 1-hydroxyphenazine plays an important role in lung tissue damage of *PA* infected CF patients.[2,43]

The mechanism of virulence of 1-hydroxyphenazine is not well studied. It is therefore imperative to investigate the chemical properties of 1-hydroxyphenazine. This might help to explain its biological activities.

1.4. Biologically-relevant chemical properties studied on phenazines:

Early studies suggest that pyocyanin is a redox pigment which undergoes redox cycling inside the cell and generates ROS which cause oxidative stress inside the cell.[28,29,27,30-36,16] Moreover Katsuyuki *et al.,*[44,45] reported that reductive activation of

phenazine-di-*N*-oxide upon treatment with DTT/NADPH (by accepting one electron) produced a stable radical intermediate (**Scheme 3)** which under aerobic and anaerobic conditions generates superoxide and hydroxyl radicals respectively. Both superoxide and hydroxyl radicals lead to DNA cleavage which may be one of the causes of cytotoxicity in cell.[44,45]

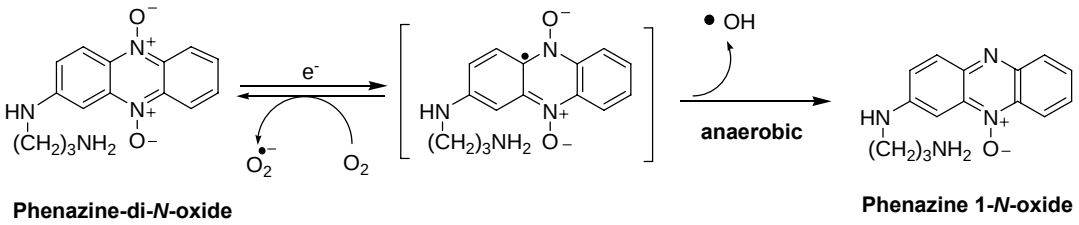

Scheme 3: Proposed mechanism for the reductive activation of phenazine-di-*N*-oxide as described by Katsuyuki *et al*.[44,45]

1.5. Hypothesis:

Based on early studies we noticed that both pyocyanin and phenazine-di-*N*-oxides are electron deficient species due to containing positive charged nitrogen atom. So, as a result they can easily get reduced by one electron reducing system and can undergo redox cycling in presence of oxygen.[44,45,16,37] Although 1-hydroxyphenazine (OHP) is structurally similar to pyocyanin (**Figure 2**) its redox behavior might be different from pyocyanin to some extent as 1-hydroxyphenazine does not contain any electron deficient species (**Figure 2**). The one electron reduction potential of pyocyanin in neutral acetonitrile solution is -0.78 V whereas for OHP it is -1.67 V which suggests that pyocyanin is a better redox pigment compare to OHP.[31] Early studies suggest that OHP

may act as an electron acceptor as OHP blocks mitochondrial electron transport in mouse liver.[43] Moreover other studies have shown that 1-hydroxyphenazine is reduced by NADPH at physiological pH.[43] So, on the basis of previous literatures we thought that OHP might undergo one electron reduction in cell by reducing system like NADPH or NADPH:cytochrome P450 reductase enzyme and then the reduced intermediate of OHP undergoes redox cycling in presence of molecular oxygen to generate ROS like super oxide radicals, H_2O_2, hydroxyl radicals (shown in **Scheme 4)**. Generation of ROS cause oxidative stress inside the *P.aeruginosa* infected lung cell which can lead to lung tissue damage in CF patients.

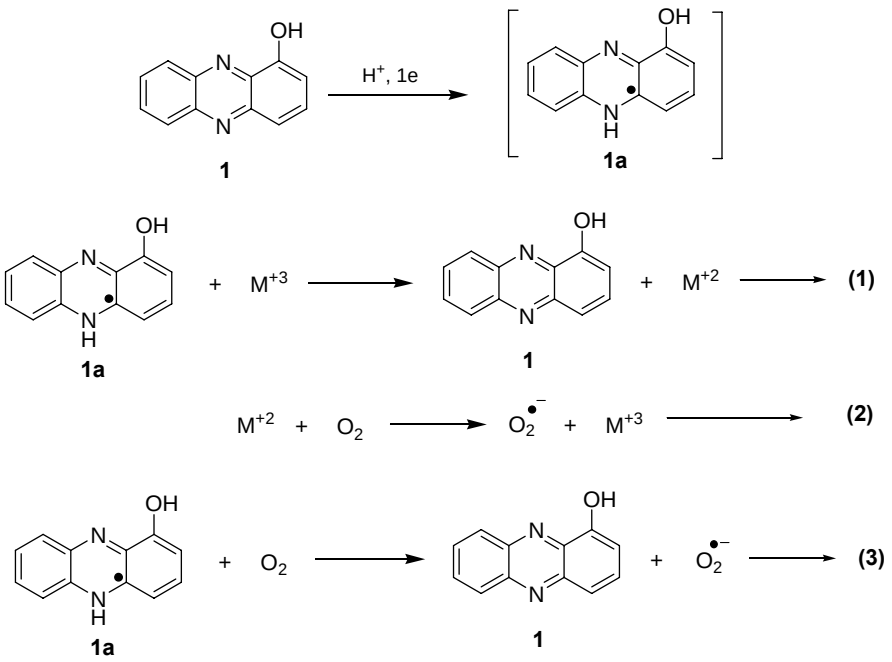

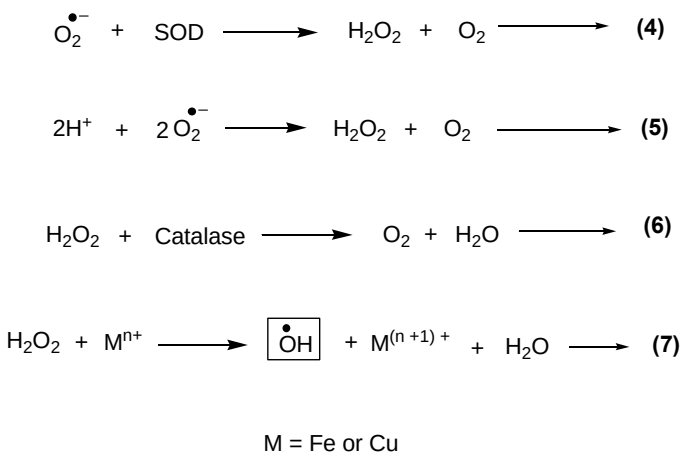

Scheme 4: Proposed mechanism for generation of ROS by 1-hydroxyphenazine (**1**).

1.6. Goal: Accordingly, our goal was to investigate whether OHP is capable to create oxidative stress inside the cell due to redox cycling. So, we used plasmid based DNA damage assay as a tool to elucidate the chemistry of oxidative stress caused by OHP *in vitro*. Our *in vitro* study was followed by cell culture experiments that demonstrated the generation of oxidative stress by OHP inside a human lung cell line.

1.7. Enzyme system used for reductive activation of OHP: OHP requires one electron reductive activation under aerobic condition to undergo redox cycling. In this work the enzyme systems used for the activation of OHP were xanthine/xanthine oxidase and NADPH:cyochrome P450 reductase systems.

1.7.1. The xanthine/xanthine oxidase system (X/XO): The X/XO system is one of the one electron reducing enzyme systems which are used in the bioassays with 1-hydroxyphenazines and heterocyclic *N*-oxides. Xanthine oxidase (XO) catalyzes the oxidation of hypoxanthine to xanthine and xanthine to uric acid.[46,47] Xanthine oxidase is

found in various types of species including mamals.[47,48] Xanthine oxidase consists of iron-sulfur center, flavin adenine dinucleotide (FAD) and molybdenum (MO) centers.[47,49] Xanthine oxidase catalyzes oxidation of hypoxanthine to xanthine and xanthine to uric acid by subsequent reduction of metal molybdenum from +VI to +IV oxidation state.[47,50] Then the electrons are transferred from molybdenum to FAD via the iron-sulfur centers with formation of $FADH_2$ and then $FADH_2$ deposits electrons to molecular oxygen with the formation of superoxide radicals and hydrogen peroxide (**Figure 3**).[47,48] The yield of hydrogen peroxide and superoxide radical per molecule of FAD depends on the reducing state of molybdenum or the enzyme.[47,51] Organic and inorganic nitrates and nitrites have been known to act as terminal electron acceptors and produce nitric oxide by accepting electrons.[47,52,53]

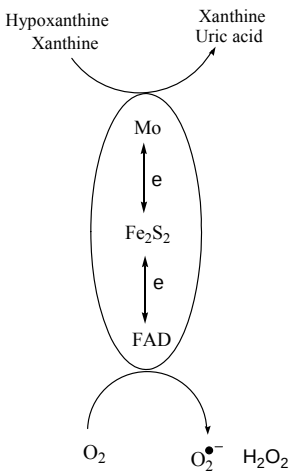

Figure 3: Schematic diagram of oxidation of hypoxanthine, xanthine and reduction of oxygen by xanthine oxidase.[47,48]

In our study, we used X/XO as a reducing system for the one-electron reductive activation of OHP and its heterocyclic-*N*-oxides. Xanthine oxidase catalyzes the transfer of electrons from xanthine to organic molecules through the oxidation of xanthine (**Figure 4**). Each molecule of xanthine is converted into uric acid by transferring two

electrons to XO and then XO transfers either one or two electron at a time to OHP or heterocyclic-*N*-oxides.[46,47]

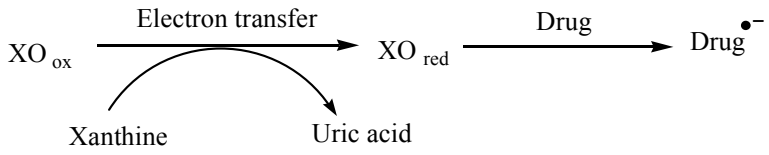

Figure 4: Reductive activation of organic molecule or drug catalyzed by X/XO.[47]

1.7.2. NADPH:cytochrome P450 reductase system:

NADPH:cytochrome P450 reductase is found in wide range of mammals including human.[54,55] It is an obligate one-electron reducing system in cell which catalyzes the transfer of electrons from NADPH to cytochrome P450.[55,56] Cytochrome P450 is one of the most important families of proteins that involved in the metabolism of foreign chemicals in the living organism.[55] NADPH:cytchrome P450 reductase belongs to flavoprotein family which consists of two cofactors FAD and FMN.[57] FAD accepts two electrons from NADPH and FMN carries out those electrons one at a time from FAD to the acceptor cytochrome P450 or organic molecules with appropriate redox potential.[58] It has been shown that under physiological condition the enzyme cycles between one and three electron reduced forms (**Figure 5**).[58]

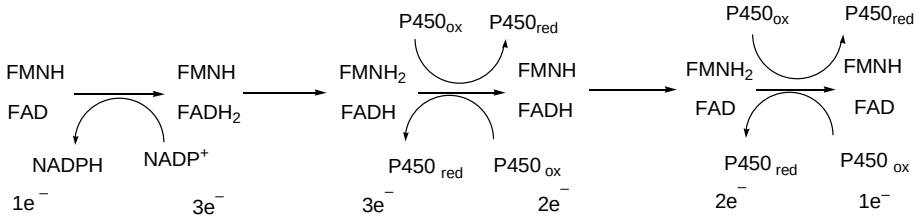

Figure 5: Schematic diagram of the redox cycle of NADPH:cytochrome P450 reductase system.[47]

It has been studied that hypoxia selective bioreductive drugs like tirapazamine, 3-amino-2-quinoxaline 1,2,4-benzotriazine 1,4-dioxide, mytomycin C etc and phenazine-di-*N*-oxides for example, myxin, methylmyxin etc exhibit their biological activity by accepting one or two (in case of mytomycin C) electrons from NADPH:cytochrome P450 reductase and X/XO. [47,59,60,61]

1.8. Synthesis of OHP: The synthesis of 1-hydroxyphenazine was carried out by modifying previously published precedure.[62] First, *N*-oxides of 1-hydroxyphenazine were obtained by a cycloaddition reaction between benzofuranoxide and 1,2-cyclohexanedione. Then, 1-hydroxyphenazine was produced by reduction of *N*-oxides by sodium dithionite. According to the method used by Haddadin *et al.* benzofuranoxide (**2**) was treated with 1,2 cyclohexanedione (**3**) in triethylamine under N_2 atmosphere for 7-8 h.[62] A deep brown colored reaction mixture was obtained which, upon acidification, produced a mixture of *N*-oxides (**5**, **6** & **7,**). Crude *N*-oxides of 1-hydroxyphenazine (**5**, **6** and **7**,) were then reduced by sodium dithionite to produce 1-hydroxyphenazine (**1**) (**Scheme 5**).[62]

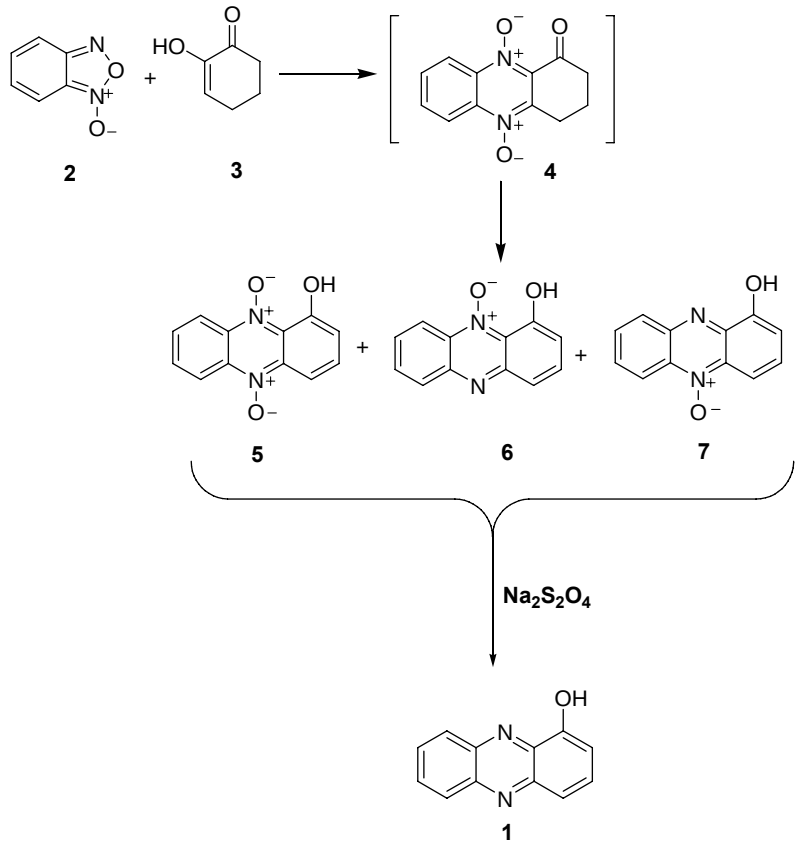

Scheme 5: Synthesis of 1-hydroxyphenazine.[62]

1.9. Aerobic DNA cleavage by 1-hydroxyphenazine in the presence of enzymatic reducing system: Based on literature it has been suggested that 1-hydroxyphenazine causes progressive lung tissue destruction in cystic fibrosis patients[2,43] in addition to other virulence like down regulating the ciliary beat frequency of respiratory epithelial cells,[24] increasing the rate of release of lysozymes by activated neutrophils etc.[20] According to our hypothesis 1-hydroxyphenazine or OHP might lead to the generation of superoxide radical by reaction with NADPH or NADPH:cytochrome P450 reductase (**Scheme 4**, equations **1,2 and 3**). Superoxide radical decomposes into hydrogen peroxide and finally hydroxyl radical under physiological condition as shown in **Scheme 4,** equations **4, 5, 6**

and 7 where metal could be iron or copper.[63] Generation of ROS like superoxide radical, hydrogen peroxide, hydroxyl radical in cell cause various types of deleterious effects for example, oxidative DNA damage, destruction of protein, lipids and also cause cytotoxicity.[36,63-65,66-68,69,70] We used a plasmid based DNA damaging assay as a readout of generation of ROS like superoxide radical by 1-hydroxyphenazine under aerobic condition in presence of NADPH:cytochrome P450 reductase.[47,59,60,71,72,73] Superoxide radicals cause the generation of hydroxyl radical via a cascade of reactions which are shown in **Scheme 4** and this hydroxyl radical leads to oxidative DNA damage.[63,74-77]

In a typical plasmid based DNA damage assay, the ability of a compound to initiate single strand break of supercoiled plasmid DNA is evidenced by the nicked and the liner form of the plasmid, which show different migration rates in an agarose gel.

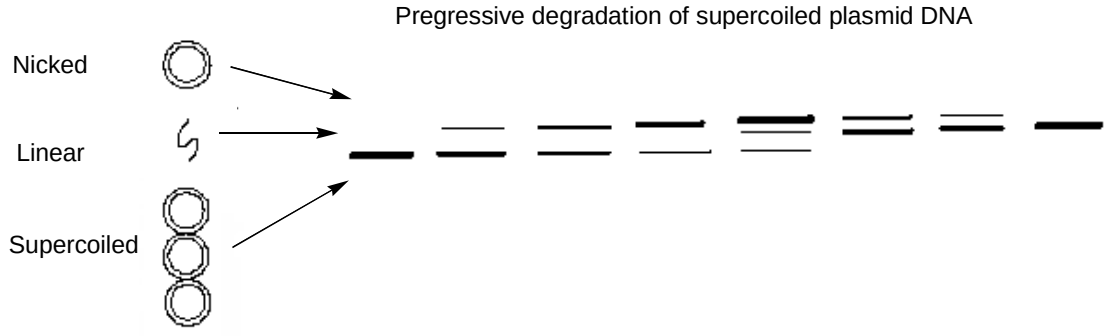

Figure 6 : Schematic diagram of degradation of supercoiled plasmid DNA to its nicked circular and linear form which is shown in agarose gel.[78]

We determined DNA cleavage efficiency of 1-hydroxyphenazine by measuring the number of strand breaks per plasmid molecule (S value) at various concentration of OHP. One electron reductive activation was achieved by using NADPH:cytochrome

P450 reductase system. SOD, Catalase and desferal (**Scheme 6**) were used as mechanistic tools to examine species involved in DNA strand cleavage from Fenton chemistry. The reaction mixture was incubated for 12 hours by wrapped with aluminium foil to prevent exposure of light.

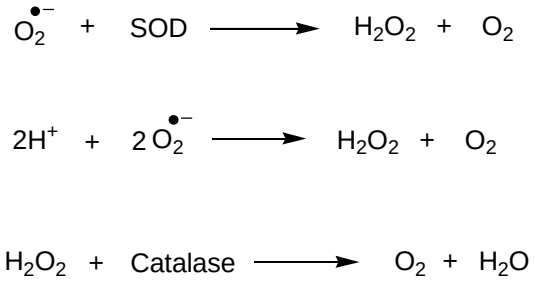

Scheme 6: Reaction of SOD and catalase with superoxide radical and hydrogen peroxide.[63,74]

A.

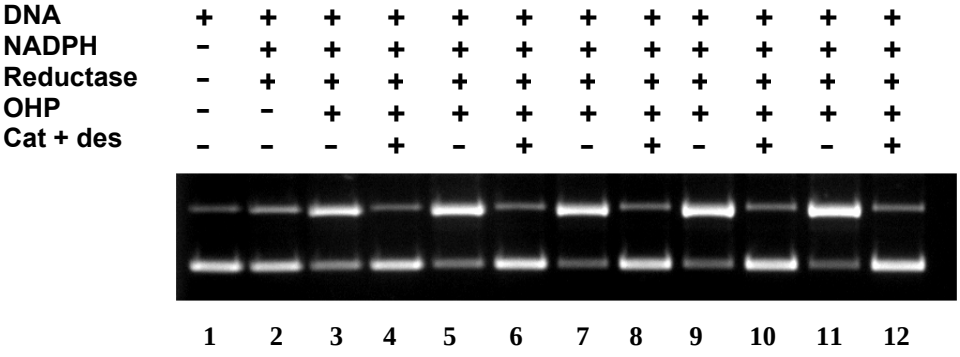

B.

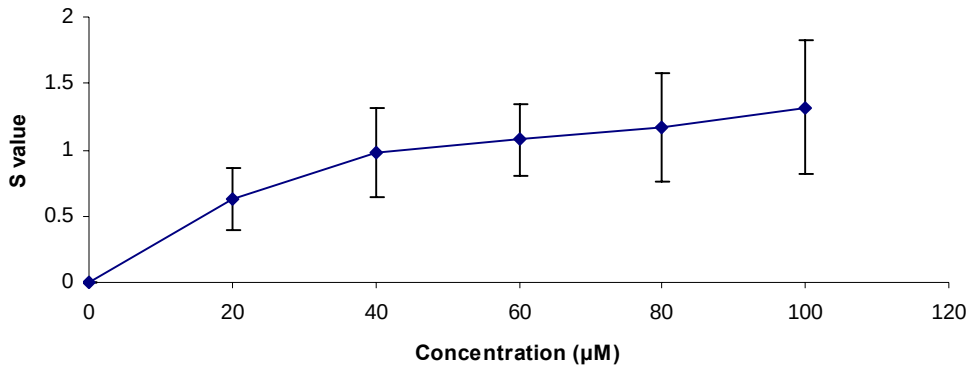

Figure 7: DNA cleavage efficiency of various concentrations of **1** in the presence of NADPH:cytochrome P450 reductase system. Supercoiled plasmid DNA (1 μg) was incubated with **1** (20-100 μM), NADPH (100 μM), cytochrome P450 reductase (0.05 U/mL), sodium phosphate buffer (50 mM, pH 7.0), and with catalase (100 μg/mL), desferal (1 mM) as control reactions in a total volume 40 μL under aerobic condition at room temperature (24^{o}C) for 12 hours, followed by agarose gel electrophoresis. **A)** Agarose gel: lane 1, DNA alone; lane 2, NADPH (100 μM) + reductase (0.05 U/mL); (lane 3, 5, 7, 9,11), **1** (20-100 μM)+ NADPH (100 μM) + reductase (0.05 U/mL); lane 3 (20 μM **1**, S = 0.63 ± 0.24); lane 5 (40 μM **1**, S = 0.98 ± 0.34); lane 7 (60 μM **1,** S = 1.07 ± 0.27); lane 9 (80 μM **1,** S = 1.16 ± 0.41); lane 11 (100 μM **1,** S = 1.32 ± 0.51); (lane 4, 6, 8, 10, 12), **1** (20-100 μM) + NADPH (100 μM) + reductase (0.05 U/mL) + catalase (100 μg/mL) + desferal (1mM). **B)** Plot of S value vs. various concentrations of OHP. The values, S, represent the mean number of strand breaks per plasmid molecule and were calculated using the equation S = -ln f_1 where f_1 is the fraction of plasmid present as in the supercoiled form I. S values of different concentration of **1** were obtained by calculating background cleavage subtraction. Standard deviation was determined from three repeats.

The DNA cleavage assay showed that compound **1,** in presence of one-electron reducing system (NADPH:cytochrome P450 reductase system), induced DNA cleavage. Controls show that NADPH:cytochrome P450 reductase system generates minimal amounts of superoxide radicals due to one electron reduction with molecular oxygen which leads to very low amounts of DNA cleavage. Addition of compound **1** to NADPH:cytochrome P450 reductase system caused increase in concentration dependent DNA cleavage. DNA cleavage by **1** was inhibited by addition of catalase and desferal as both catalase and desferal destroy ROS (**Scheme 4 & 6**).

1.10. DNA cleavage efficiency of 1-hydroxyphenazine in presence of chemically reducing system NADPH and reductive enzyme system NADPH:cytochrome P450 reductase system:

Our initial result (discussed above) clearly showed that 1-hydroxyphenazine cleaved DNA in presence of NADPH:cytochrome P450 reductase system. Now, we wanted to examine in addition to cytochrome P450 reductase whether any other biological reducing agent such as NADPH which is present in significant amount in cell[79] can facilitate this event. Along these lines, Hecht and coworkers studied that 3-substituted phenazine di-*N*-oxide cleaves DNA followed by one electron reductive activation by NADPH, DTT (**Scheme 3**).[44,45] Moreover it is known that pyocyanin undergoes redox cycling by accepting electrons nonenzymatically either from NADH or NADPH.[16,27,28,29,30-36,37] So, accordingly we investigated whether NADPH can activate OHP to induce DNA cleavage. DNA cleavage assays were performed in presence of OHP with or without presence of various concentrations of NADPH and NADPH:cytochrome P450 reductase system under aerobic condition.

A.

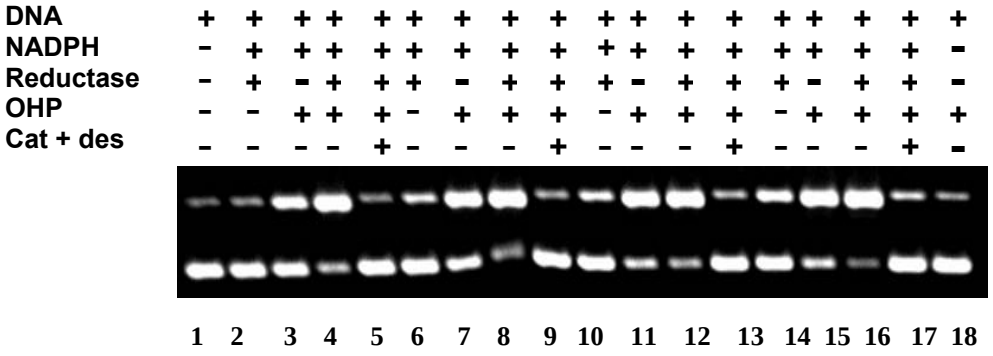

B.

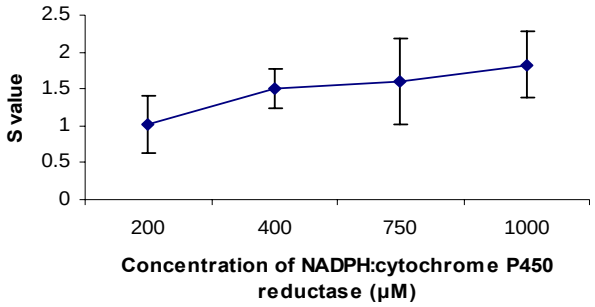

C.

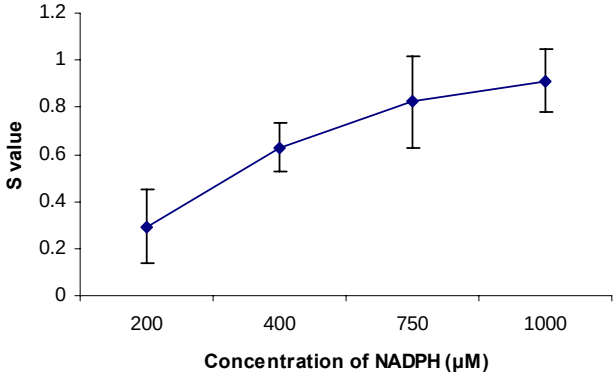

Figure 8: DNA-cleavage efficiency of **1** in the presence of various concentrations of NADPH (200 µM, 400 µM, 750 µM, 1 mM) or NADPH:cytochrome P450 reductase (0.05 U/mL) system. Supercoiled plasmid DNA (1 µg) was incubated with **1** (100 µM), NADPH (200 µM, 400 µM, 750 µM, 1 mM), cytochrome P450 reductase (0.05 U/mL), sodium phosphate buffer (50 mM, pH 7.0), and with catalase (100 µg/mL), desferal (1 mM) as control reactions in a total volume 40 µL under aerobic condition at room temperature (24^{o}C) for 12 hours, followed by agarose gel electrophoresis. **A)** Agarose gel: lane 1, DNA alone; lane 2, 6, 10 & 14, DNA + NADPH (200 µM, lane 2, 400 µM, lane 6, 750 µM, lane 10 & 1mM, lane 14) + reductase (0.05 U/mL); lane 3, 7, 11 & 15, DNA + **1** (100 µM) + NADPH (200 µM, 400 µM, 750 µM, 1mM); lane 3 (200 µM **NADPH**, S = 0.29 ± 0.16); lane 7 (400 µM **NADPH**, S = 0.63 ± 0.10); lane 11 (750 µM **NADPH,** S = 0.82 ± 0.19); lane 15 (1 mM **NADPH,** S = 0.91 ± 0.13); lane 4, 8, 12 & 16, DNA + NADPH (200 µM, 400 µM, 750 µM, & 1mM) + reductase (0.05 U/mL); lane 4 (200 µM **NADPH**, S = 1.02 ± 0.39); lane 8 (400 µM **NADPH**, S = 1.52 ± 0.27); lane 12 (750 µM **NADPH,** S = 1.61 ± 0.58); lane 16 (1 mM **NADPH,** S = 1.83 ± 0.44); lane 5, 9, 13 & 17, control (control: 1 mM desferal & 100 µg/mL catalase); lane 18, **1** alone. B) Plot of S-value vs. increasing concentration of NADPH. **C)** Plot of S-value vs. increasing concentration of NADPH:cytochrome P450 reductase system. The values, S, represent the mean number of strand breaks per plasmid molecule and were calculated using the equation S = -ln f_1 where f_1 is the fraction of plasmid present as in the supercoiled form I. S values of different concentration of **NADPH** were obtained by calculating background cleavage subtraction. Standard deviation was determined from three repeats.

We found that NADPH alone facilitates DNA damage event of OHP and DNA damage efficiency of OHP increases with increasing concentration of NADPH. Addition of enzyme cytochrome P450 reductase increases the yield of DNA damage. We also noticed that OHP alone couldn't cleave DNA. So, this result clearly demonstrated that OHP required one electron reductive activation either by chemical reducing system like NADPH or by reducing enzyme like NADPH:cytochrome P450 reductase system to induce DNA damage.

1.11. Is redox cycling is the cause of DNA damage by OHP under aerobic condition?

Based on our initial results (discussed above) we know that OHP caused aerobic DNA cleavage by one-electron reductive activation. Now, these preliminary results led us to study the mechanism of aerobic DNA cleavage by OHP. Previous studies showed that heterocyclic-*N*-oxides undergo redox cycling under aerobic condition in the presence of one electron reducing system and generate superoxide radicals which lead to oxidative DNA damage.[44,45] Moreover pyocyanin, the precursor of 1-hydroxyphenazine, is also a redox cyclic agent.[16,27,28,29,30-36] Thus based on these precedents, it might be suggested that OHP undergoes one electron reductive activation in presence of one electron reducing system and generates superoxide radical in presence of molecular oxygen as a result of redox cycling (**Scheme 4**). After that superoxide radical on treatment with superoxide dismutase (SOD) produce H_2O_2 which on treatment with metal generates well known DNA damaging agent hydroxyl radical via Fenton chemistry (**Scheme 4 & 6**). In cellular system both SOD and catalase remove superoxide radical and H_2O_2 respectively

as shown in **Scheme 6**[63,74] and removal of superoxide radical and H_2O_2 finally inhibit the generation of hydroxyl radical. The metal chelating agent desferal also prevents production of hydroxyl radical by inhibiting Fenton chemistry. Thus, SOD, catalase and desferal inhibit DNA damage by preventing formation of hydroxyl radical from Fenton chemistry.

To examine whether aerobic DNA cleavage by OHP is a result of redox cycling we performed plasmid based DNA cleavage assays in presence of NADPH:cytochrome P450 reductase system and also studied the effect of addition of SOD, catalase and desferal into the DNA damage reactions.

A.

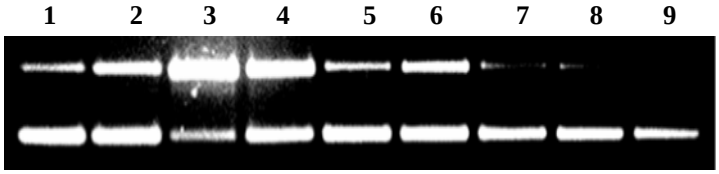

B.

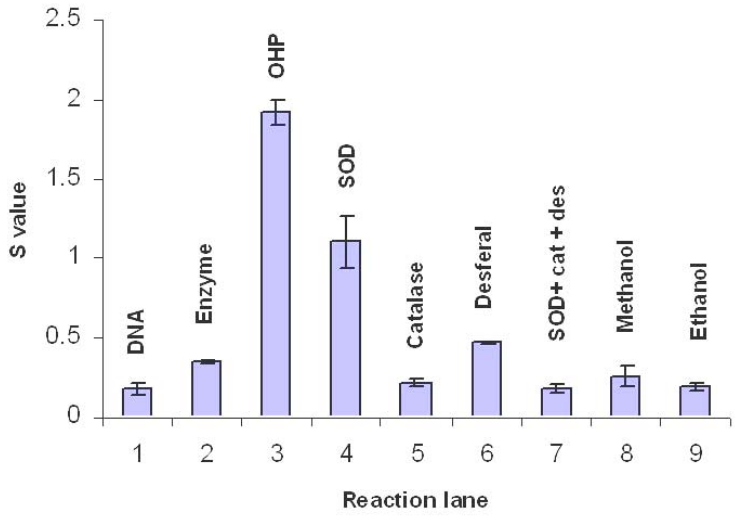

Figure 9: Cleavage of Supercoiled Plasmid DNA by 1-hydroxyphenazine (**1**) in the presence of enzyme system NADPH:cytochrome P450 reductase as an activating system. All reactions contained DNA (1 μg), **1** (100 μM), NADPH (200 μM), cytochrome P450 reductase (0.05 U/mL), sodium phosphate buffer (50 mM, pH 7.0), in a total volume 40 μL and SOD (100 μg/mL), catalase (100 μg/mL), desferal (1 mM) as control reactions were incubated in aerobic condition at room temperature (24^{o}C) for 12 hours, followed by agarose gel electrophoresis. **A)** Agarose gel: lane 1, DNA alone (S = 0.18 ± 0.04); lane 2, NADPH (200 μM) + cytochrome P450 reductase (0.05 U/mL) (S = 0. 0.35 ± 0.01); Lane 3-9, **1** (100 μM) + NADPH (200 μM) + reductase (0.05 U/mL , lane 3) (S = 1.92 ± 0.08); SOD (100 μg/mL, lane 4) (S = 1.11 ± 0.16); catalase (100 μg/mL, lane 5) (S = 0.22 ± 0.03); desferal (1mM, lane 6) (S = 0.48 ± 0.007); SOD+ catalase + desferal (100 μg/mL+ 100 μg/mL+ 1 mM, lane 7) (S = 0.18 ± 0.03); methanol (1 mM, lane 8) (S = 0.25 ± 0.06); ethanol (1 mM, lane 9) (S = 0.19 ± 0.02). **B.** Bar graph of S-values of all reaction lanes. The values, S, represent the mean number of strand breaks per plasmid molecule and were calculated by using the equation S = -ln f_1 where f_1 is the fraction of plasmid present as in the supercoiled form I. Standard deviation was determined from three repeats.

We found that DNA cleavage by OHP in presence of NADPH:cytochrome P450 reductase was inhibited by addition of 100 μg/mL SOD, 100 μg/mL catalase and 1 mM desferal . This result led us to conclude that OHP caused DNA damage due to redox cycling in presence of NADPH:cytochrome P450 reductase system as shown in **Scheme 4 & 6**.

DNA cleavage assay of OHP was also carried out in presence of X/XO system under aerobic condition and SOD, catalase and desferal were used as control.

A.

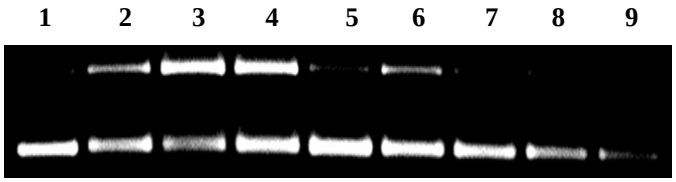

B.

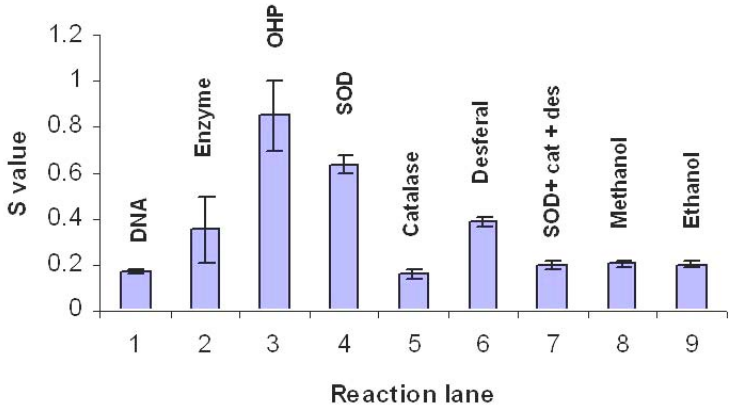

Figure 10: Cleavage of Supercoiled Plasmid DNA by 1-hydroxyphenazine (**1**) in the presence of enzyme system X/XO as an activating system. All reactions contained DNA (1 μg), 1-hydeoxyphenazine (100 μM), xanthine (50 μM), XO (0.6 U/mL), sodium phosphate buffer (50 mM, pH 7.0) and SOD (200 μg/mL), catalase (200 μg/mL), desferal (1 mM) as control reactions in a total volume 40 μL were incubated in aerobic condition at room temperature (24^{o}C) for 6 hours, followed by agarose gel electrophoresis. **A)** Agarose gel: Lane 1, DNA alone (S = 0.17 ± 0.01); lane 2, xanthine (50 μM) + XO (0.6 U/mL) (S = 0.35 ± 0.14); lane 3-9, **1** (100 μM) + xanthine (50 μM) + XO (0.6 U/mL, lane 3) (S = 0.85 ± 0.15); SOD (200 μg/mL, lane 4) (S = 0.63 ± 0.04); catalase (200 μg/mL, lane 5) (S = 0.16 ± 0.02); desferal (1mM; lane 6) (S = 0.39 ± 0.02); SOD+ catalase + desferal (200 μg/mL+ 200 μg/mL+ 1mM; lane 7) (S = 0.19 ± 0.02); methanol (1mM, lane 8) (S 0.20 ± 0.02); ethanol (1mM, lane 9) (S = 0.20 ± 0.02). **B.** Bar graph of S-values of all reaction lanes. The values, S, represent the mean number of strand breaks per plasmid molecule and were calculated by using the equation S = -ln f_1 where f_1 is the fraction of plasmid present as in the supercoiled form I. Standard deviation was determined from three repeats.

X/XO system was also able to drive DNA strand cleavage by OHP and provided evidence of formation of superoxide radical by OHP. Although X/XO system itself can generate superoxide radicals (**Figure 10, lane 2**) that leads to DNA damage, we found significant increase of DNA damage after addition of OHP into X/XO medium (**Figure 10, lane 3**). DNA damage was inhibited by addition of SOD, catalase and desferal (**Figure 10, lane 4-7**). The incubation time for reaction mixture contained X/XO was lower compare to NADPH:cytochrome P450 reductase system which results lesser amount of DNA cleavage in case of X/XO compare to NADPH:cytochrome P450 reductase system. We also noticed larger amount of background cleavage in case of X/XO compare to NADPH:cytochrome P450 reductase system as X/XO is a better source of generation of superoxide radical compare to NADPH:cytochrome P450 reductase system.

To understand whether DNA damage by OHP is radical mediated we performed plasmid based DNA cleavage assay in presence of various radical scavengers like methanol and ethanol which usually quench hydroxyl radicals. We found that DNA cleavage was inhibited by addition of methanol and ethanol (**Lane 8 and 9** in both **Figure 9 and 10**) which is simply consistent with ROS.

We also examined DNA cleavage efficiency of OHP under anaerobic condition in presence of NADPH:cytochrome P450 reductase. We didn't notice any significant yield of DNA cleavage (**Figure 11**).

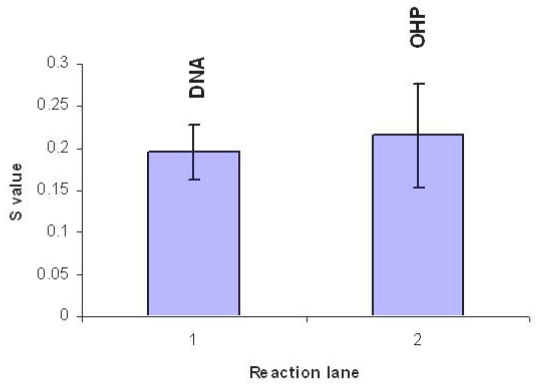

Figure 11: DNA cleavage efficiency of OHP under anaerobic condition. Supercoiled plasmid DNA (1 μg) was incubated with OHP (100 μM), NADPH (200 μM), cytochrome P450 reductase (0.05 U/mL) in presence of 50 mM sodium phosphate buffer for 5-6 h under anaerobic condition. SOD (100 μg/mL), catalase (100 μg/mL) and desferal (1 mM) were used in the reaction mixture to prevent DNA damage due to redox cycling. Bar graph of S-values of all reaction lanes are shown above. The values, S, represent the mean number of strand breaks per plasmid molecule and were calculated by using the equation $S = -\ln f_1$ where f_1 is the fraction of plasmid present as in the supercoiled form I. Lane 1= DNA alone (0.19 ± 0.22), lane 2= DNA + OHP + NADPH:cytochrome P450 reductase under anaerobic condition (S = 0.21 ± 0.06). Standard deviation was determined from two repeats.

Therefore, from these studies we conclude that OHP generates superoxide radical, H_2O_2 and hydroxyl radical in presence of one electron reducing system due to redox cycling that leads to DNA damage.

1.12. Comparison of DNA damage efficiency of OHP with well known redox cycling agent menadione and DMNQ:

Menadione and DMNQ are well known redox cycling agents which cause DNA damage due to redox cycling.[80,81,82,83] Both menadione and DMNQ have a 1,4-napthaquinone moiety. Many clinically important anticancer drugs for example, anthracyclines, mitoxantrones, saintopin etc contain quinone moiety and it has been studied that 1,4-napthaquinone analogues inhibit human DNA topoisomerase I that leads

to cytotoxicity.[83] Moreover another important characteristic of 1,4-napthaquinone analogs is that they undergo redox cycling in presence of NADPH:cytochrome P450 reductase and generate superoxide radicals which lead to formation of DNA cleaving agent hydroxyl radical.[83] In addition to exhibit significant antitumor activity 1,4-naphthoquinone derivatives also display other pharmacological activity such as antibacterial, antifungal, anti-inflammatory activity etc.[83] DMNQ derivatives show cytotoxicity against L1210 and P388 cancer cells.[83] Both menadione and DMNQ also generate oxidative stress inside the cell due to formation of ROS via redox cycling.[84]

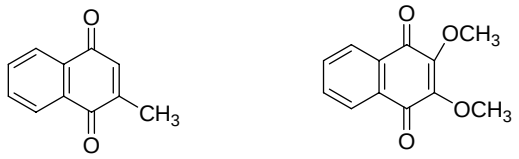

Menadione **DMNQ**

Figure 12: Structure of menadione and DMNQ

As our studies suggested that OHP cleaved DNA due to redox cycling, we compared DNA damage efficiency of OHP with menadione and DMNQ by performing a plasmid based DNA damage assay of OHP or menadione or DMNQ in presence of NADPH:cytochrome P450 reductase.

A.

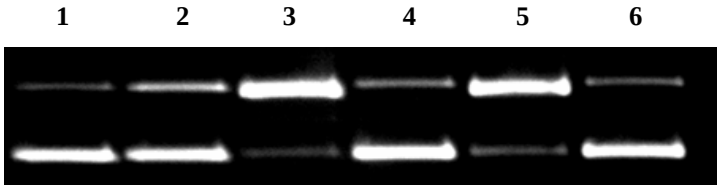

B.

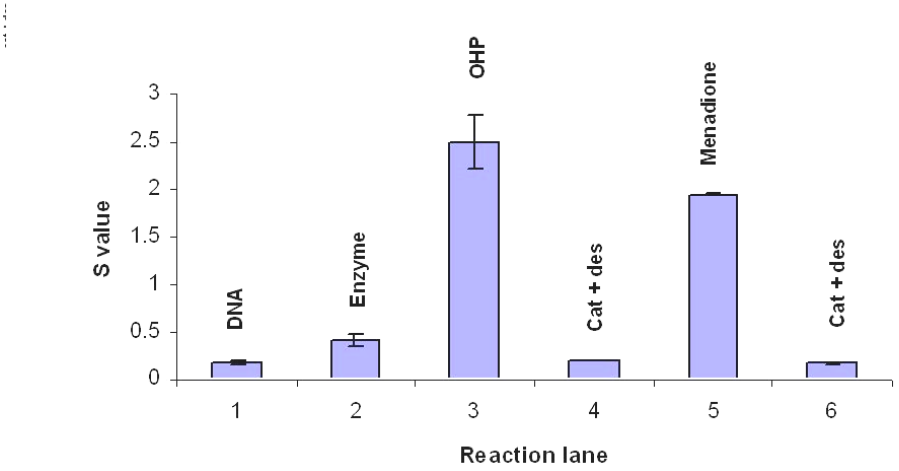

Figure 13: Comparison of DNA cleavage by **1** with menadione a well known redox cycling agent in presence of enzyme system NADPH and cytochrome P450 reductase. Supercoiled plasmid DNA (1 μg) was incubated with **1** (100 μM) or menadione (100 μM) in presence of NADPH (200 μM), cytochrome P450 reductase (0.05 U/mL) and catalase (100 μg/mL), desferal (1 mM) as control reactions in a total volume 40 μL under aerobic condition at room temperature (24^{o}C) for 12 hours, followed by agarose gel electrophoresis. **A)** lane 1, DNA alone (S = 0.17 ± 0.03); lane 2, NADPH (200 μM) + reductase (0.05 U/mL) (S = 0.41 ± 0.07); lane 3 & 5, **1** (lane 3, 100 μM) (S = 2.5 ± 0.28) or **menadione** (lane 5, 100 μM) (S = 1.94 ± 0.007) + NADPH (200 μM) + reductase (0.05 U/mL); lane 4 (S = 0.19 ± 0) & 6 (S = 0.165 ± 0.007), control (control: 1 mM desferal & 100 μg/mL catalase). **B.** Bar graph of S-values of all reaction lanes. The values, S, represent the mean number of strand breaks per plasmid molecule and were calculated by using the equation S = -ln f_1 where f_1 is the fraction of plasmid present as in the supercoiled form I. Standard deviation was determined from two repeats.

A.

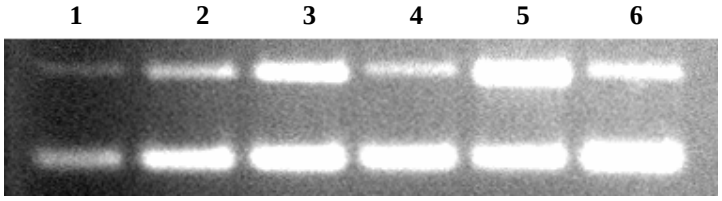

B.

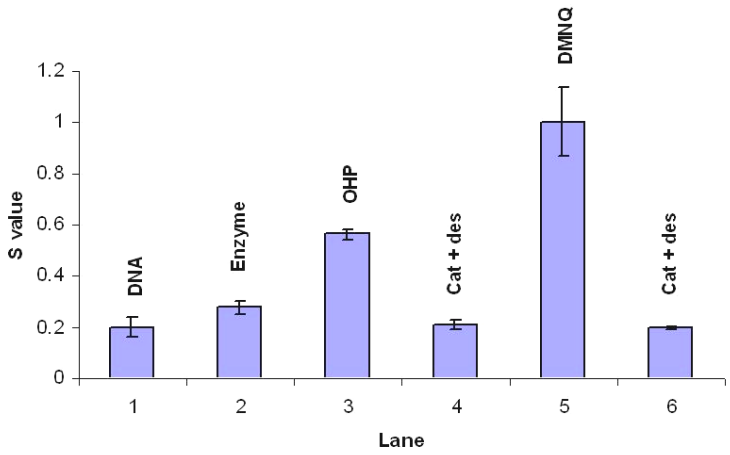

Figure 14: Comparison of DNA cleavage by **1** with DMNQ in presence of NADPH and cytochrome P450 reductase. Supercoiled plasmid DNA (1 μg) was incubated with **1** (100 μM) or DMNQ (100 μM) in presence of NADPH (200 μM), cytochrome P450 reductase (0.05 U/mL) and catalase (100 μg/mL), desferal (1 mM) as control reactions in a total volume 40 μL under aerobic condition at room temperature (24^{o}C) for 3 hours, followed by agarose gel electrophoresis. **A)** Agarose gel: lane 1, DNA alone (S = 0.20 ± 0.04); lane 2, NADPH (200 μM) + reductase (0.05 U/mL) (S = 0.28 ± 0.03); lane 3 & 5, **1** (lane 3, 100 μM) (S = 0.56 ± 0.02) or **DMNQ** (lane 5, 100 μM) (S = 1.00 ± 0.13) + NADPH (200 μM) + reductase (0.05 U/mL); lane 4 (S = 0.21 ± 0.01) & 6 (S = 0.20 ± 0.004), control (control: 1 mM desferal & 100 μg/mL catalase). **B.** Bar graph of S-values of all reaction lanes. The values, S, represent the mean number of strand breaks per plasmid molecule and were calculated by using the equation S = -ln f_1 where f_1 is the fraction of plasmid present as in the supercoiled form I. Standard deviation was determined from two repeats.

We found that DNA cleavage efficiency of OHP is comparable with well known redox cycling agents menadione and DMNQ.

1.13. In vitro metabolism of OHP:

Redox cycling agents act as catalyst which remains unchanged and not consumed during the reaction. Accordingly, we checked to see if OHP is consumed during the reaction with NADPH:cytochrome P450 reductase. Thus, we incubated OHP with NADPH:cytochrome P450 reductase at pH 7 buffer for over night and then analyzed the reaction mixture by performing normal phase HPLC and LC/MS. LC/MS analysis was performed by using TSQ7000 triple-quadruple mass spectrometer where we used same normal phase HPLC method as used in HPLC analysis to detect the metabolites and used APCI-MS (atmospheric pressure chemical ionization) operating in positive ion mode to determine the mass (m/z = M+H) of metabolites.

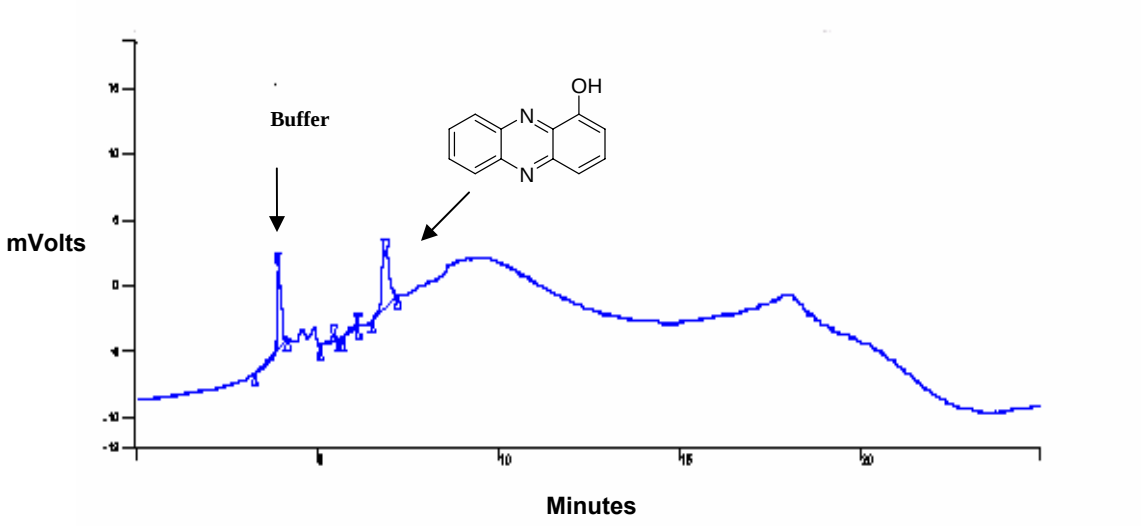

Figure 15: Metabolism study of 1-hydroxyphenazine (**1**) by HPLC analysis. A 200 µL solution of sodium phosphate buffer (pH 7.0, 50 mM), **1** (100 µM) was incubated with NADPH (500µM) and cytochrome P450 reductase (0.05 U/mL) at room temperature (24^{o}C) under aerobic condition for 12 hours followed by HPLC analysis.

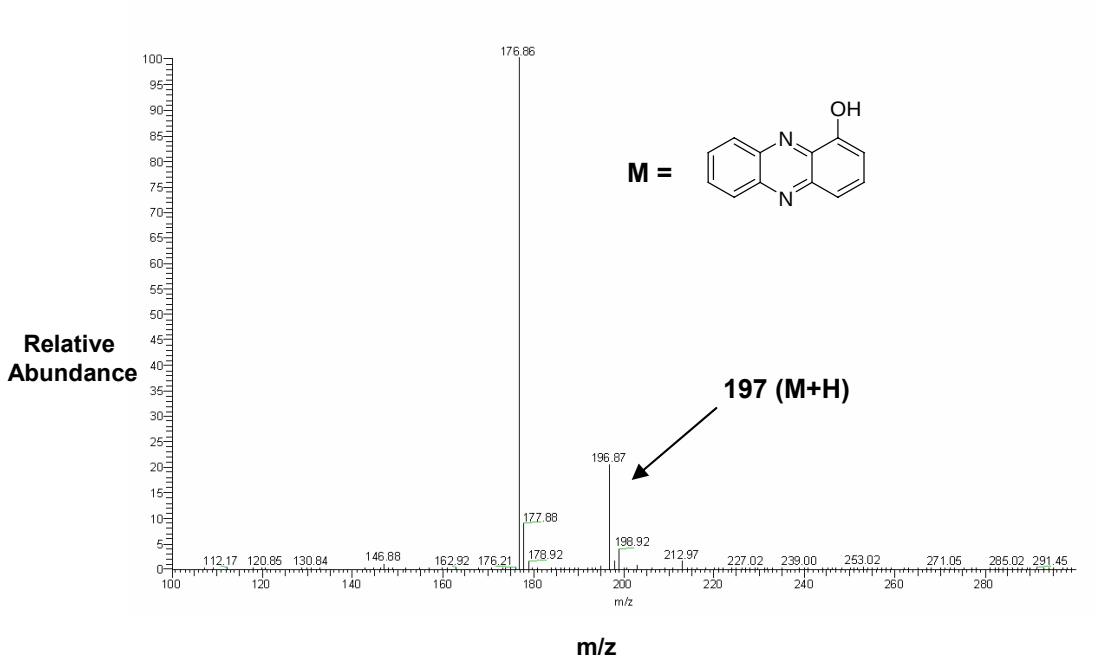

Figure 16: Metabolism study of 1-hydroxyphenazine (**1**) by using LC/MS where the compound was detected by using normal phase HPLC method and mass of the peak (m/z = 197) of retention time 6.56 minutes was determined by using APCI positive ion mode. The mass spectrum shows M+H ion of **6** at m/z 197 obtained using LC-APCI/MS operating in the positive ion mode. A 200 µL solution of sodium phosphate buffer (pH 7.0, 50 mM), **1** (100 µM) was incubated with NADPH (500µM) and cytochrome P450 reductase (0.05 U/mL) at room temperature (24^{o}C) under aerobic condition for 12 hours followed by LC/MS analysis.

HPLC analysis detected the peak of OHP coming at retention time 6.8 minutes and didn't show any other OHP derived peaks. Moreover we also found that OHP was not consumed during the reaction, almost 95% OHP was remained at the end of the assay. LC/MS analysis also identified the molecular ion peak of mass m/z = **197** ($M+H^+$; APCI positive ion mode**)** coming at 6.8 minutes which correspond to OHP.

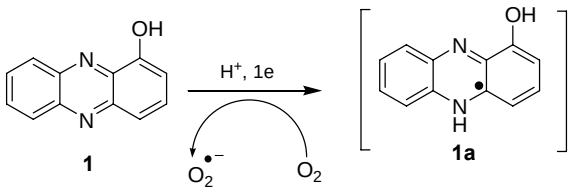

Scheme 7: Redox cycling of OHP under aerobic condition.

Therefore both HPLC and LC/MS analysis are consistent with redox cycling mechanism of OHP (**Scheme 7**).

1.14. OHP generates reactive oxygen species (ROS) in macrophage:

Our *in vitro* study established that OHP undergoes one-electron reductive activation on treatment with one electron reducing enzyme and generates ROS like superoxide radical, H_2O_2 and hydroxyl radical due to redox cycling. Our next goal was to investigate whether OHP can generate ROS inside the cell to strengthen our hypothesis regarding the virulence by OHP. Accordingly the *in vivo* study was carried out by our cell biology collaborator Jarek and Qian Li, center for Free Radical Biology, the University of Alabama Birmingham. They performed the cell-based assay to detect ROS caused by OHP in the RAW264.7 murine macrophage cells by using DCF fluorescence dye.[85] DCF (2'-7'-dichlorofluorescein) is the oxidized form of 2'-7'-dichlorofluorescin (DCFH). DCFH doesn't fluoresce. While DCFH is oxidized into fluorescent DCF in presence of oxidizing agent like H_2O_2, superoxide radical then it produces green signal inside the cell (**Scheme 8**).

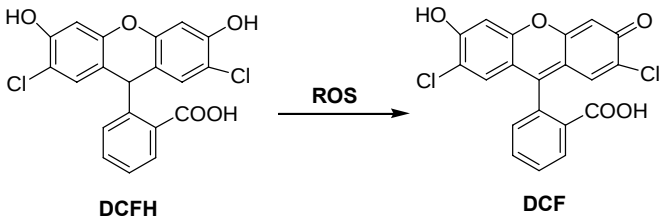

DCFH DCF

Scheme 8: Oxidation of DCFH into DCF by ROS.[87,88]

DCF is used to detect oxidative stress inside the cell.[86,87] In this cell based assay, OHP was incubated with RAW264.7 murine macrophage cells at 37^{o} for 30 min. Then DCF was added and fluorescence microscopy was performed 10 minutes later.[85]

A.

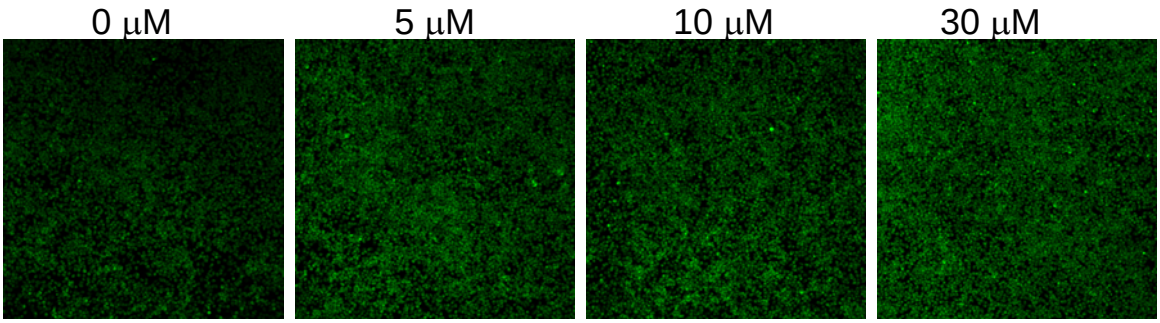

B.

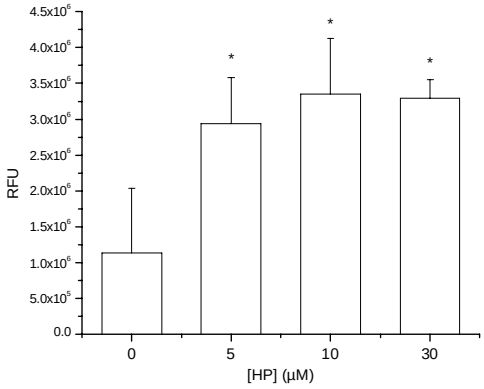

Figure 17: **A)** Detection of ROS in RAW264.7 murine macrophage cells by using fluorescent dye DCF. **B)** Bar graphs represent the fluorescence intensity with or without presence of OHP.[85]

Incubation of macrophage with OHP produced a significant increase in fluorescence compared to the macrophage cell incubated without OHP. Fluorescent intensity was not increased in an appreciable amount with increasing concentration of OHP. Limited concentration dependence may be due to saturation of relevant enzyme systems by OHP under the conditions of assay. This remains to be tested. In conclusion it can be clearly demonstrated that OHP generates ROS inside the macrophage.

1.15. Conclusion:

On the basis of our both *in vitro* and *in vivo* studies it can be clearly demonstrated that 1-hydroxyphenazine generates ROS via redox cycling in presence of NADPH:cytochrome P450 reductase system. It is well known that generation of ROS produce oxidative stress inside the cell which leads to cytotoxicity. Our future goal will be to detect oxidative stress inside lung cells as *P. aeruginosa* infects lung airways of cystic fibrosis patients. Therefore, overall this study establishes a possible mechanism underlying the virulence properties of 1-hydroxyphenazine. As our study clearly demonstrated that 1-hydroxyphenazine generates ROS inside the cell and generation of ROS can cause oxidative stress inside the cell therefore this mechanism study would lead us to design an antioxidant which can be used as therapeutics for *P. aeruginosa* infected cystic fibrosis patients.

Material and methods:

Materials: Materials with highest purity were bought from the following suppliers. benzofuroxan, sodium phosphate, xanthine, menadione, triethylamine and TLC plates from Aldrich Chemical Co. (Milwaukee, WI); Sodium hydrosulfite 85% and 1,2 cyclohexanedione, 98% from Acros Organics (Pittsburgh, PA); NADPH, acetonitrile, desferal, cytochrome P450 reductase, catalase and SOD from Sigma Chemical Co. (St. Louis, MO); agarose from Seakem; HPLC grade solvents (methanol, ethanol, ethyl acetate, heptane), ethyl acetate, hexane, NaOH, HCl and acetic acid from Fisher Scientific (Pittsburg, PA); xanthine oxidase and ethidium bromide from Roche Molecular Biochemicals (Indianapolis, IN); Silica gel (0.04-0.063 mm pore size) for column chromatography from Merck; The plasmid pGL2BASIC was prepared using standard protocols, [Sambrook, J.; Fritsch, E. F.; Maniatis, T. (1989) *Molecular Cloning: A Lab Manual,* Cold Spring Harbor Press, Cold Spring Harbor. NY]. 1-Hydroxyphenazine, 1-*N*-oxide and di-*N*-oxide of 1-hydroxyphenazine were synthesized by following the literature methods.[30] High resolution mass spectroscopy was performed at the University of Illinois Urbana-Champaign Mass Spectroscopy facility and low resolution mass spectroscopy and LC/MS study were performed at University of Missouri-Columbia Mass Spectroscopy facility. NMR spectra were taken using Bruker DRX 300 and 500 MHz instruments at the University of Missouri-Columbia.

Synthesis of 1-hydroxyphenazine: At first *N*-oxides of 1-hydroxyphenazine were prepared by following the synthetic route used by Haddadin and coworkers with slight modification.[62] Benzofuranoxide (1gm, 0.00543 moles) was dissolved in 10 mL TEA (triethylamine) by heating and stirring the solution under N_2 gas. Then 1,2 cyclohexanedione (450mg, .0040 moles) was added drop wise to the reaction mixture under N_2 gas. After that the reaction mixture was stirred in ice bath for 30 minutes and 7-8 hours in room temperature (RT). The color of the reaction mixture was turned into deep brown. Then the reaction mixture was diluted in crushed ice and acidified (pH 5) by HCl. After that the reaction mixture was extracted in distilled ethyl acetate and dried over anhydrous Na_2SO_4. The solvent was evaporated and the reaction mixture was purified by gravity column chromatography (elute solvent: 1:3 distilled ethyl acetate and hexane) to obtain mixture of *N*-oxides of 1-hydroxyphenazine (26%). Crude *N*-oxides of 1-hydroxyphenazine (**5**, **6** & **7**, 50 mg) was dissolved in 5% 2.5 mL sodium hydroxide solution. After that 40% 1mL $Na_2S_2O_4$ was added in the reaction mixture and the reaction mixture was gently heated at 70^oC for 2 h. After that the reaction mixture was acidified to pH 4 by HCl. Upon acidification the reaction mixture was turned into brownish yellow color. Then the product was extracted in distilled ethyl acetate and dried over anhydrous Na_2SO_4. The solvent was evaporated and the crude product was purified by gravity column chromatography (elute solvent: ethyl acetate and hexane) to obtain product **1** (14.6%). R_f = 0.4 (1: 3 EtOAc/hexane). ^{1}H-NMR of **1** (300 MHz, Acetone-d_6) δ 9.27 (1H, s), 8.27 (1H, dd, J_1= 2.4 Hz, J_2= 4.2 Hz; 1H, dd, J_1= 2.1 Hz, J_2= 4.2 Hz), 7.99 (1H, ddt, J_1= 2.1 Hz, J_2= 6.6 Hz, J_3= 5.1 Hz; 1H, ddt, J_1= 2.1 Hz, J_2= 6.3 Hz, J_3= 5.1), 7.87 (1H, dd, J_1= 7.5 Hz, J_2= 8.5 Hz), 7.76 (1H, dd, J_1= 8.5 Hz, J_2= 1 Hz), 7.26 (1H, dd, J_1= 7.5 Hz, J_2=

1 Hz) ppm; ^{13}C-NMR (Acetone-d_6, 125 MHz) δ 153.79, 145.00, 144.88, 142.16, 136.04, 132.73, 131.74, 131.45, 130.54, 130.16, 120.58, 110.19 ppm; LRMS: ESI-MS $[M+H]^+$= 196.91; HRMS: 197.0714, calculated mass: 197.0715 (PPM: -0.5).

In all assays OHP was used as 10% acetonitrile in water (by volume).

Cleavage of Supercoiled Plasmid DNA by OHP: In a typical DNA cleavage assay, supercoiled plasmid DNA (1 μg) was incubated with 1-hydroxyphenazine (100 μM), NADPH (200 μM), cytochrome P450 reductase (0.05 U/mL), sodium phosphate buffer (50 mM, pH 7.0) in a total volume 40 μL. SOD (100 μg/mL), catalase and (100 μg/mL), desferal (1 mM) were added in the reaction mixture in case of control reactions. Some assays were performed by using xanthine (X) (50 μM) and xanthine oxidase (XO) (0.6 U/mL) in place of NADPH:cytochrome P450 reductase. Reactions were initiated by addition of cytochrome P450 reductase or XO. Reaction mixture was wrapped with aluminium foil to prevent exposure of light and incubated under aerobic condition at room temperature (24^{o}C) for 12 hours in case of NADPH:cytochrome P450 reductase system and 6 hours in case of X/XO system. In case of anaerobic assay, except DNA, NADPH and enzymes, OHP (100 μM), sodium phosphate buffer (50 mM, pH 7), desferal (1 mM) and water were taken in pyrex tubes and degassed by three cycles of freeze-pump-thaw to remove dissolved oxygen. Then the pyrex tubes containing degassed solutions were sealed, scored and opened in an argon filled glove bag. Next SOD (100 μM/mL), catalase (100 μM/mL), NADPH (200 μM) and cytochrome P450 reductase (0.05U/mL) were prepared by using degassed water. SOD, catalase and desferal were used in all lanes to prevent DNA damage due to redox cycling. The reaction was initiated

by addition of NADPH and cytochrome P450 reductase and the reaction mixture was incubated in argon filled glove bag for 5-6 hours. After incubation, the reaction was stopped by addition of 6.6 μL of 50% glycerol loading buffer, and the resulting reaction mixture was loaded onto a 0.9% agarose gel. The gel was electrophoresed for approximately 2 h at 90 V in 1 x TAE buffer and then stained in a solution of ethidium bromide (0.3 μg/mL) for 3 hours. DNA in the gel was visualized by UV-transillumination and the amount of DNA in each band was quantified using an Alpha Innotech IS-1000 digital imaging system. DNA-cleavage assay containing radical scavengers was performed as described above with the exception that radical scavengers such as methanol (1 mM) or ethanol (1 mM) were added to the reaction mixture before addition of enzymes.

Cleavage of Supercoiled Plasmid DNA with increasing concentration of OHP and NADPH:cytochrome P450 reductase system: In a typical DNA damage assay supercoiled plasmid DNA (1 μg) was incubated with increasing concentration of 1-hydroxyphenazine (20-100 μM), NADPH (100 μM), cytochrome P450 reductase (0.05 U/mL), sodium phosphate buffer (50 mM, pH 7) and with catalase (100 μg/mL), desferal (1 mM) as control reactions in a total volume 40 μL. In some assays DNA (1 μg) was incubated with OHP (100 μM) and increasing concentration of NADPH (200 μM, 400 μM, 750 μM, 1 mM) or NADPH:cytochrome P450 reductase (0.05 U/mL) system. The reactions were initiated by addition of cytochrome P450 reductase, then wrapped with aluminium foil to prevent exposure of light and incubated under aerobic condition at room temperature (24^{o}C) for 12 hours. Following incubation, the reaction was stopped by

addition of 6.6 μL of 50% glycerol loading buffer, and the resulting reaction mixture was loaded onto a 0.9% agarose gel. The gel was electrophoresed for approximately 2 h at 90 V in 1 x TAE buffer and then stained in a solution of ethidium bromide (0.3 μg/mL) for 3 hours. DNA in the gel was visualized by UV-transillumination and the amount of DNA in each band was quantified using an Alpha Innotech IS-1000 digital imaging system.

Comparison of DNA damage ability of 1-hydroxyphenazine with menadione and DMNQ: In a typical plasmid based DNA damage assay DNA (1 μg) was incubated with 1-hydroxyphenazine (100 μM) or menadione (100 μM), NADPH (200 μM), cytochrome P450 reductase (0.05 U/mL), sodium phosphate buffer (50 mM, pH 7) and with catalase (100 μg/mL), desferal (1 mM) as control reactions in a total volume 40 μL at room temperature (24^{o}C) under aerobic condition for 12 hour. In a similar way DNA (1 μg) was incubated with 1-hydroxyphenazine (100 μM) or DMNQ (100 μM), NADPH (200 μM), cytochrome P450 reductase (0.05 U/mL), sodium phosphate buffer (50 mM, pH 7) and with catalase (100 μg/mL), desferal (1 mM) as control reactions in a total volume 40 μL at room temperature (24^{o}C) under aerobic condition for 3 hour. The reaction mixture was wrapped by aluminium foil to prevent exposure of light. After that the reaction was stopped by addition of 6.6 μL of 50% glycerol loading buffer, and the resulting reaction mixture was loaded onto a 0.9% agarose gel. The gel was electrophoresed for approximately 2 h at 90 V in 1 x TAE buffer and then stained in a solution of ethidium bromide (0.3 μg/mL) for 3 hours. DNA in gel was visualized by UV-transillumination and the amount of DNA in each band was quantified using an Alpha Innotech IS-1000 digital imaging system.

Metabolism study of 1-Hydroxyphenazine in presence of NADPH:cytochrome P450 reductase system: In a typical assay a solution of 200 uL containing 1-hydroxyphenazine (100 μM) and sodium phosphate buffer (50 mm, pH 7) alone or 1-hydroxyphenazine (100 μM), sodium phosphate buffer (50 mM, pH 7), NADPH (500 μM) and cytochrome P450 reductase (0.05 U/mL) were incubated at room temperature (24^{o}C) under aerobic condition for 12 hours. Two control experiments were done by addition of catalase (100 μg/mL) and desferal (1 mM) or without addition of 1-hydroxyphenazine in the reaction mixture. After incubation, the proteins were removed by centrifugation through Amicon Microcon (YM3) filters. The filtrate was extracted in 50:50 ethyl acetate: hexane mixture and then analyzed by HPLC employing a Microsorb-MV-100 NH_2 normal phase column (5 um particle size, 25 cm length, 100 A^{o} pore size and 4.6 mm i.d.) eluted with gradient solvent system starting with 40% A (0.5 % acetic acid in ethylacetate) and 60 % B (0.5 % acetic acid in heptane) followed by linear increase to 55 % A from 0 minute to 2 minute, 70% A from 2 to 4 minute. Then 70% A was held for next 13 minutes and in next 2 minutes again A is reached to 40% and gets equilibrated for next 8 minutes. The flow rate was 0.7 mL/min and the products were monitored by UV-absorbance at 284 nm. In vitro metabolism of 1-hydroxyphenazine yield only 1-hydroxyphenazine which was not consumed during the reaction with NADPH:cytochrome P450 reductase system, almost 95% OHP was remained at the end of the reaction. 1-Hydroxyphenazine was identified by co-injection of reaction mixture with authentic standard and by LC/MS. LC/MS analysis was performed by using TSQ7000 triple-quadruple mass spectrometer where we used same normal phase HPLC method as described above with the exception of UV-absorbance detected at 274 nm

instead of 284 nm and used APCI-MS (atmospheric pressure chemical ionization) operating in positive ion mode to determine the mass (m/z = M+H) of metabolites.

References:

1. Kerr, J. *Infect. Dis. Rev.* **2000**, *2*, 184-194.
2. Laursen, J.; Nielsen, J. *Chem. Rev.* **2004**, *104*, 1663-1685.
3. Weigele, M.; Maestrone, G.; Mitrovic, M.; Leimgruber, W. *Antimicro. Agents. Chemother.* 1**970**, 46-49.
4. Hollstein, U.; Butler, P. L. *Biochemistry* **1972**, *11*, 1345-1350.
5. Hollstein, U.; Gemert, R. J. V. *Biochemistry* **1971**, *10*, 497-504.
6. Behki, R. M.; Lesley, S. M. *J. Bacteriol.* **1972**, *109,* 250-261.
7. Baron, S. S.; Terranova, G.; Rowe, J. J. *Curr. Microbiol*. **1997**, *18,* 223-230.
8. Abken, H. J.; Tietze, M.; Brodersen, J.; Baumer, S.; Beifuss, U.; Deppenmeier, U. *J. Bacteriol*. **1998**,*180*, 2027-2032.
9. Beifuss, U.; Tietze, M.; Baumer, S.; Deppenmeier, U. *Angew. Chem. Int. Ed*. **2000**, *39,* 2470-2472.
10. Bjarnsholt, T.; Givskov, M. *Anal. Bioanal. Chem.* **2007**, *387*, 409-414.
11. Hassett, D. J. *et al. Adv. Drug. Deliv. Rev.* **2002**, *54*, 1425-1443.
12. Lu, C. D.; Winteler, H.; Abdelal, A.; Hass, D. *J. Bacteriol*. **1999**, *181*, 2459-2464.
13. Lau, G. W.; Hassett, D. J.; Britigan, B. E. *Trends in Microbiology* **2005**, *13*, 389-397.
14. Ruxana T.; Blackwell, T. S.; Christman, J. W.; Prince, A. S. *American Journal of Respiratoty and Critical Care Medicine* **2005**, *171*, 1209-1223.
15. http://www.nhlbi.nih.gov/health/dci/Diseases/cf/cf_causes.html.
16. Lau, G. W.; Hassett, D. J.; Ran, H.; Kong, F. *Trends in Molecular Medicine* **2004**, *10*, 601-606.

17. http://www.msu.edu/~luckie/About_MSUCF.html.

18. http://www.bioscience.org/news/scientis/virulenc.htm.

19. http://mvirdb.llnl.gov/.

20. Ras, G. J.; Anderson, R.; Taylor, G. W. *J. Infect. Dis.* **1990**, *162,* 178-185.

21. Sorensen, R. U.; Klinger, J. D.; Cash, H. A.; Chase, P. A.; Dearborn, D. G. *Infect. Immun.* **1983**, *41,* 321-330.

22. Berk, R.; Nelson, E. L.; Pickett, M. J. *J. Infect. Dis.* **1960,** *107,* 183-188.

23. Sorensen, R. U.; Klinger, J. D. *Antibiotic. Chemother.* **1987**, *39,* 113-124.

24. Wilson, R.; Pitt, T.; Taylor, G. *J. Clin. Invest.* 1**987**, *79,* 221-229.

25. Munro, N. C.; Barker, A.; Rutman, A. *J. Appl. Physiol.* **1989**, *76,* 316-323.

26. Denning, G. M.; Wollenweber, L. A.; Railsback, M. A.; Cox, C. D.; Stoll, L. L.; Britigan, B. E. *Infect. Immun.* **1998**, *66,* 5777-5784.

27. Friedheim, EAH. *J. Exp. Med.* **1931**, *54,* 207-221.

28. Baron, S. S.; Rowe, J. J. *Antimicrob Agents Chemother.* **1981**, *20,* 814-820.

29. Kerr, J. R.; Taylor, G. W.; Rutman, A.; Hoiby, N.; Cole, P. J.; Wilson, R. *J. Clin. Pathol.* **1999**, *52,* 385-387.

30. Morrison, M. M.; Sawyer, D.T. *J. Am. Chem. Soc.* **1978**, *100,* 211-213.

31. Morrison, M. M.; Seo, E. T.; Howie, J. K.; Sawyer, D. T. *J. Am. Chem. Soc.* **1978**, *100,* 207-211.

32. Dickens, F.; Mcllwain, H. *Biochem. J.* **1938**, *32,* 1615-1625.

33. Friedheim, EAH.; Michaelis, L. *J. Biol. Chem.* **1931**, *91,* 355-368.

34. Massey, V.; Singer, T. P. *J. Biol. Chem.* **1957**, *229,* 755-762.

35. Zaugg, W. S. *J. Biol. Chem.* **1964**, *239,* 3964-3970.

36. Hassan, H. M.; Fridovich, I. *J. Bacteriol.* **1980**, *141,* 156-163.

37. Muller, M. *Free. Rad. Biol. Med.* **2002**, *33*, 1527-1533.

38. Garg, T. K.; Chang, J. Y. *BMC Ophthalmology.* **2003**, *3*, 1-15.

39. Salmon, T. B.; Evert, B. A.; Song, B.; W, Paul. *Nucleic Acids Research* **2004**, *32*, 3712-3723.

40. Agarwal, A.; Said, T. M. *BJU. INT.* **2005,** *9 5*, 503 – 507.

41. http://www.cosmobio.co.jp/export_e/products/kits/products_NNS_20060421_1.asp.

42. Denning, G. M.; Iyer, S. S.; Reszka, K. J.; Malley, Y. O.; Rasmussen, G. T.; Britigam, B. E. *Am. J. Physiol. Lung. Cell. Mol. Physiol.* **2003**, *285*, L584-L592.

43. Muller, M. *Biochimica et Biophysica Acta* **1995**, 185-189.

44. Nagai, K.; Carter, J. B.; Xu, J.; Hecht, M. S. *J. Am. Chem. Soc.* **1991**, *113,* 5099-5100.

45. Nagai, K.; Hecht, M. S. *J. Biol. Chem.* **1991**, *266,* 23994-24002.

46. Voet, D.; Voet, J. G. Biochemistry; 2nd edition; John Wiley and Sons, Inc: New work, 1995.

47. DNA damage by Heterocyclic N-oxides: A novel class of antitumor agents, PhD thesis submitted by Goutam Chowdhury in **2005.**

48. Harrison, R. *Free Rad. Biol. Med.* **2002**, *33*, 774-797.

49. Wooton, J. C.; Nicloson, R. E.; Cock, J. M.; Walters, D. E.; Burke, J. F.; Doyle, W. A.; Bray, R. C. *Biochem. Biophys. Acta* **1991**, *1057*, 157-185.

50. Hille, R. *Chemistry and biochemistry of flavoenzymes*; CRC Press: Boca Raton, **1992**; Vol. III.

51. Porras, A. G.; Olson, J. S.; Palmer, G. *J. Biol. Chem.* **1981**, *256*, 9096-9103.

52. Olson, J. S.; Ballou, D. P.; Palmer, G.; Massey, V. *J. Biol. Chem.* **1974**, *249*, 4363-4382.

53. Godber, B. L. J.; Doel, J. J.; Sapkota, G. P.; Blake, D. R.; Stevens, C. R.; Eisenthal, R.; Harrison, R. *J. Biol. Chem.* **2000**, *275*, 7757-7763.

54. Dudka, J. *Ann. Nutr. Metab.* **2006**, *50*, 121-125

55. Gutierrez, A.; Grunau, A.; Painet, M.; Munro, A. W.; Wolf, C. R.; Roberts, G. C. K.; Scrutton, N. S. *Biochemical Society Transactions* **2003**, *31*, 497-501.

56. Smith, G. C. M.; Tew, D. G.; Wolf, C. R. *Proc. Natl. Acad. Sci. USA.* **1994**, *91*, 8710-8714.

57. Iyanagi, T.; Mason, H. S. *Biochemistry* **1973**, *12*, 2297-2308.

58. Vemilion, J. L.; Ballou, D. P.; Massay, V.; Coon, M. J. *J. Biol. Chem.* **1981**, *256*, 266-277.

59. Daniels, J. S.; Gates, K. S. *J. Am. Chem. Soc.* **1996**, *118*, 3380-3385.

60. Chowdhury, G.; Kotandeniya, D.; Daniels, J. S.; Gates, K. S. *Chem. Res. Toxicol*. **2004**, *17,* 1399-1405.

61. Wilson, W. R. *Lancaster* **1992**, *3*.

62. Issidorides, C. H.; Atfah, M. A.; Sabounji, J. J.; Sidani, A. R.; Haddadin, M. J. *Tetrahedron* **1978**, *34,* 217-221.

63. Halliwell, B.; Gutteridge, J. M. C. *Methods Enzymol.* **1990**, *186*, 1.

64. Bagley, A. C.; Krall, J.; Lynch, R. E. *Proc. Nat. Acad. Sci. U.S A.* **1986**, *83*, 9189.

65. Hassan, H. M.; Fridovich, I. *Arch. Biochem. Biophys.* **1979**, *196*, 385.

66. Sanchez Sellero, I.; Lopez-Rivadulla Lamas, M. *Recent Res. Dev. Drug Metab. Disp.* **2002**, *1*, 1163-275.

67. Finkel, T.; Holbrook, N. J. *Nature* **2000**, *408*, 239.

68. Davis, W.; Ronai, Z.; Tew, K. D. *J. Pharm. Exp. Ther.* **2001**, *296*, 1.

69. Arrigo, A. P.; Firdaus, W. J. J.; Mellier, G.; Moulin, M.; Paul, C.; Diaz-Latoud, C.; Kretz-Remy, C. *Methods* **2005**, *35*, 126.

70. Chen, Y.; Jungsuwadee, P.; Vore, M.; Butterfield, D. A.; Clair, St. D. K. *Mol. Interventions* **2007**, *7*, 147.

71. Mitra, K.; Kim, W.; Daniels, J. S.; Gates, K. S. *J. Am. Chem. Soc.* **1997**, *119,* 11691-11692.

72. Sivaramakrishnan, S.; Gates, K. S. *Bioorganic & Medicinal Chemistry letters* **2008**, in press.

73. Chatterji, T.; Keerthi, K. Gates, K. S. *Bioorganic & Medicinal Chemistry letters* **2005**, *15*, 3921-3924.

74. Gates, K. S. *Pergamon: New York* **1999**, *7*, 491-552.

75. Greenberg, M. M. *Org. Biolmol. Chem.* **2007**, *5*, 18.

76. Greenberg, M. M. *Chem. Res. Toxicol.* **1998**, *11*, 1235.

77. Gates, K. S. *Reviews of Reactive Intermediates* **2007**, 333-378.

78. escience.ws/b572/L2/L2.htm.

79. Santangelo, F. *Curr. Med. Chem.* **2003**, *10*, 2599-2610.

80. Paget, T.; Maroulis, S.; Mitchell, A.; Edwards, M. R.; Edward, L. *Microbiology*. **2004**, *150*, 1231-1236.

81.Winston, A. M.; Kaler, B.; Bach, P. H. *Toxicology letters*. **1998**, *94*, 209-215.

82. Shi, M. M.; Kugelman, A.; Iwamoto, T.; Tian, L.; Forman, H. J. *J. Biol. Chem.* **1994**, *269*, 26512-26517.

83. Chung, Y.; Yoo, J.; Park, S. Hyun.; Kim, B. H.; Chen, Xi.; Zhan, C. G.; Cho, H. *Bull. Korean Chem. Soc*. **2007**, 28, 691-694.

84. Seung, S. A.; Lee, J. Y.; Lee, M.Y.; Park, J. S.; Chung, J. H. *Chemico-Biological Interactions* **1998**, *113*, 133-144.

85. All cell biology experiments were carried out by Jarek and also Qian Li, Center for Free Radical Biology, Departments of Anesthesiology, Physiology & Biophysics and Environmental Health Sciences,The University of Alabama Birmingham and got e-mail permission to put their data on my thesis.

86. Rota, C.; Chignell, C. F.; Mason, R. P. *Free. Radic. Biol. Med.* **1999**, *27*, 873-881.

87. Chignell, C. F.; Sik, R. H. *Free. Radic. Biol. Med.* **2003**, *34*, 1029-1034.

^{1}H-NMR Spectra of 1-hydroxyphenazine (**1**) in $(CD_3)_2CO$

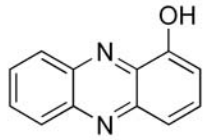

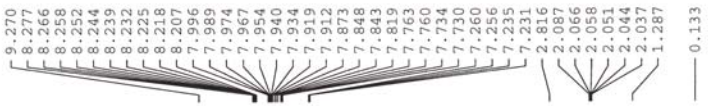

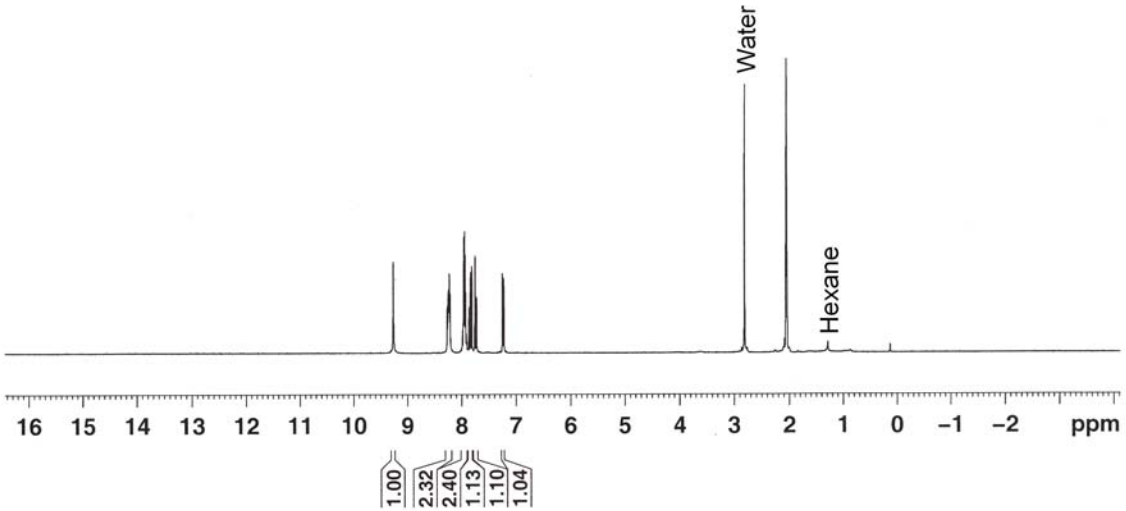

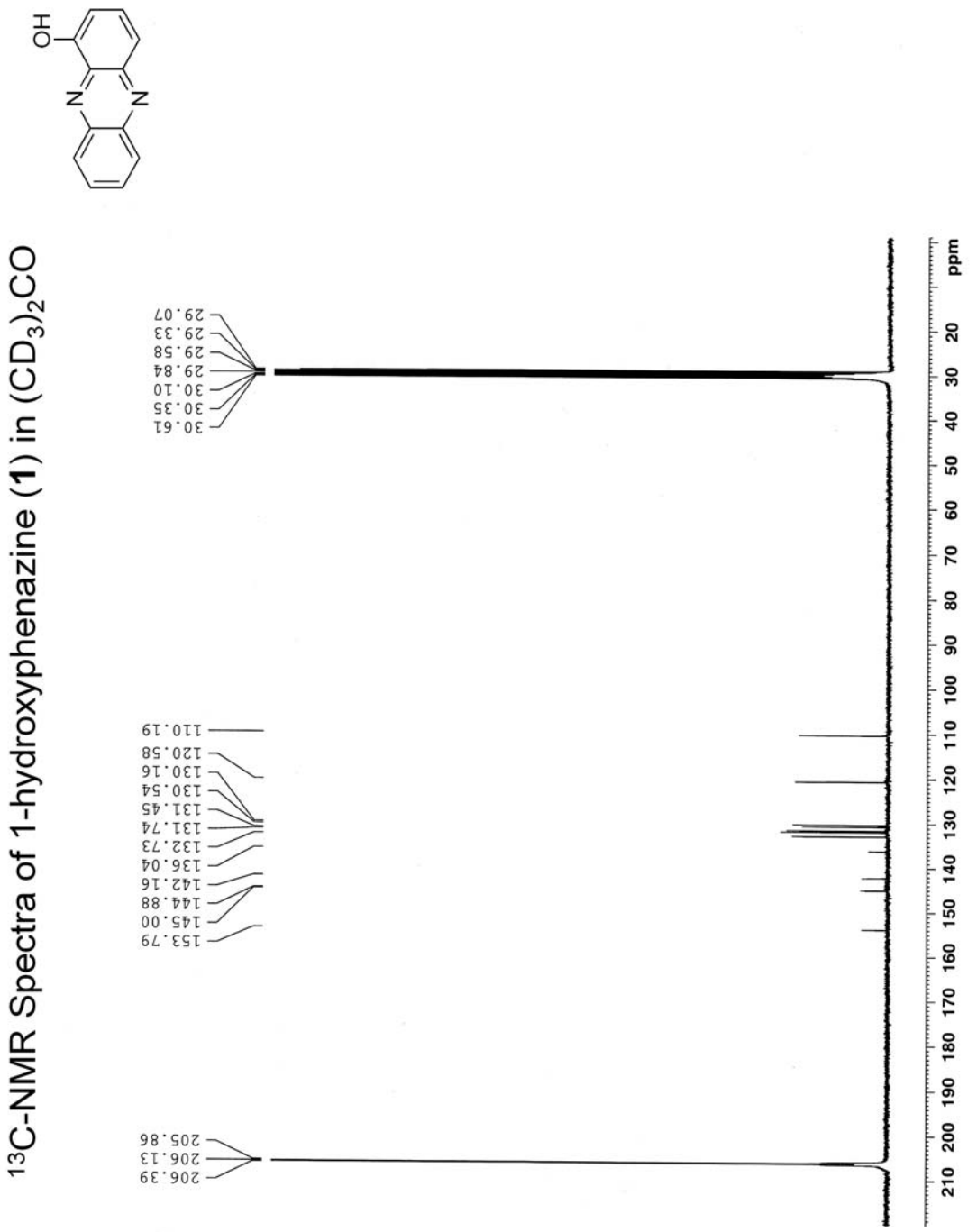
^{13}C-NMR Spectra of 1-hydroxyphenazine (1) in $(CD_3)_2CO$
OH
N
N
206.39
206.13
205.86
153.79
145.00
144.88
142.16
136.04
132.73
131.74
131.45
130.54
130.16
120.58
110.19
30.61
30.35
30.10
29.84
29.58
29.33
29.07
ppm

Chapter 2: Oxidative DNA damage by cytotoxic *N*-oxides of 1-hydroxyphenazine: Towards a molecular understanding of the bacterial virulence factor 1-hydroxyphenazine

2.1. Introduction:

Colonization of *Pseudomonas aeruginosa (PA)* in the lung airways of cystic fibrosis patients induces immune responses in the host cell and the function of immune responses or, in other words, host defense is clearance of *P.aeruginosa* from the lung airways.[1] Immune responses in the host cell functions by the coordinated effort of different types of immune cells including respiratory tract epithelium, macrophages and neutrophils. The respiratory epithelium cell plays an important role to resist colonization of bacteria. Its function is to provide mucosal barrier and contribute the clearance of bacterial cells by ciliary action.[1] Apart from this, bacterial invasion also induces numerous signaling cascades in host immune cell that results in expression of mucins in epithelium,[2] production of antimicrobial peptides,[3,4] and chemokines to recruit and stimulate neutrophils.[5-7] The role of macrophages is to ingest bacteria and generate important inflammatory mediators for host defense. Macrophages interact with *P.aeruginosa* via multiple receptors which are present in the cell surface and by the formation of pseudopods.[1] Moreover host immune cell polymorphonuclear neutrophils provide resistance against bacterial pathogenesis through the release of toxins that kill bacteria.[20] Beside these events in response to bacterial invasion in host, macrophages and neutrophils of the host generate ROS (reactive oxygen species) and RNS (reactive nitrogen species).[1,19] Based on early studies it can be demonstrated that ROS are able to kill *P.aeruginosa* both *in vitro* and *in vivo* [1] and ROS are generated due to the presence of

nicotinamide adenine dinucleotide phosphate-reduced oxidase or NADPH-oxidase (N_{ox}) in both macrophages and neutrophils.[1] Nitric oxide (NO) is a reactive nitrogen species which is generated at the infection site by NO synthase and plays an important role in inflammation.[1] NO has antimicrobial activity against a wide variety of pathogens.[23] Therefore, based on early studies it can be suggested that in response to *P.aeruginosa* infection in host, immune cells of host including neutrophils, macrophages get activated and generate ROS and RNS like H_2O_2, hypochorous acid, NO, OH radicals and peroxynitrite to kill bacteria. Stelios *et al.* measured the concentration of exhaled H_2O_2 in bronchiectasis patients and also compared the concentration of exhaled H_2O_2 of the patients having *P.aeruginosa* colonization with the patients without *P.aeruginosa* colonization.[8] They determined that the concentration of exhaled H_2O_2 is higher in case of bronchiectasis patients (1.1 μM) compare to normal human being (0.3 μM)[8] and they also studied that bronchiectasis patients having *P.aeruginosa* infection contain significantly higher amount of H_2O_2 (1.6 μM) compare to the patients without *P.aeruginosa* infection (0.8 μM).[8] Furthermore it has been studied by Jobsis *et al.* that antibiotic treatment reduced the concentration of H_2O_2 which has been produced in a significantly higher amount in cystic fibrosis patients (during treatment H_2O_2 decreases from 0.28 μM to 0.16 μM).[9] Besides these, it has been studied by Elizabeth *et al.* that *P.aeruginosa* invades endothelial cells during colonization of the lung airways in cystic fibrosis patients and induces production of large amounts of ROS like superoxide radical, H_2O_2 and according to their study the concentration of H_2O_2 in *P.aeruginosa* infected endothelial cell is 9 μM.[10] Therefore, based on early studies it can be demonstrated that in response to *P.aeruginosa* invasion in the lung airways of cystic fibrosis patients host

immune cell like neutrophils, macrophages or endothelium generate a significantly higher amount of ROS and RNS compared to non-infected cell. So, it might be possible that 1-hydroxyphenazine (OHP) can get oxidized into its *N*-oxides either by immune cell derived H_2O_2, hypochlorite, peroxynitrite or by molecular oxygen as *P.aeruginosa* infects lung airways which creates highly aerobic atmosphere. Such an oxidation process could yield a potent cytotoxin, as described in the following paragraph.

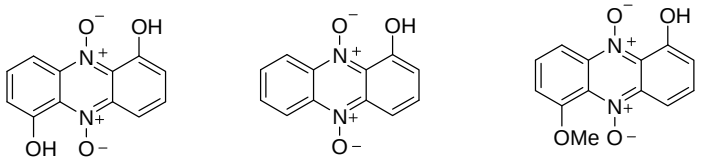

Figure 1: Examples of phenazine-*N*-oxides.[11,12,14]

Phenazine-*N*-oxides are cytotoxic and one of the reasons for their cytotoxicity is their ability to interact with DNA.[13,14,24] Early studies suggest that phenazine-*N*-oxides cause extensive DNA damage.[13,14,24] For example, myxin causes extensive degradation of cellular DNA in *E. Coli* cells.[24] Katsuyuki *et al.*[13] reported that reductive activation of phenazine-di-*N*-oxide on treatment with DTT/NADPH (by accepting one electron) produced a stable radical intermediate (**Scheme 3** in **Chapter 1)** which under aerobic and anaerobic condition generates superoxide and hydroxyl radical respectively. Both superoxide and hydroxyl radicals lead to DNA cleavage which may be one of the causes of cytotoxicity in cell. Moreover it has been studied in our lab that naturally-occurring phenazine-*N*-oxides methylmyxin and myxin caused oxidative DNA cleavage due to

redox cycling (**Scheme 1**) and the release of hydroxyl radical (**Scheme 2**), respectively, under aerobic condition in presence of one electron reducing system xanthine/xanthine oxidase or NADPH:cytochrome P450 reductase system.[14]

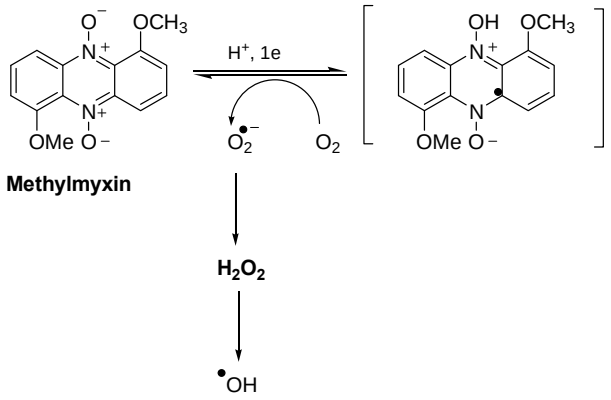

Scheme 1: Proposed mechanism of DNA damage by methylmyxin under aerobic condition.[14]

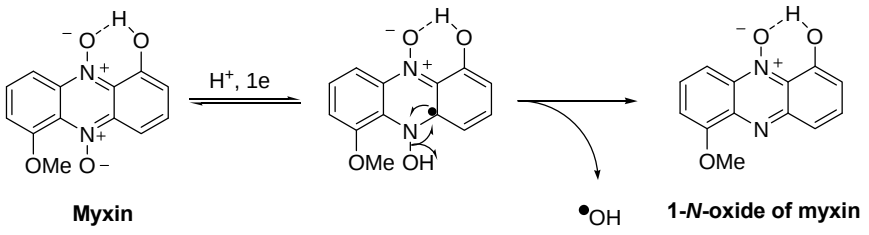

Scheme 2: Proposed mechanism of DNA damage by myxin under aerobic condition.[14]

2.2. Hypothesis: Based on early studies we hypothesized that 1-hydroxyphenazine (OHP) might be oxidized into cytotoxic phenazine-*N*-oxides by immune cell derived ROS and RNS like H_2O_2, hypohlorous acid, peroxynitrite at the infection site of the lung

airways of cystic fibrosis patients. These *N*-oxides of 1-hydroxyphenazine may, in turn, cause cell killing and tissue damage in analogy with other phenazine-*N*-oxides.

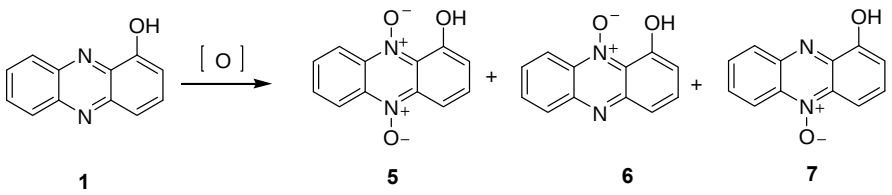

Scheme 3: Oxidation of 1-hydroxyphenazine (**1**) to its mono (**6** and **7**) and di-*N*-oxides (**5**).

The following pathway can be envisioned for cell killing properties of OHP *N*-oxides. Phenazine-di-*N*-oxide (**5**) and mono-*N*-oxides (**6, 7**) of OHP can undergo one electron enzymatic reduction by NADPH:cytochrome P450 reductase system to produce activated radical intermediate **5a** or **5b** in case of **5** and **6a** or **7a** in case of **6** and **7** respectively as shown in **Scheme 4** and **5**, which can generate reactive oxygen species (ROS) like superoxide radical, H_2O_2 and hydroxyl radical either via redox cycling or the activated radical intermediates **5a** / **5b** or **6a** / **7a** can release hydroxyl radical through homolysis of N-OH bond. Generation of ROS in cell cause various types of deleterious effects for example, oxidative DNA damage, destruction of protein, lipids and also cause cytotoxicity.[29-34]

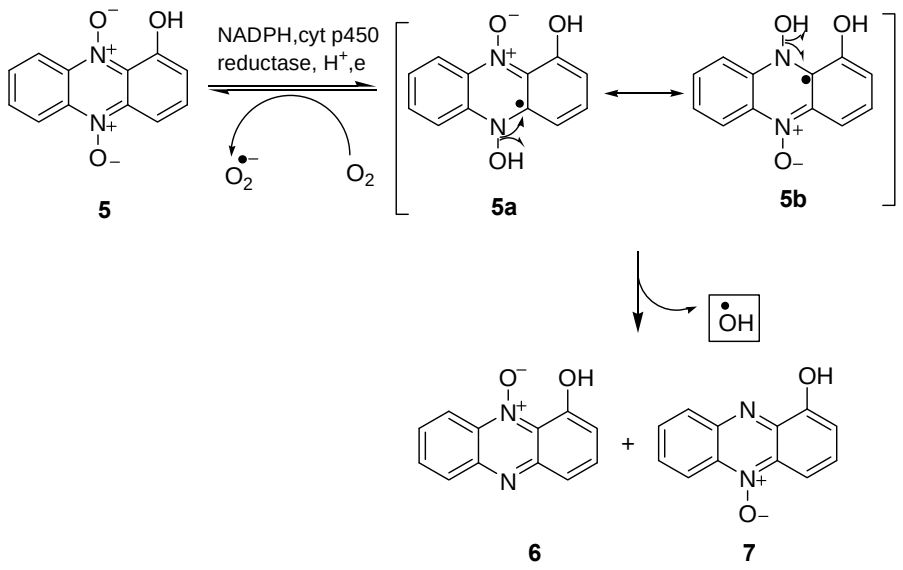

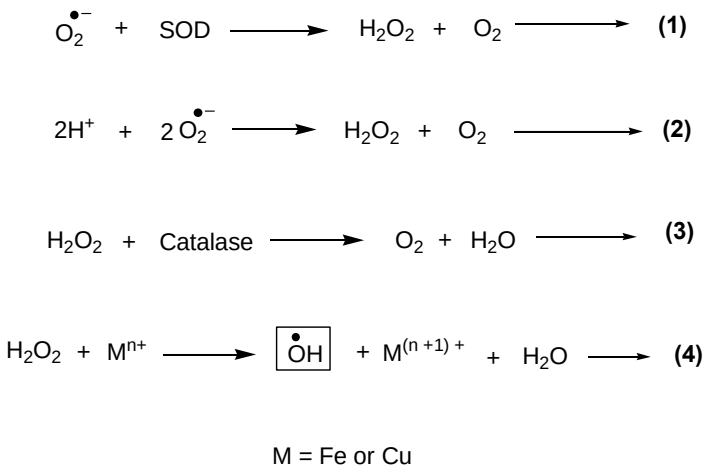

Scheme 4: Proposed mechanism for generation of ROS by of di-*N*-oxide of OHP (**5**).

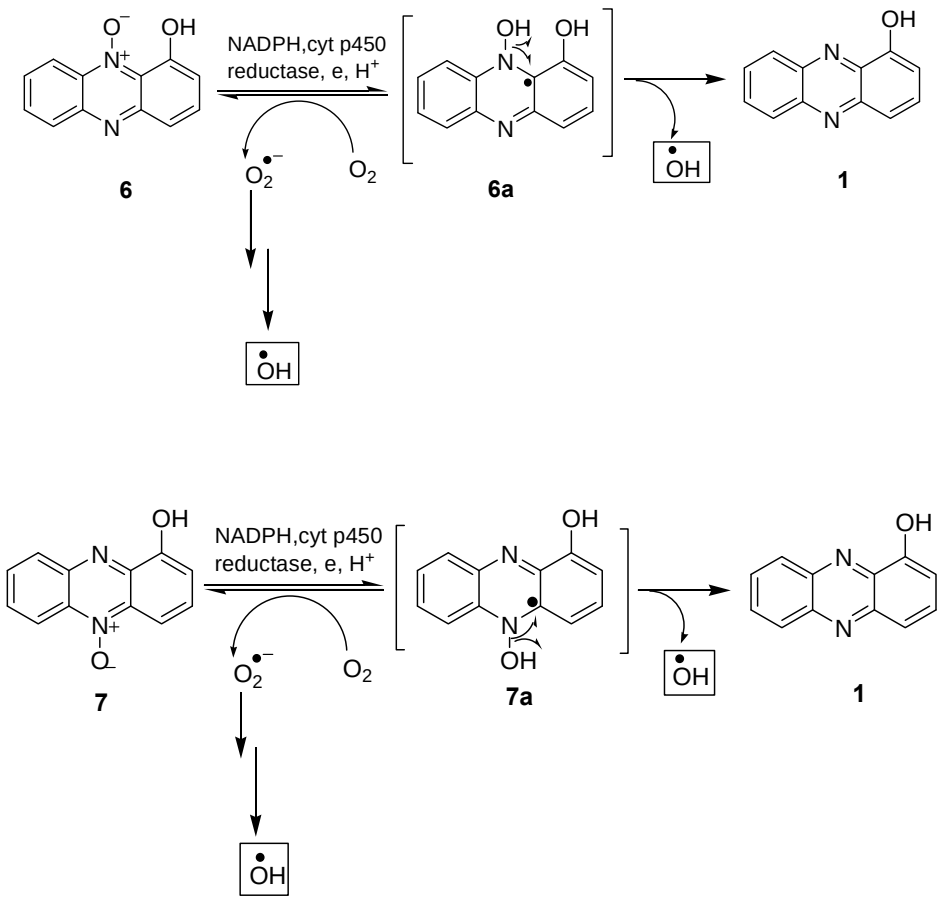

Scheme 5: Proposed mechanism for generation of ROS by mono-*N*-oxides of OHP (**6** and **7)**.

2.3. Goal: Our goal was to investigate whether 1-hydroxyphenazine (OHP) can be oxidized into cytotoxic *N*-oxides by molecular oxygen, H_2O_2, hypochlorous acid and peroxynitrite *in vitro* and to examine whether *N*-oxides of OHP can generate ROS in presence of one electron reducing enzyme. This might help explaining the virulence properties of 1-hydroxyphenazine inside the *P.aeruginosa* infected lung airways of cystic fibrosis patients. We used plasmid based DNA damage assay as a tool to elucidate the chemistry of oxidative stress caused by *N*-oxides of OHP *in vitro.*

2.4. Synthesis of di-*N*-oxide and mono-*N*-oxide of 1-hydroxyphenazine:

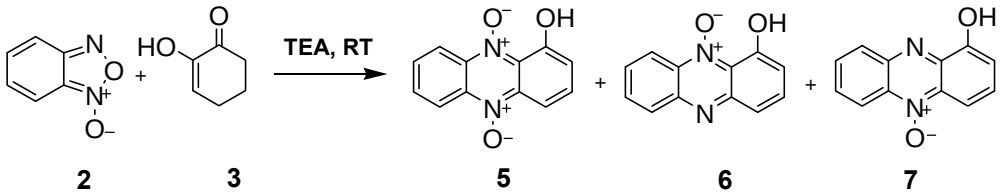

Scheme 6: Synthesis of di-*N*-oxide and mono-*N*-oxide of 1-hydroxyphenazine.[15]

N-oxides of 1-hydroxyphenazine were synthesized by the cycloaddition reaction between benzofuranoxide and 1,2-cyclohexanedione at room temperature[15] which gave a deep brown colored reaction mixture of *N*-oxides of OHP. By purifying the crude reaction mixture of *N*-oxides we obtained di-*N*-oxide of OHP **5** as major product and also obtained a minor product. Based on proton NMR, ^{13}C and high resolution mass spectroscopy we characterized the minor product as 1-hydroxyphenazine 10-*N*-oxide or up-*N*-oxide **6.** Interpretation of ^{1}H NMR for the characterization of **6** was discussed below.

The phenolic OH of **6** will form intramolecular hydrogen bonding with oxygen attached to nitrogen whereas phenolic OH of 1-hydroxyphenazine 5-*N*-oxide or down-*N*-oxide **7** wouldn't form any intramolecular hydrogen bonding (**Figure 2**).

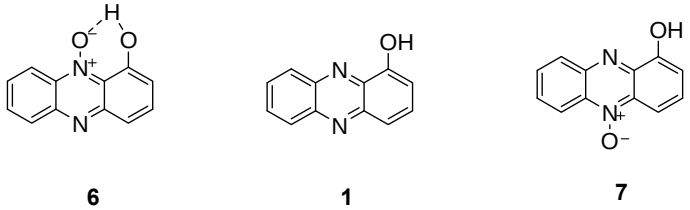

Figure 2: Structure of OHP **1** and both mono-*N*-oxides of OHP **6** and **7**.

Recent literature reveals that chemical shift of phenolic proton is shifted towards downfield significantly due to formation of intramolecular hydrogen bonding compare to the reference compounds and chemical shift of that phenolic proton is independent of concentration.[35] For example, chemical shift of phenolic proton of 2-(1-Methoxycarbonyl-2-naphthyl)methylphenol is shifted towards downfield (7.36 ppm) compare to 2-methylphenol (4.52 ppm) due to formation of 9-membered intramolecular hydrogen bonding as shown in **Figure 3** and chemical shift of phenolic proton of 2-(1-Methoxycarbonyl-2-naphthyl)methylphenol doesn't change with changing its concentration.[35]

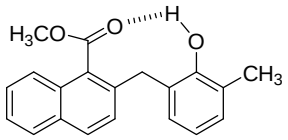

2-(1-Methoxycarbonyl-2-naphthyl)methylphenol

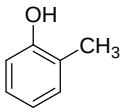

2-Methylphenol

Figure 3: Structure of 2-(1-Methoxycarnonyl-2-naphthyl)methylphenol and 2-methylphenol.[35]

We observed the chemical shift of phenolic proton of mono-*N*-oxide of 1-hydroxyphenazine is 13.785 ppm whereas chemical shift of phenolic proton corresponds to 1-hydroxyphenazine **1** is 9.3 ppm. The chemical shift of phenolic proton of mono-*N*-oxide of OHP is independent with concentration. So, based on resent literature it can be demonstrated that in case of down-*N*-oxide **7** (**Figure 2**) the phenolic proton wouldn't shift towards downfield due to absence of intramolecular hydrogen bonding and the chemical shift of the phenolic proton should be 9.3 ppm as we observed in case of 1-

hydroxyphenazine. Thus, we characterize the compound mono-*N*-oxide as up-*N*-oxide or 1-hydroxyphenazine10-*N*-oxide **6** since we observed the chemical shift of phenolic proton is 13.785 ppm and it doesn't change with changing concentration. Moreover, previous study in our lab provides information that chemical shift of phenolic proton of 1-hydroxy-6-methoxyphenazine 10-*N*-oxide or up-*N*-oxide is shifted significantly towards downfield (13.6 ppm) compare to down-*N*-oxide or 1-hydroxy-6-methoxyphenazine 5-*N*-oxide (8 ppm) (**Figure 4**).[14]

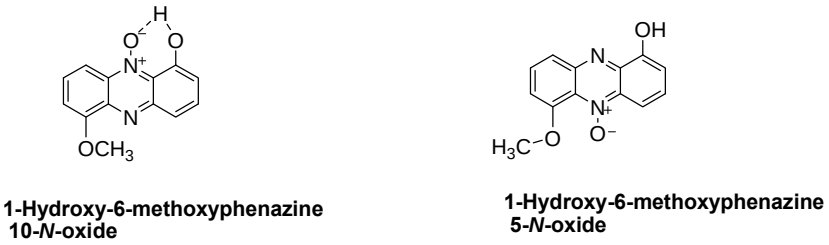

1-Hydroxy-6-methoxyphenazine 10-*N*-oxide

1-Hydroxy-6-methoxyphenazine 5-*N*-oxide

Figure 4: Structure of 1-hydroxy-6-methoxyphenazine 10-*N*-oxide and 1-hydroxy-6-methoxyphenazine 5-*N*-oxide.[14]

In addition to this, it is known that H situated beside the *N*-oxide in **8** (**Figure 5**) has chemical shift value 8.75 ppm whereas in **9** chemical shift of H situated besides heteroatom nitrogen is 8.22 ppm.[25] Accordingly in case of **6** the chemical shift of H_b and H_c should be 8.6 ppm and 8.2 ppm respectively. The chemical shift of H_a will be shifted towards up field 7.68 δ due to conjugation effect of phenolic OH which increases electron density at the *p*-position of phenolic OH containing aromatic ring through delocalization of electrons. In case of **7** the chemical shift of H_a will be shifted towards more down field as H_a is situated beside *N*-oxide which exhibit strong electron withdrawing effect and

consequently the chemical shift of H_a in **7** should be in the range of 7.9-8.3 δ. We didn't get any peak in this range in our ^{1}H NMR but we get a peak at 7.68 δ.

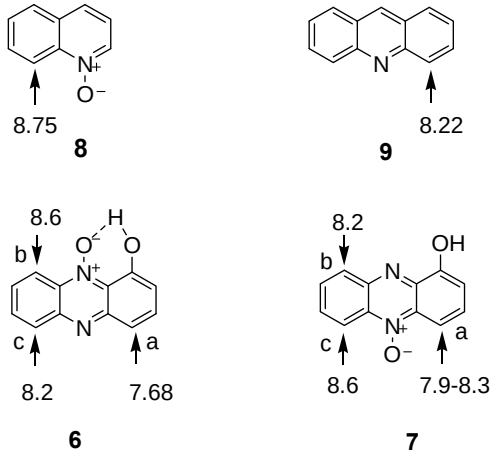

Figure 5: Chemical shift values of different protons of different types of heteroaromatics.[25,26]

So, based on the overall ^{1}H NMR interpretation and previous literatures we characterize the minor product as 1-hydroxyphenazine 10-*N*-oxide or **6**.

2.5. Aerobic DNA damage by *N*-oxides of OHP in presence of one electron reducing system:

Early studies supported that phenazine-*N*-oxides cause DNA damage in presence of one electron reducing system and DNA damage might be the one of the causes of phenazine mediated cytotoxicity in cell.[13,14] Therefore, based on early studies about phenazine-*N*-oxides we thought that, both *N*-oxides of OHP **5** & **6** might generate ROS following one electron reductive activation as described in **Scheme 4** and **5** which can cause oxidative stress. We used plasmid based DNA damage assay as readout of oxidative stress. Therefore, to examine DNA damage ability of *N*-oxides of OHP we performed a plasmid based DNA damage assay with both **6** and **5** in presence of one

electron reducing enzyme NADPH:cytochrome P450 reductase under aerobic condition.[14,16-18]

Compounds **6** or **5** was incubated with NADPH:cytochrome P450 reductase in presence of sodium phosphate buffer at 23^0C under aerobic conditions for 5-6 h and resulting DNA cleavage was examined by agarose gel. To examine whether DNA damage by both *N*-oxides of OHP was due to ROS, we performed parallel DNA damage assays in presence of SOD, catalase and desferal. The role of these additives is to destroy ROS and consequently prevent ROS mediated DNA damage as shown in **Scheme 7**.[29,36]

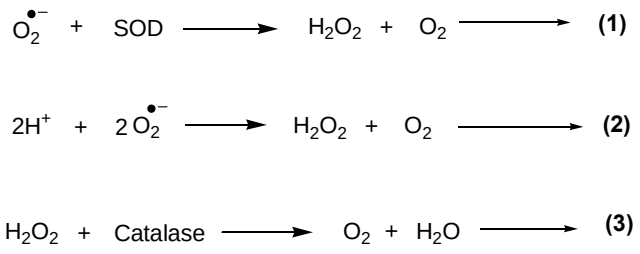

Scheme 7: Reaction of SOD and catalase with superoxide radical and hydrogen peroxide.[29,36]

A.

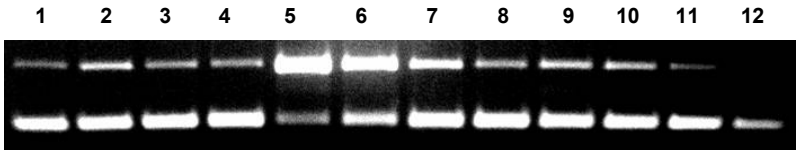

B

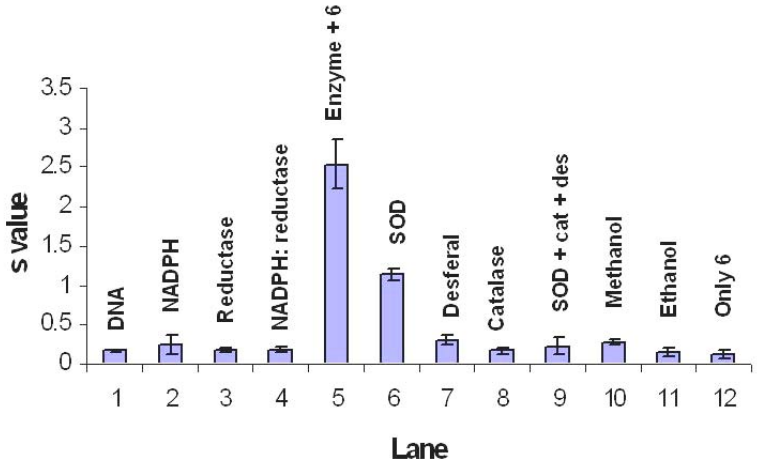

Figure 6: Cleavage of Supercoiled Plasmid DNA by mono-*N*-oxide of OHP (**6**) in the presence of NADPH:cytochrome P450 reductase as an activating system. All reactions contained DNA (1 μg) **6** (100 μM), NADPH (200 μM), cytochrome P450 reductase (0.05 U/mL), sodium phosphate buffer (50 mM, pH 7.0), in a total volume 40 μL and SOD (100 μg/mL), catalase (100 μg/mL), desferal (1 mM) as control reactions were incubated in aerobic condition at room temperature (24°C) for 5-6 hours, followed by agarose gel electrophoresis. **A.** Agarose gel: lane 1, DNA alone (S = 0.16 ± 0.01); lane 2, **6** + NADPH (200 μM) (S = 0.24 ± 0.11); lane 3, **6** + cytochrome P450 reductase (S = 0.17 ± 0.02); lane 4, NADPH (200 μM) + cytochrome P450 reductase (0.05 U/mL) (S = 0.17 ± 0.04); Lane 5-11, **6** (100 μM) + NADPH (200 μM) + reductase (0.05 U/mL , lane 5) (S = 2.54 ± 0.32); SOD (100 μg/mL, lane 6) (S = 1.14 ± 0.07); desferal (1mM, lane 7) (S = 0.29 ± 0.05); catalase (100 μg/mL, lane 8) (S = 0.16 ± 0.03); SOD+ catalase + desferal (100 μg/mL+ 100 μg/mL+ 1 mM, lane 9) (S = 0.22 ± 0.11); methanol (1 mM, lane 10) (S = 0.27 ± 0.03); ethanol (1 mM, lane 11) (S = 0.15 ± 0.04); lane 12 **6** only (S = 0.13 ± 0.05). **B.** Bar graph of S values of all reaction lanes. The values, S, represent the mean number of strand breaks per plasmid molecule and were calculated by using the equation $S = -\ln f_1$ where f_1 is the fraction of plasmid molecule as form I.

A.

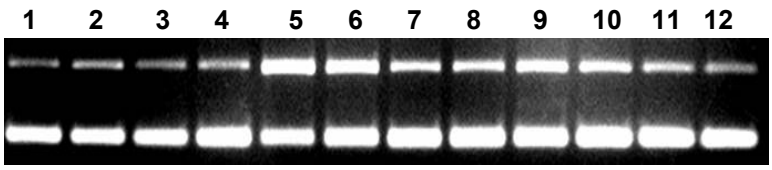

B.

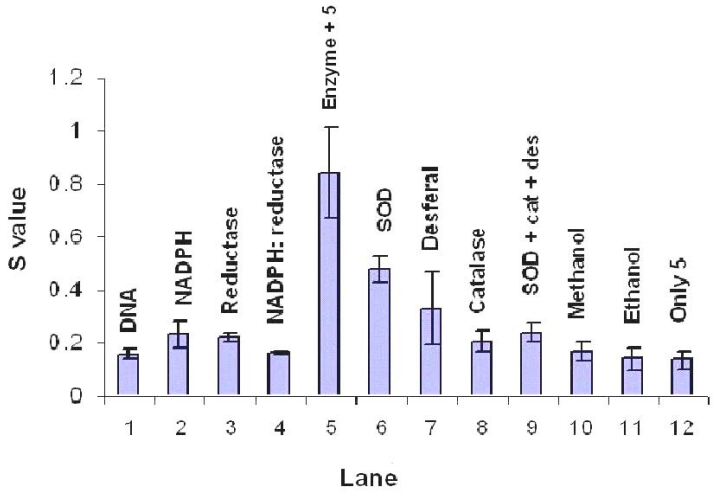

Figure 7: Cleavage of Supercoiled Plasmid DNA by di-*N*-oxide of OHP (**5**) in the presence of NADPH:cytochrome P450 reductase as an activating system. All reactions contained DNA (1 μg) **5** (100 μM), NADPH (200 μM), cytochrome P450 reductase (0.05 U/mL), sodium phosphate buffer (50 mM, pH 7.0), in a total volume 40 μL and SOD (100 μg/mL), catalase (100 μg/mL), desferal (1 mM) as control reactions were incubated in aerobic condition at room temperature (24^{o}C) for 5-6 hours, followed by agarose gel electrophoresis. **A.** Agarose gel: lane 1, DNA alone (S = 0.16 ± 0.02); lane 2, **5** + NADPH (200 μM) (S = 0.23 ± 0.05); lane 3, **5** + cytochrome P450 reductase (S = 0.22 ± 0.02); lane 4, NADPH (200 μM) + cytochrome P450 reductase (0.05 U/mL) (S = 0.16 ± 0.00); Lane 5-11, **5** (100 μM) + NADPH (200 μM) + reductase (0.05 U/mL , lane 5) (S = 0.84 ± 0.17); SOD (100 μg/mL, lane 6) (S = 0.48± 0.05); desferal (1mM, lane 7) (S = 0.33 ± 0.14); catalase (100 μg/mL, lane 8) (S = 0.21 ± 0.04); SOD+ catalase + desferal (100 μg/mL+ 100 μg/mL+ 1 mM, lane 9) (S = 0.24 ± 0.03); methanol (1 mM, lane 10) (S = 0.17 ± 0.04); ethanol (1 mM, lane 11) (S = 0.14 ± 0.04); lane 12 **5** only (S = 0.14 ± 0.03). **B.** Bar graph of S-values of all reaction lanes. The values, S, represent the mean number of strand breaks per plasmid molecule and were calculated by using the equation S = -ln f_1 where f_1 is the fraction of plasmid molecule as form I.

We found that both *N*-oxides of OHP **5** and **6** caused DNA damage in presence of NADPH:cytochrome P450 reductase system. These *N*-oxides didn't damage DNA alone and also didn't damage DNA in presence of either NADPH or cytochrome P450

reductase. Moreover we observed that DNA damage by both **5** and **6** was inhibited completely in presence of SOD, catalase and desferal which lead to the conclusion that both *N*-oxides of OHP caused DNA damage due to redox cycling. Furthermore, to examine whether DNA damage was radical mediated, we also performed plasmid based DNA damage assay with both **5** and **6** in presence of radical scavenger methanol and ethanol. We noticed that in both cases (***Figure 6 & 7*** lanes10 & 11) DNA cleavage was inhibited in presence of radical scavengers which proved that DNA cleavage by *N*-oxides of OHP was radical mediated.

Therefore, from this study it can be clearly demonstrated that both mono-*N*-oxide **6** and di-*N*-oxide **5** of OHP caused DNA damage due to redox cycling in presence of one electron reducing enzyme system NADPH:cytochrome P450 reductase and this DNA damage was radical mediated. As both *N*-oxides generates superoxide radical, H_2O_2 and OH radical under aerobic condition due to redox cycling it provides indirect evidence that both *N*-oxides of OHP can generate ROS inside the cell and generation of ROS leads to cytotoxicity in cell.

2.6. Concentration dependent DNA damage by *N*-oxides of OHP:

Our previous study demonstrated that *N*-oxides of OHP caused DNA damage due to redox cycling in presence of one electron reducing system and DNA damage was radical mediated. After that we performed concentration dependent DNA damage assay by both *N*-oxides of OHP in presence of NADPH:cytochrome P450 reductase system.[14,16-18] In a typical plasmid based DNA damage assay, various concentrations of

either **5** or **6** were incubated with NADPH:cytochrome P450 reductase system under physiological pH at 23^{o}C under aerobic condition for 5-6 hours

A

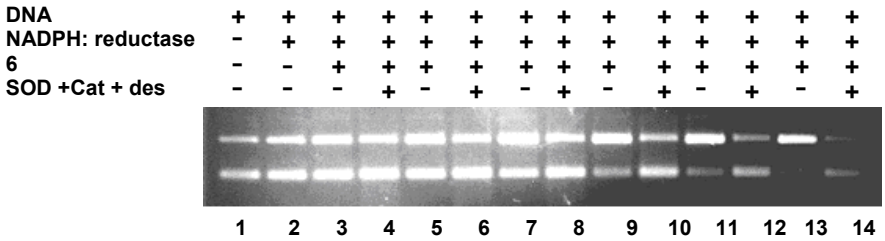

.

B.

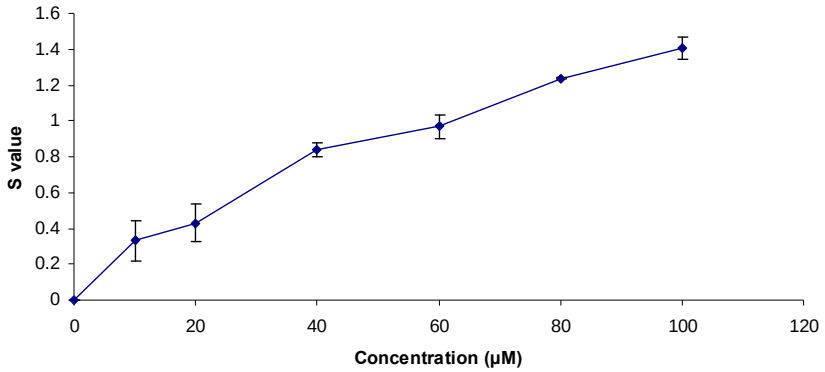

Figure 8: DNA cleavage efficiency by various concentrations of mono-*N*-oxide of OHP, **6** in the presence of NADPH:cytochrome P450 reductase system. Supercoiled plasmid DNA (1 μg) was incubated with **6** (10-100 μM), NADPH (200 μM), cytochrome P450 reductase (0.05 U/mL), sodium phosphate buffer (50 mM, pH 7.0), and with SOD (100 μg/mL), catalase (100 μg/mL), desferal (1 mM) as control reactions in a total volume 40 μL under aerobic condition at room temperature (24^{o}C) for 5-6 hours, followed by agarose gel electrophoresis. **A.** Agarose gel: lane 1, DNA alone; lane 2, NADPH (200 μM) + reductase (0.05 U/mL); (lane 3, 5, 7, 9,11,13), **6** (10-100 μM)+ NADPH (200 μM) + reductase (0.05 U/mL); lane 3 (10 μM **6**, S = 0.33 ± 0.11); lane 5 (20 μM **6**, S = 0.43 ± 0.10); lane 7 (40 μM **6,** S = 0.84 ± 0.04); lane 9 (60 μM **6,** S = 0.97 ± 0.06); lane 11 (80 μM **6,** S = 1.24 ± 0.00); lane 13 (100 μM **6,** S = 1.41 ± 0.06); (lane 4, 6, 8, 10, 12, 14), **6** (10-100 μM) + NADPH (200 μM) + reductase (0.05 U/mL) + SOD (100 μg/mL) + catalase (100 μg/mL) + desferal (1mM). **B.** Plot of S value vs. various concentrations of **6**. The values, S, represent the mean number of strand breaks per plasmid molecule and were calculated by using the equation S = -ln f_1 where f_1 is the fraction of plasmid molecule as form I. S values of different concentration of **6** were obtained by calculating background cleavage subtraction.

A.

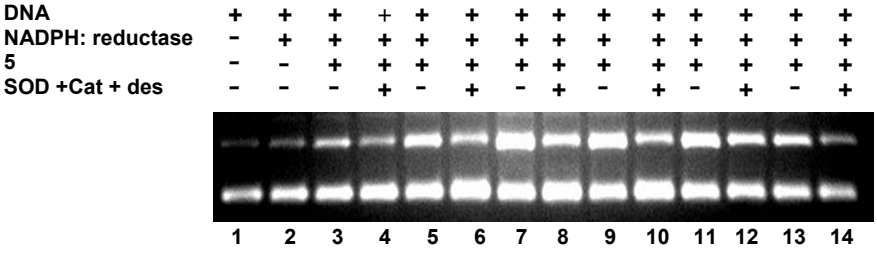

B.

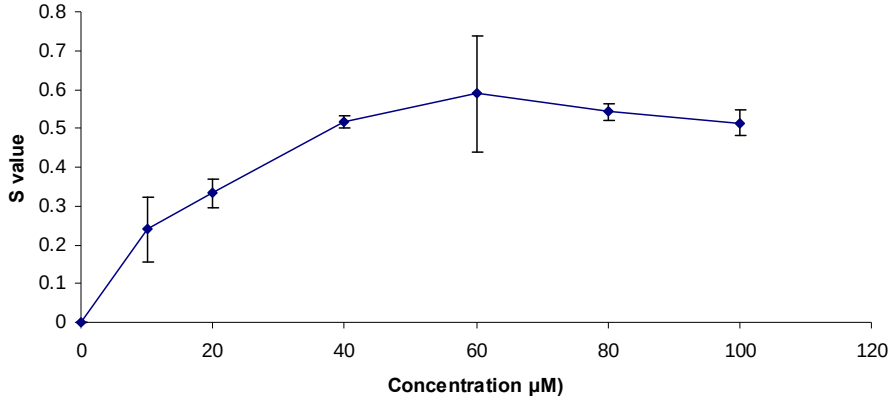

Figure 9: DNA cleavage efficiency by various concentrations of di-*N*-oxide of OHP, **5** in the presence of NADPH:cytochrome P450 reductase system. Supercoiled plasmid DNA (1 µg) was incubated with **5** (10-100 µM), NADPH (200 µM), cytochrome P450 reductase (0.05 U/mL), sodium phosphate buffer (50 mM, pH 7.0), and with SOD (100 µg/mL), catalase (100 µg/mL), desferal (1 mM) as control reactions in a total volume 40 µL under aerobic condition at room temperature (24^{o}C) for 5-6 hours, followed by agarose gel electrophoresis. **A.** Agarose gel: lane 1, DNA alone; lane 2, NADPH (200 µM) + reductase (0.05 U/mL); (lane 3, 5, 7, 9,11,13), **5** (10-100 µM)+ NADPH (200 µM) + reductase (0.05 U/mL); lane 3 (10 µM **5**, S = 0.24 ± 0.08); lane 5 (20 µM **5**, S = 0.33 ± 0.04); lane 7 (40 µM **5,** S = 0.52 ± 0.01); lane 9 (60 µM **5,** S = 0.59 ± 0.15); lane 11 (80 µM **5,** S = 0.54 ± 0.02); lane 13 (100 µM **5,** S = 0.51 ± 0.03); (lane 4, 6, 8, 10, 12, 14), **5** (10-100 µM) + NADPH (200 µM) + reductase (0.05 U/mL) + SOD (100 µg/mL) + catalase (100 µg/mL) + desferal (1mM). **B.** Plot of S value vs. various concentration of OHP. The values, S, represent the mean number of strand breaks per plasmid molecule and were calculated by using the equation $S = -\ln f_1$ where f_1 is the fraction of plasmid molecule as form I. S values of different concentration of **5** were obtained by calculating background cleavage subtraction.

These results clearly demonstrated that both mono-*N*-oxide **6** and di-*N*-oxide of OHP **5** lead to DNA damage in presence of NADPH:cytochrome P450 reductase via a

redox cycling mechanism involving production of superoxide radical and the yield of DNA damage was concentration dependent.

2.7. DNA damage efficiency of *N*-oxides of OHP was comparable with redox cycling agent menadione:

Menadione is a well known redox-cycling agent which causes DNA damage due to redox cycling.[21,22] Our previous studies suggested that DNA damage by *N*-oxides of OHP is due to redox cycling. So, we compared DNA damage efficiency of the *N*-oxides of OHP with menadione. Early studies suggest that TPZ is a hypoxia selective anti cancer drug which causes extensive DNA damage under anaerobic condition whereas in presence of molecular oxygen TPZ does redox cycling that also leads to DNA damage in a lesser extent.[14,16-18] So, we also compared DNA damage efficiency of *N*-oxides of OHP with TPZ in addition to menadione.

A.

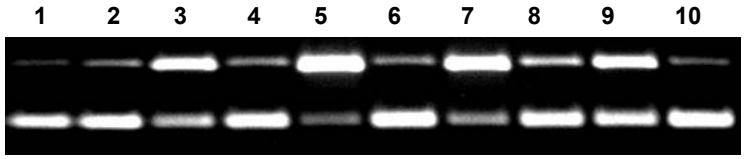

B.

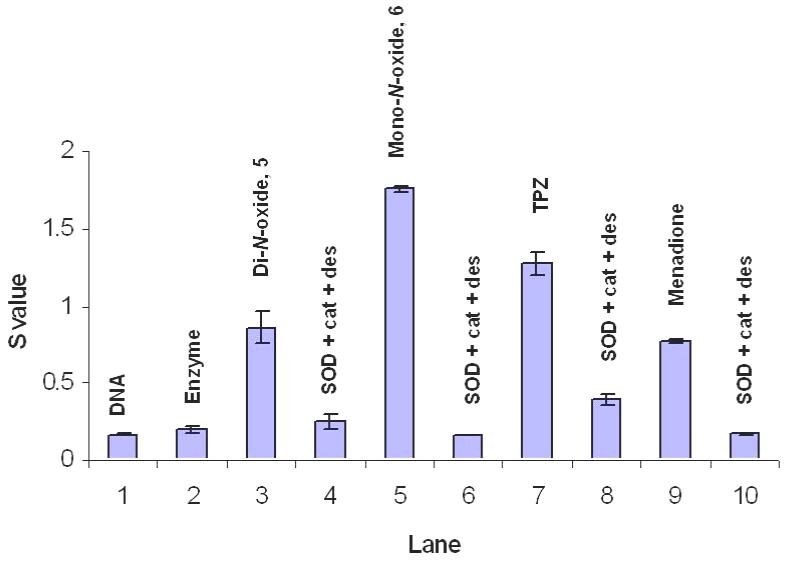

Figure 10: Comparison of DNA cleavage by *N*-oxides of OHP, **5** & **6** with menadione a well known redox cycling agent and with TPZ in presence of NADPH and cytochrome P450 reductase. Supercoiled plasmid DNA (1 μg) was incubated with **5** (100 μM) or **6** (100 μM) or menadione (100 μM) or TPZ (100 μM) in presence of NADPH (200 μM), cytochrome P450 reductase (0.05 U/mL) and with SOD (100 μg/mL), catalase (100 μg/mL), desferal (1 mM) as control reactions in a total volume 40 μL under aerobic condition at room temperature (24^{o}C) for 5-6 hours, followed by agarose gel electrophoresis. **A.** Agarose gel: lane 1, DNA alone (S = 0.17 ± 0.00); lane 2, NADPH (200 μM) + reductase (0.05 U/mL) (S = 0.20 ± 0.02); lane 3, **5** (100 μM) + NADPH (200 μM) + reductase (0.05 U/mL) (S = 0.85 ± 0.09); lane 5, **6** (100 μM) + NADPH (200 μM) + reductase (0.05 U/mL) (S = 1.75 ± 0.02); lane 7, **TPZ** (100 μM) + NADPH (200 μM) + reductase (0.05 U/mL) (S = 1.27 ± 0.08); lane 9, **menadione** (100 μM) + NADPH (200 μM) + reductase (0.05 U/mL) (S = 0.77 ± 0.01); lanes 4 (S = 0.26 ± 0.04); lane 6 (S = 0.16 ± 0.00); lane 8 (S = 0.4 ± 0.03); and lane 10 (S = 0.17 ± 0.00) were control lanes (control: 1 mM desferal + 100 μg/mL SOD + 100 μg/mL catalase). **B.** Bar graph of comparison of DNA damage of *N*-oxides of OHP with TPZ and menadione. The values, S, represent the mean number of strand breaks per plasmid molecule and were calculated by using the equation S = -ln f_1 where f_1 is the fraction of plasmid molecule as form I.

These experiments reveal that DNA cleavage efficiency of *N*-oxides of OHP is comparable with well known redox cycling agent menadione.

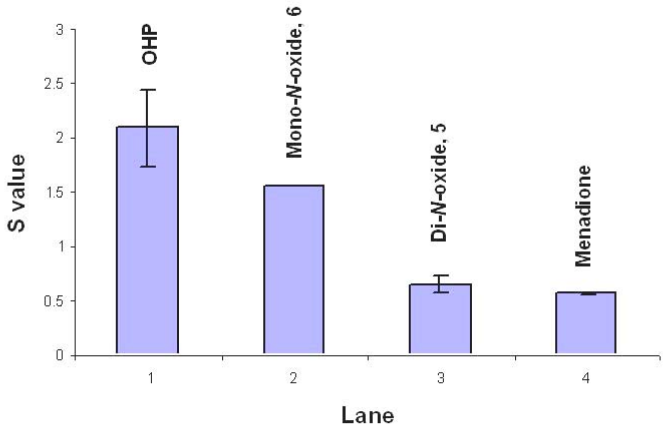

Figure 11: Comparative study of DNA cleavage efficiency between OHP and its *N*-oxides with menadione. OHP or its *N*-oxides or menadione were incubated with NADPH:cytochrome P450 reductase system at 23^{o}C under aerobic condition for 5-6 h. Lane 1 OHP **1** (100 μM) (S= 2.09 ± 0.35); lane 2 mono-*N*-oxide of OHP **6** (100 μM) (S= 1.55 ± 0.00); lane 3 di-*N*-oxide of OHP **5** (100 μM) (S= 0.65 ± 0.07); lane 4 menadione (100 μM) (S= 0.56 ± 0.01). The values, S, represent the mean number of strand breaks per plasmid molecule and were calculated by using the equation S = -ln f_1 where f_1 is the fraction of plasmid molecule as form I.

We observed that DNA damage efficiency of OHP is highest and DNA damage efficiency is decreased in this order OHP > mono-*N*-oxide **6**> di-*N*-oxide of OHP **5** as shown in **Figure 11**. DNA damage efficiency of OHP and its *N*-oxides is comparable with menadione.

2.8. Metabolism study of both mono-*N*-oxide and di-*N*-oxide of OHP:

If *N*-oxides of OHP produce ROS like superoxide radical, hydroxyl radical via redox cycling, then they act as catalysts that remain unchanged during the reaction

process. Accordingly, we followed the fate of these molecules during ROS-producing reaction. We incubated **6** or **5** with NADPH:cytochrome P450 reductase at pH 7 buffer for overnight and then analyzed the reaction mixture by HPLC and LC/MS.

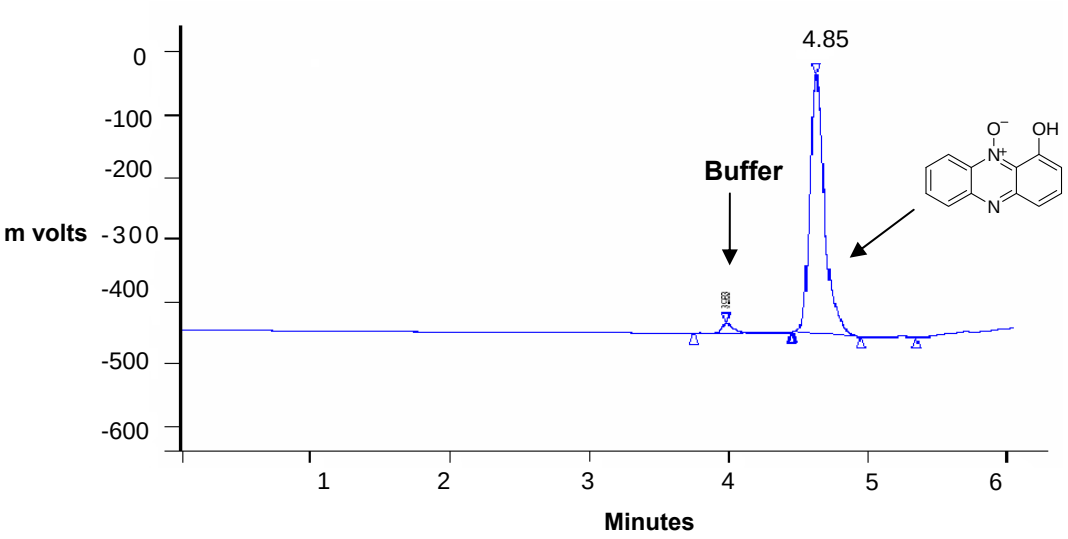

Figure 12: Metabolism study of mono-*N*-oxide of 1-hydroxyphenazine (**6**) results in only **6**. A 200 µL solution of **6** was incubated with NADPH:cytochrome P450 reductase at room temperature (24°C) under aerobic condition for 12 hours followed by HPLC analysis.

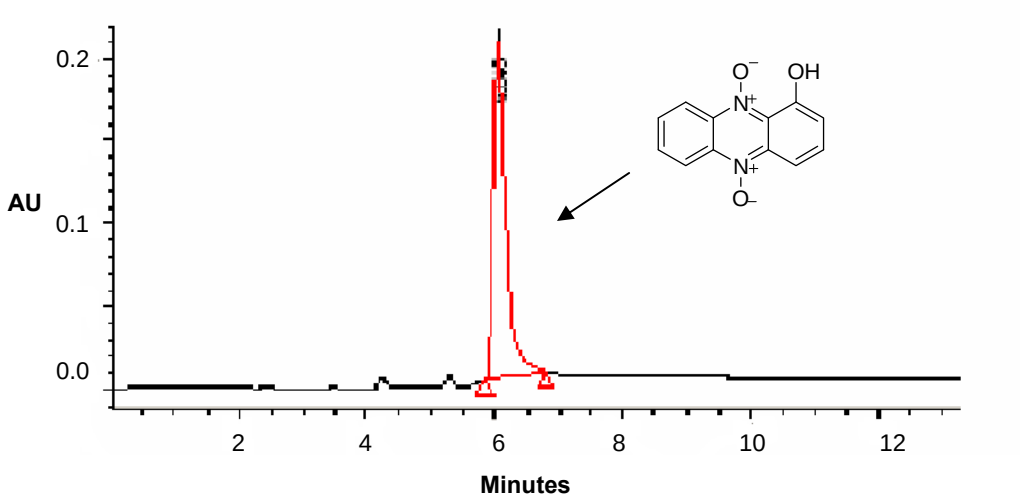

Figure 13: Metabolism study of di-*N*-oxide of 1-hydroxyphenazine (**5**) detects **5**. A 200 µL solution of **5** was incubated with NADPH:cytochrome P450 reductase at room temperature (24°C) under aerobic condition for 12 hours followed by HPLC analysis.

In both cases HPLC analysis of the reaction mixture containing either **6** or **5** with NADPH:cytochrome P450 reductase (***Figure 12 & 13***) revealed that the compounds are not extensively degraded during the reaction. The identity of peak **6** and **5** was confirmed by co-injecting with the authentic standards and by LC/MS. LC/MS analysis was performed by using TSQ7000 triple-quadruple mass spectrometer where we used same HPLC method which was used in HPLC analysis to detect the metabolites and used APCI-MS (atmospheric pressure chemical ionization) operating in positive ion mode to determine the mass (m/z = M+H) of the metabolites.

LC/APCI-MS analysis determined only 1-hydroxyphenazine 5,10-di-*N*-oxide **5** and 1-hydroxyphenazine 10-*N*-oxide **6** but didn't detect any deoxygenated products of *N*-oxides.

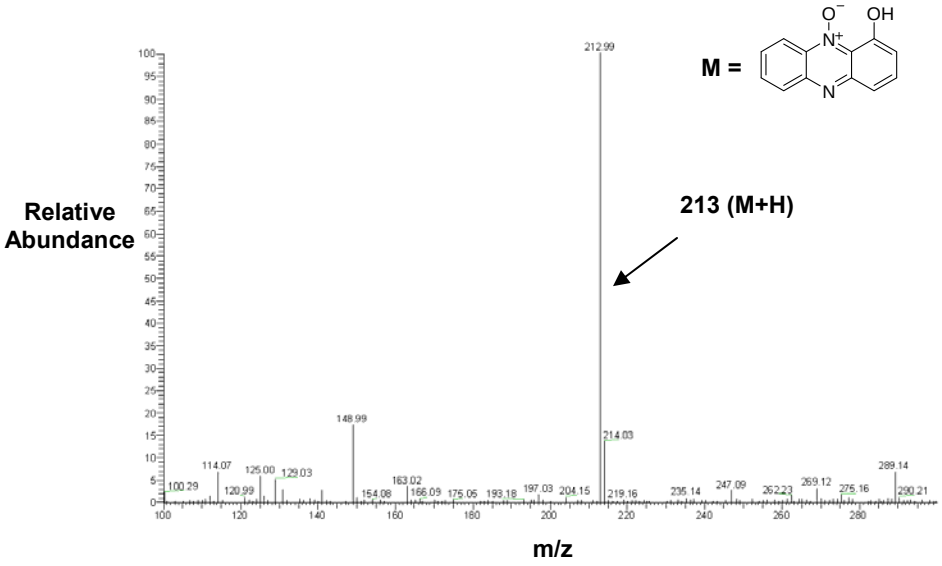

Figure 14: Identification of mono-*N*-oxide of 1-hydroxyphenazine (**6**) by LCMS analysis where the compound was detected by using normal phase HPLC method and mass of the peak (m/z = 213) of retention time 4.80 minutes was determined by using APCI positive ion mode. The mass spectrum shows M+H ion of **6** at m/z 213 obtained using LC-APCI/MS operating in the positive ion mode. A 200 µL solution of sodium phosphate buffer (pH 7.0, 50 mM), **6** (100 µM) was incubated with NADPH (500µM) and cytochrome P450 reductase (0.05 U/mL) at room temperature (24^{o}C) under aerobic condition for 12 hours followed by LC/MS analysis.

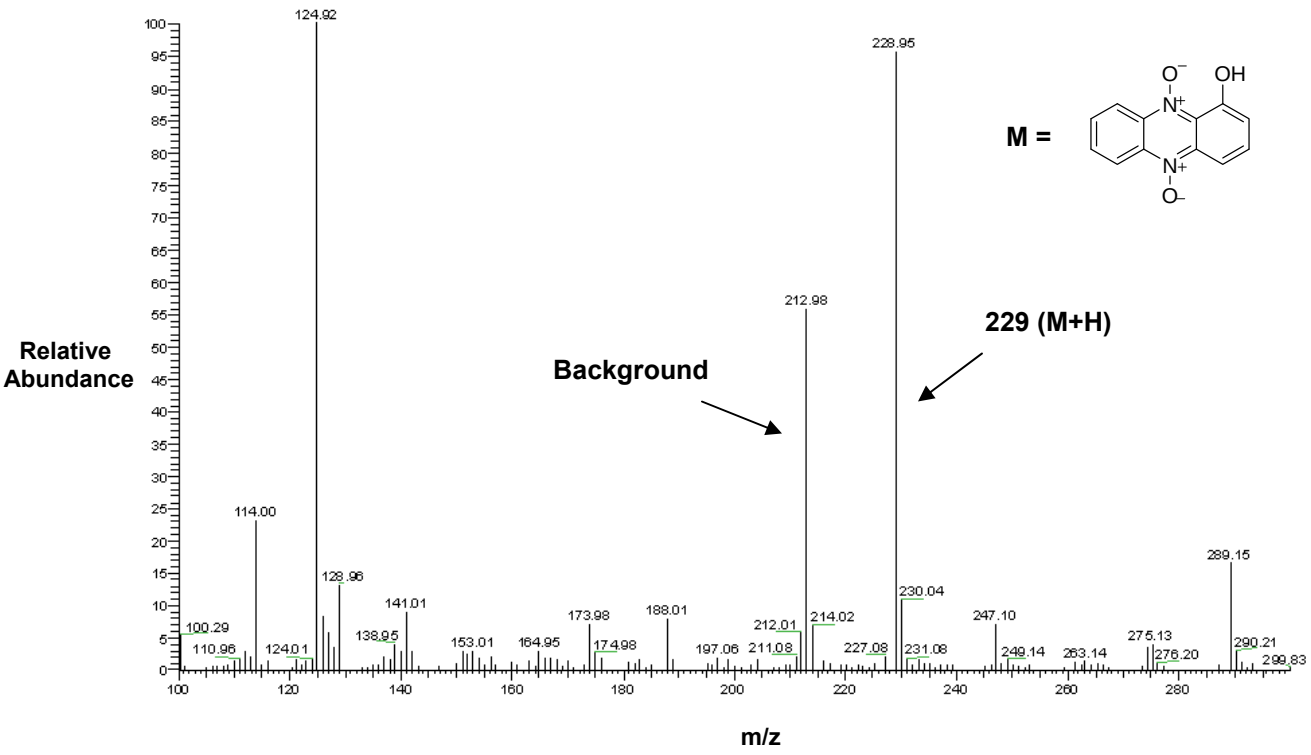

Figure 15: Identification of di-*N*-oxide of 1-hydroxyphenazine (**5**) by LCMS analysis where the compound was detected by using normal phase HPLC method and mass of the peak (m/z = 229) of retention time 5.85 minutes was determined by using APCI positive ion mode. The mass spectrum shows M+H ion of **5** at m/z 229 obtained using LC-APCI/MS operating in the positive ion mode. A 200 µL solution of sodium phosphate buffer (pH 7.0, 50 mM), **5** (100 µM) was incubated with NADPH (500µM) and cytochrome P450 reductase (0.05 U/mL) at room temperature (24^{o}C) under aerobic condition for 12 hours followed by LC/MS analysis.

Therefore both HPLC and LCMS analysis supported redox cycling mechanism of both *N*-oxides of OHP as shown in **Scheme 8** and **9**

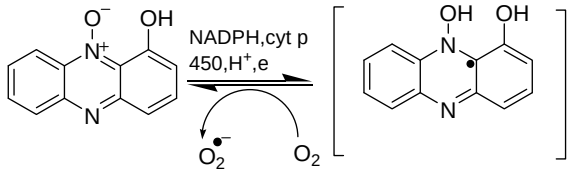

Scheme 8: Redox cycling mechanism of mono-*N*-oxide of OHP **6**.

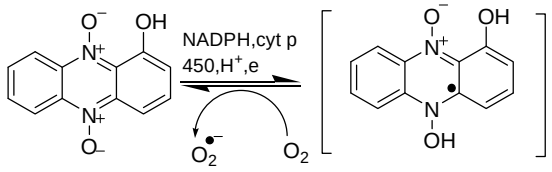

Scheme 9: Redox cycling mechanism of di-*N*-oxide of OHP **5**.

2.9. Oxidation of 1-hydroxyphenazine (OHP) into its di-*N*-oxide and mono-*N*-oxide:

We suggest that OHP might oxidize into its *N*-oxides by infected immune cell derived H_2O_2, peroxynitrite and hypochlorous acid. To examine our hypothesis we performed *in vitro* study where we carried out an oxidation reaction of OHP with molecular oxygen, H_2O_2 and peroxynitrite for qualitative detection of any *N*-oxides products of OHP (**Scheme 3**). In a typical assay OHP was incubated with H_2O_2 at pH 7 buffer at 23^{o}C and then we extracted the reaction mixture into 50:50 ethyl acetate: hexane mixture and next injected into HPLC. The reaction mixture was analyzed by normal phase HPLC eluted with 0.5% acetic acid in ethyl acetate and heptane.

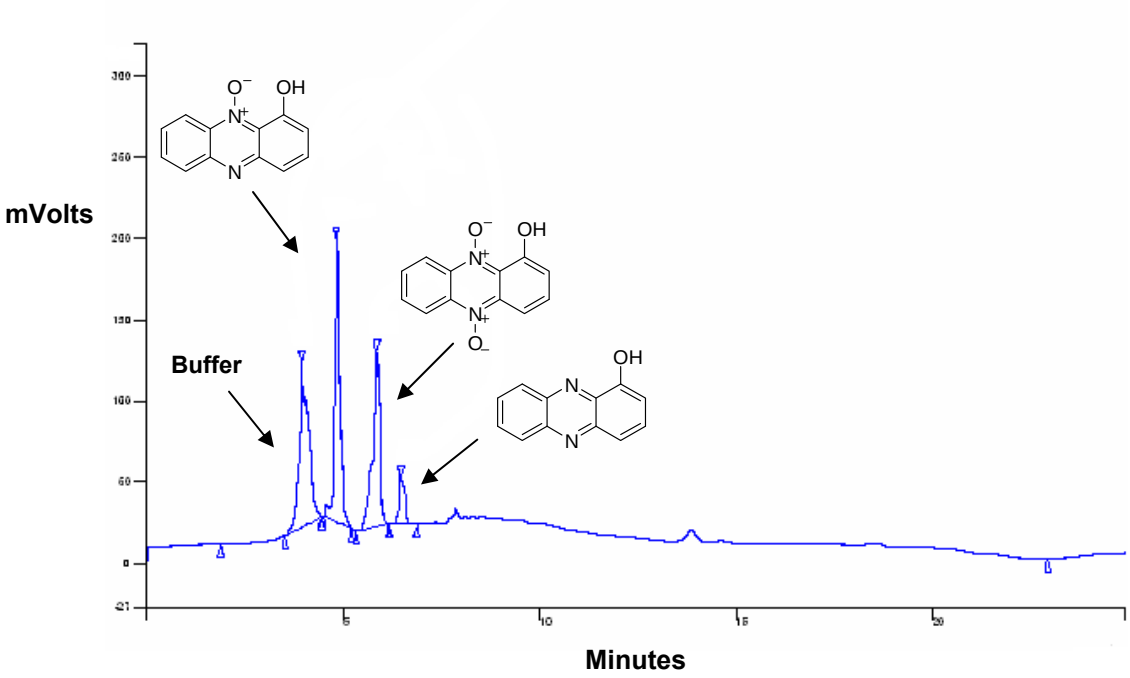

Figure 16: HPLC chromatogram for the oxidation reaction of OHP by H_2O_2. OHP was oxidized into its *N*-oxides **5** and **6**. OHP (500 µM) was incubated with H_2O_2 (8.5 mM) at pH 7 buffer at 23°C under aerobic condition and then the reaction mixture was analyzed by normal phase HPLC.

We found that OHP is oxidized into both *N*-oxides **5** and **6** by total 18 day's incubation with H_2O_2 at 23°C under aerobic condition and these oxidized products were confirmed by co-injecting the reaction mixture with authentic standards. The mono-*N*-oxide of OHP **6** was the major product whereas di-*N*-oxide **5** was a minor product. Thus, to understand the reasons of getting mono-*N*-oxide as a major product and di-*N*-oxide as a minor product we performed oxidation reaction between OHP and H_2O_2 with two control reactions. In a typical assay, OHP was incubated with H_2O_2 in presence of sodium phosphate buffer at room temperature for 17 hours as alongside control reactions containing a) mono-*N*-oxide of OHP **6** + H_2O_2, b) di-*N*-oxide of OHP **5** + H_2O_2. Next the reaction mixtures including controls were analyzed by HPLC. We found that OHP was

oxidized into mono-*N*-oxide **6** whereas the mono-*N*-oxide **6** didn't oxidize into di-*N*-oxide **5**. Moreover, we noticed that di-*N*-oxide didn't degrade in presence of H_2O_2. Based on these observations we propose the following pathway for the formation of **5** and **6**.

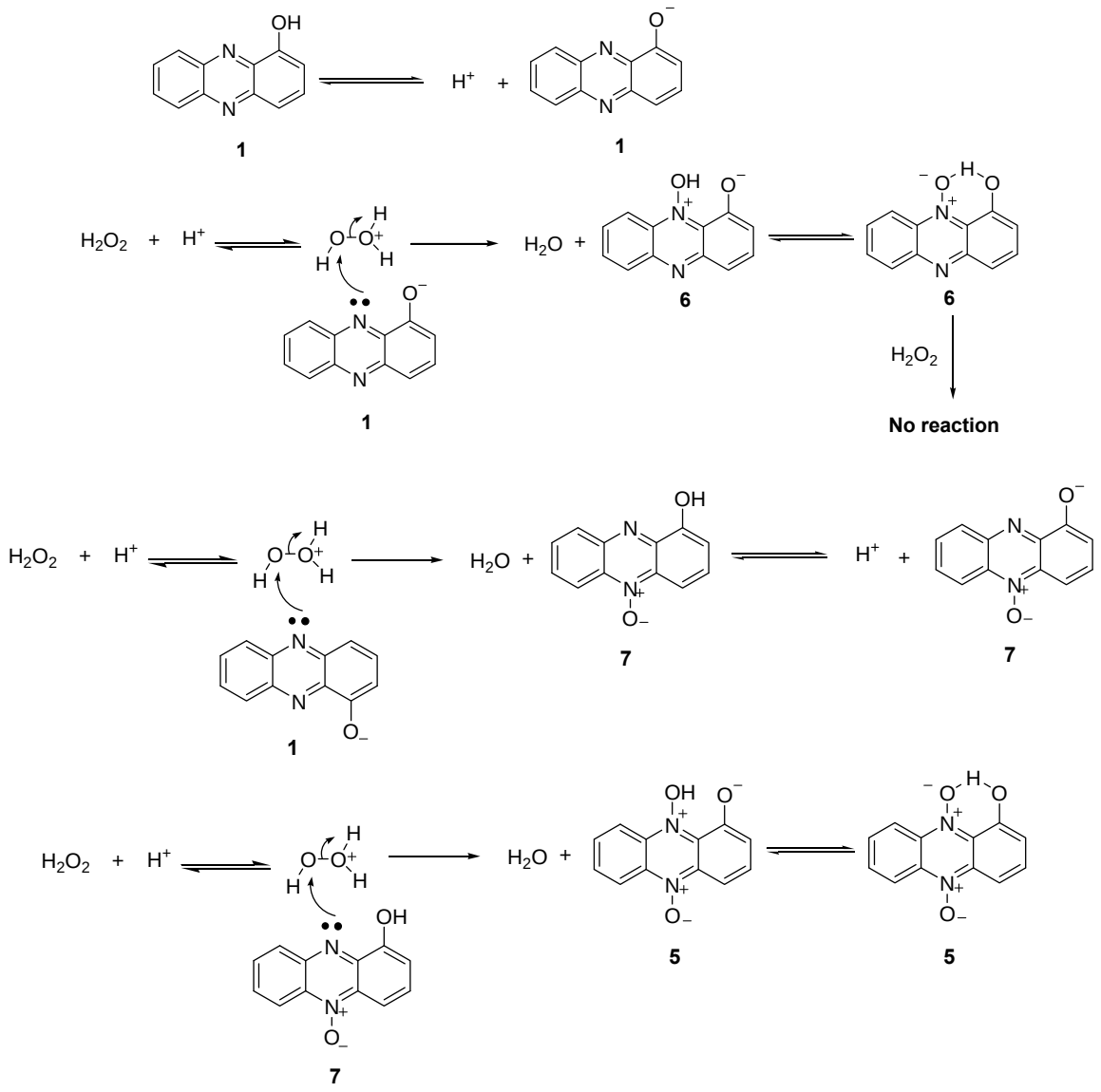

Scheme 10: Proposed pathway for formation of **5** and **6** by reaction of OHP with H_2O_2.

Thus, on the basis of our results, it can be suggested that both mono-*N*-oxides **6** and **7** are produced by oxidation of OHP with H_2O_2. But evidently only **7** converts further into the di-*N*-oxide of OHP **5**.

In addition to H_2O_2 we performed oxidation reaction of OHP with molecular oxygen and peroxynitrite for qualitative detection of any *N*-oxidized products of OHP under physiological condition. When OHP (***Figure 17 and 18***) was incubated at 37°C at pH 7.5 sodium phosphate buffers for 24 h it was found that OHP was oxidized into its mono-*N*-oxide **6** and the oxidized product was identified by observation of the mass of M+H ion in LC/MS in APCI positive ion mode.

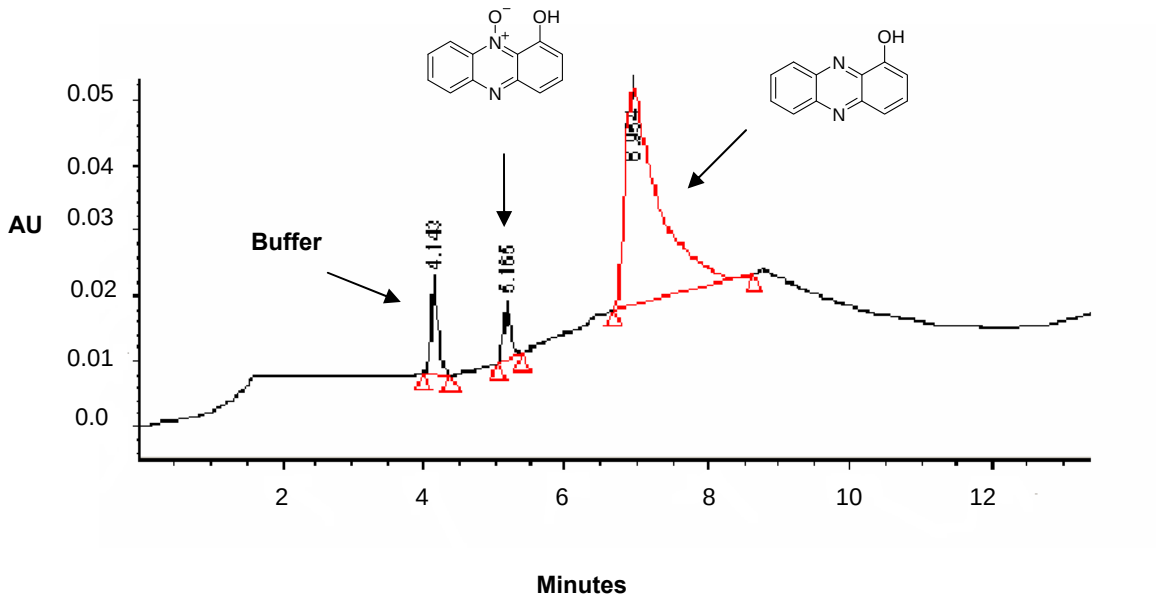

Figure 17: HPLC chromatogram for the oxidation reaction of OHP by oxygen where OHP was oxidized into mono-*N*-oxide **6** by reaction with molecular oxygen. OHP (500 µM) was incubated at pH 7.5 buffer at 37°C under aerobic condition for 24 hours and then the reaction mixture was analyzed by normal phase HPLC (eluting solvent: 0.5% acetic acid in ethyl acetate and heptane).

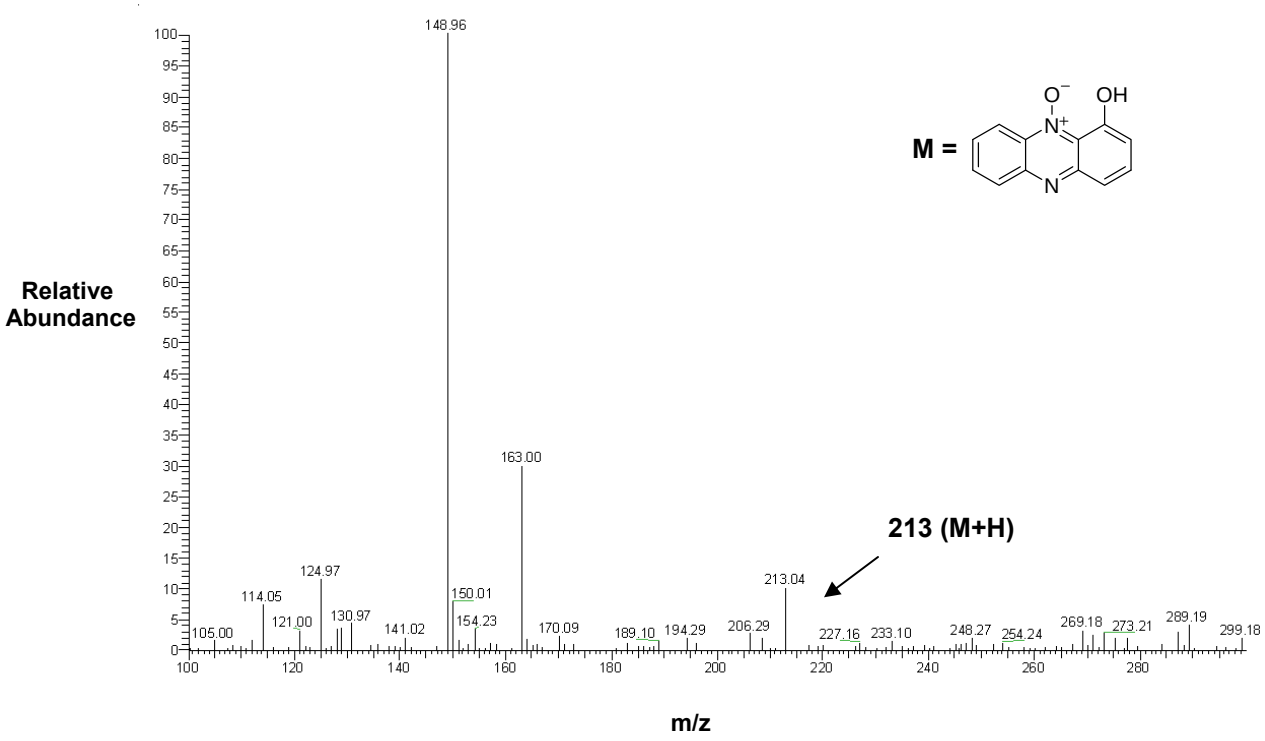

Figure 18: Identification of mono-*N*-oxide of OHP **6** by LC/MS analysis where the compound was detected by using normal phase HPLC method and mass of the peak (m/z = 213) of retention time 4.9 minutes was determined by using APCI positive ion mode. The mass spectrum shows M+H ion of **6** at m/z 213 obtained using LC-APCI/MS operating in the positive ion mode.

Angeli's salt is known to produce peroxynitrite by undergoing decomposition at 37^{o}C at pH 7.5.[27,28] So, to investigate whether OHP can be oxidized by peroxynitrite we incubated OHP with Angeli's salt [27,28] in presence of sodium phosphate buffers at pH 7.5 at 37^{O}C for 4:30h- 24 hours (***Figure 19 and 20***) followed by HPLC and LCMS analysis in a similar way as described above. Both HPLC and LC/MS analysis detected time dependent formation of mono-*N*-oxide **6**.

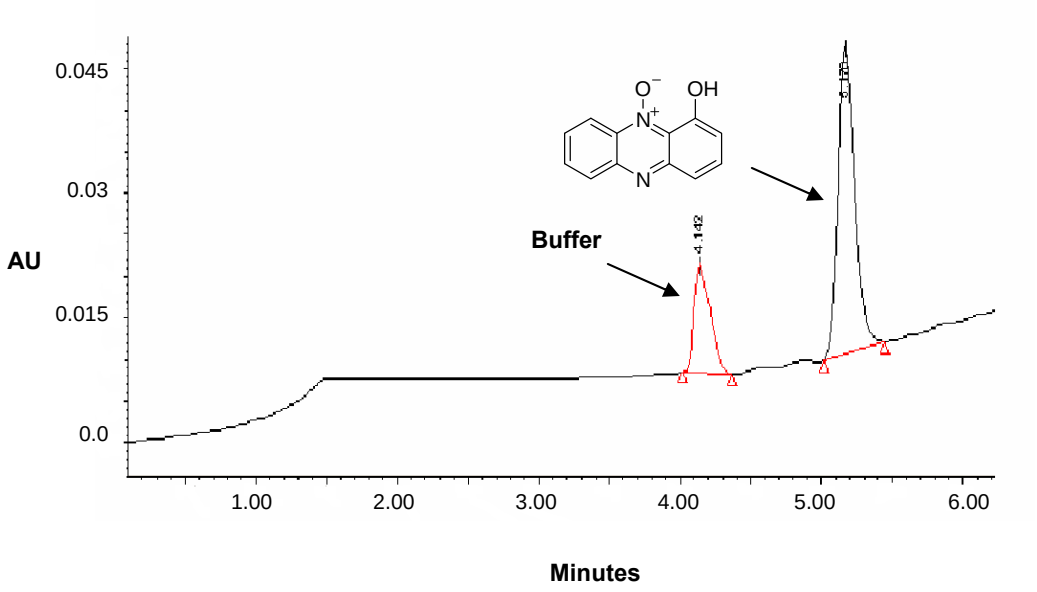

Figure 19: HPLC chromatogram for the oxidation reaction of OHP by peroxynitrite. OHP was oxidized into mono-*N*-oxide **6** by oxidation with peroxynitrite. OHP (500 µM) was incubated with Angeli's salt (10 mM) at pH 7.5 buffer at 37^{O}C under aerobic condition for 24 hours and then the reaction mixture was analyzed by normal phase HPLC (eluting solvent: 0.5% acetic acid in ethyl acetate and heptane).

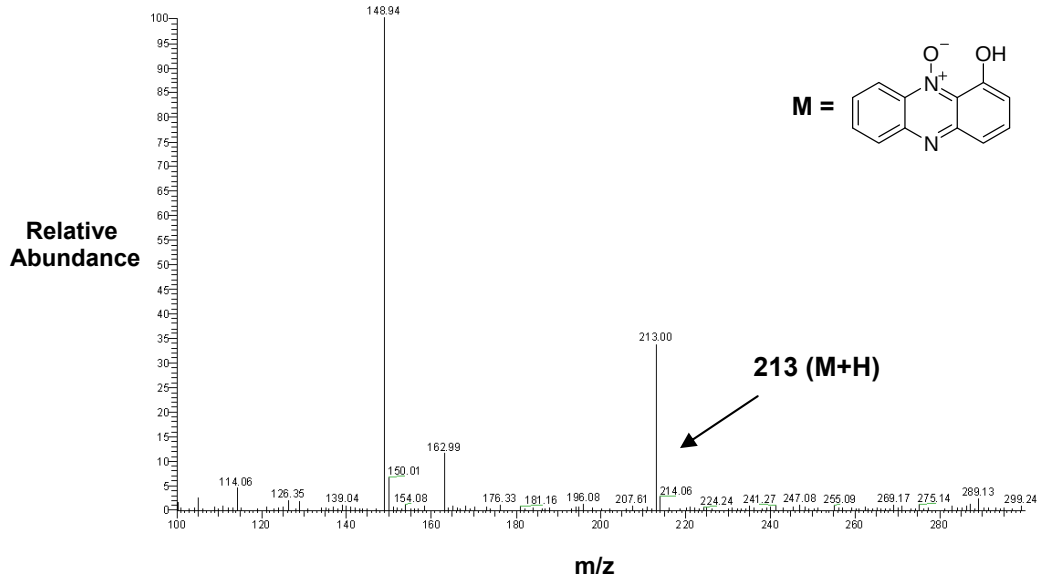

Figure 20: Identification of mono-*N*-oxide of OHP **6** by LC/MS analysis where the compound was detected by using normal phase HPLC method and mass of the peak (m/z = 213) of retention time 4.8 minutes was determined by using APCI positive ion mode. The mass spectrum shows M+H ion of **6** at m/z 213 obtained using LC-APCI/MS operating in the positive ion mode.

Therefore our in vitro study provided evidence that OHP is oxidized by molecular oxygen, H_2O_2 and peroxynitrite at physiological pH and produce both mono-*N*-oxide **6** and di-*N*-oxide **5** of OHP which strengthen our hypothesis that OHP might get oxidized in *P.aeruginosa* infected lung cell by neutrophils and endothelium derived ROS.

2.10. Conclusion:

We have already discussed in our first chapter that 1-hydroxyphenazine the secondary metabolite of *P.aeruginosa* produces ROS inside the cell via enzyme-driven redox cycling. Generation of ROS causes oxidative stress inside the cell which might be the one of the reasons of lung tissue damage in case of cystic fibrosis patients. In this chapter, we have provided first direct evidence that 1-hydroxyphenazine has the potential to be converted to di-*N*-oxide **5** and mono-*N*-oxide of OHP **6** upon oxidation by oxygen, H_2O_2 and peroxynitrite. Mono-*N*-oxide **6** appears resistant to further oxidation while presumed intermediate **7** proceeds to give di-*N*-oxide **5**. Both **5** and **6** can cause efficient enzyme-driven production of ROS, via a redox cycling mechanism under aerobic conditions. Therefore, generation of ROS by both 1-hydroxyphenazine and *N*-oxides of OHP (discussed in this chapter) could explain the virulence of OHP as well as the *P.aeruginosa* associated lung tissue damage in cystic fibrosis patients.

Material and methods:

Materials: Materials with highest purity were bought from the following suppliers. Benzofuroxan, sodium phosphate, menadione, triethylamine, 30% H_2O_2 and TLC plates from Aldrich Chemical Co. (Milwaukee, WI); Sodium hydrosulfite 85% and 1,2 cyclohexanedione, 98% from Acros Organics (Pittsburgh, PA); NADPH, acetonitrile, desferal, cytochrome P450 reductase, catalase and SOD from Sigma Chemical Co. (St. Louis, MO); agarose from Seakem; HPLC grade solvents (methanol, ethanol, ethylacetate, heptane), ethylacetate, hexane, NaOH, HCl and acetic acid from Fisher Scientific (Pittsburg, PA); ethidium bromide from Roche Molecular Biochemicals (Indianapolis, IN); Silica gel (0.04-0.063 mm pore size) for column chromatography from Merck. Angeli's salt is bought from Cayman Chemicals (Ann Arbor, MI). The plasmid pGL2BASIC was prepared using standard protocols, [Sambrook, J.; Fritsch, E. F.; Maniatis, T. (1989) *Molecular Cloning: A Lab Manual,* Cold Spring Harbor Press, Cold Spring Harbor. NY]. 1-Hydroxyphenazine, **5** and **6** were synthesized by following the literature methods.[15] High resolution mass spectroscopy was performed at the University of Illinois Urbana-Champaign Mass Spectroscopy facility and low resolution mass spectroscopy and LCMS study were performed at University of Missouri-Columbia Mass Spectroscopy facility. NMR spectra were taken using Bruker DRX 300 and 500 MHz instruments at the University of Missouri-Columbia.

Synthesis of di-*N*-oxide and mono-*N*-oxide of 1-hydroxyphenazine: At first *N*-oxides of 1-hydroxyphenazine were prepared by following the synthetic route used by

Haddadin and coworkers with slight modification.[15] Benzofuranoxide (1gm, 7.3 millimols) was dissolved in 10 mL TEA (triethylamine) by heating and stirring the solution under N_2 gas. Then 1,2 cyclohexanedione (450 mg, 4 millimols) was added drop wise to the reaction mixture under N_2 gas. After that the reaction mixture was stirred in ice bath for 30 minutes and then for 7-8 hours at 25^0C. The color of the reaction mixture was turned into deep brown. Then the reaction mixture was diluted in crushed ice and acidified (pH 5) by HCl. After that the reaction mixture was extracted in distilled ethyl acetate and dried over anhydrous Na_2SO_4. The solvent was evaporated and the reaction mixture was purified by gravity column chromatography (elute solvent: 1:3 distilled ethyl acetate and hexane) to obtain mixture of *N*-oxides of 1-hydroxyphenazine (26%). Both di-*N*-oxide **5** and mono-*N*-oxide of OHP **6** were obtained by purifying the crude reaction mixture by using gravity column chromatography (elute solvent: ethyl acetate and hexane). ^{1}H-NMR of **5** (300 MHz, Acetone-d_6) δ 14.84 (1H, s), 8.66 (2H, m), 8.01 (3H, m), 7.79 (1H, dd, J_1= 8.1 Hz, J_2= 9.0 Hz), 7.13 (1H, dd, J_1= 8.1 Hz, J_2= 0.9 Hz) ppm; ^{13}C-NMR (DMSO-d_6, 125 MHz) δ 153.25, 137.14, 135.77, 133.49, 132.60, 132.20, 131.86, 126.20, 119.34, 118.74, 113.70, 108.12 ppm; LRMS: ESI-MS $[M+H]^+$= 228.82; HRMS: 229.0623, calculated mass: 229.0613 (PPM: 4.4). ^{1}H-NMR of **6** (500 MHz, Acetone-d_6) δ 13.78 (1H, s), 8.60 (1H, d, J= 9.0 Hz), 8.20 (1H, d, J= 9.0 Hz), 8.01 (1H, t, J_1 = 9 Hz, J_2 = 6.5 Hz), 7.95 (1H, dd, J_1 = 9 Hz, J_2 = 6.5 Hz), 7.82 (1H, t, J_1 =8.5, J_2 = 8 Hz), 7.68 (1H, d, J= 9 Hz), 7.06 (1H, d, J= 7.5 Hz) ppm; ^{13}C-NMR (DMSO-d_6, 125 MHz) δ 151.53, 146.21, 144.99, 132.76, 132.36, 132.02, 131.77, 129.89, 124.37, 119.21, 117.77, 111.98 ppm; LRMS: ESI-MS $[M+H]^+$= 212.81; HRMS: 213.0656, calculated mass: 213.0664 (PPM: -3.8).

In all assays OHP *N*-oxides were used as 10% acetonitrile in water by volume. For oxidation reaction of OHP, OHP was used as 5-15% acetonitrile in water.

Oxidation of OHP into its *N*-oxides by H_2O_2, O_2 and peroxynitrite: At first 500 μM OHP (15% acetonitril in water by volume) was taken in a 10 mL round bottom flask in a total volume 1 mL. Then 50 mM sodium phosphate buffer (pH 7) was added and 50 μL 30% H_2O_2 from 100 mM stock solution was added in the reaction mixture (RM) in such a way that final concentration of 30% H_2O_2 in the reaction mixture was 5mM. Next the reaction mixture was incubated at room temperature for two days with gently stirring. After two days 25 μL 30% H_2O_2 from same 100 mM stock was added in the reaction mixture to attain the final concentration 7.5 mM. The RM is then kept at room temperature with stirring. Next 10 μL 100 mM H_2O_2 was added in the reaction mixture to attain the final concentration 8.5 mM and the reaction mixture was incubated for two more days with gently stirring. The reaction mixture was incubated total for 18 days. After that the reaction mixture was extracted in 50:50 ethyl acetate:hexane mixture and then analyzed by HPLC employing a Microsorb-MV-100 NH_2 normal phase column (5 μm particle size, 25 cm length, 100A^o pore size and 4.6 mm i.d.) eluted with gradient solvent system starting with 40% A (0.5 % acetic acid in ethyl acetate) and 60 % B (0.5 % acetic acid in heptane) followed by linear increase to 55 % A from 0 minute to 2 minute, 70% A from 2 to 4 minute. Then 70% A was held for next 13 minutes and in next 2 minutes again A is reached to 40% and gets equilibrated for next 8 minutes. The flow rate was 0.7 mL/min and the products were monitored by UV-absorbance at 284 nm. In addition to OHP we detected the peak of both mono-*N*-oxide **6** and di-*N*-oxide of OHP **5**

and both *N*-oxides of OHP was confirmed by co-injection of reaction mixture with authentic standards. So, OHP was oxidized into its *N*-oxides in presence of H_2O_2.

Moreover OHP (500 μM 5% acetonitrile in water by volume) was incubated at 37 ^oC at pH 7.5 sodium phosphate buffers for 24 hours. After that the reaction mixture was extracted in ethyl acetate and then analyzed by normal phase HPLC as described above. It was found that OHP was oxidized into its mono-*N*-oxide **6**. Moreover 500 μM OHP (5% acetonitrile in water by volume) was incubated with 10 mM Angeli's salt which produces peroxynitrite[27,28] at 37 ^oC at pH 7.5 sodium phosphate buffer for 4:30 h, 6:30 h and for 24 hours and after that the reaction mixture was extracted into ethyl acetate and next it was analyzed by HPLC as described above. We noticed that OHP was oxidized into mono-*N*-oxide **6** upon oxidation with peroxynitrite. In both cases the identity of mono-*N*-oxide **6** was confirmed by LC/MS. LC/MS analysis was performed by using TSQ7000 triple-quadruple mass spectrometer where we used same HPLC method as described above to separate and detect the compounds and used APCI (atmospheric pressure chemical ionization) positive ion mode to determine the mass (m/z = M+H) of the compounds. The mechanistic study of oxidation of OHP was carried out in a similar way as described above where 500 μM OHP was incubated with 5 mM H_2O_2 in presence of 50 mM sodium phosphate buffer at room temperature for 17 hours and as controlled two more reaction mixture contained a) 500 μM **6** + 5 mM H_2O_2, b) 500 μM di-*N*-oxide of OHP **5** + 5 mM H_2O_2 in presence of 50 mM sodium phosphate buffer were incubated for 17 hours. Next all the reaction mixture including controls were injected into HPLC and were analyzed by using similar HPLC method as described above.

Cleavage of Supercoiled Plasmid DNA by mono-*N*-oxide and di-*N*-oxide of OHP: In a typical DNA cleavage assay supercoiled plasmid DNA (1 μg) was incubated with the mono-*N*-oxide of OHP **6** (100 μM) or di-*N*-oxide of OHP **5** (100 μM), NADPH (200 μM), cytochrome P450 reductase (0.05 U/mL), sodium phosphate buffer (50 mM, pH 7.0) and with SOD (100 μg/mL), catalase (100 μg/mL) and desferal (1 mM) as control reactions in a total volume 40 μL. The reactions were initiated by addition of cytochrome P450 reductase, then wrapped with aluminium foil to prevent exposure of light and incubated under aerobic condition at room temperature (24^{o}C) for 5-6 hours. After incubation, the reactions were stopped by addition of 6.6 μL of 50% glycerol loading buffer, and the resulting reaction mixture was loaded onto a 0.9% agarose gel. The gel was electrophoresed for approximately 2 h at 90 V in 1 x TAE buffer and then stained in a solution of ethidium bromide (0.3 μg/mL) for 3 hours. DNA in gel was visualized by UV-transillumination and the amount of DNA in each band was quantified using an Alpha Innotech IS-1000 digital imaging system. DNA-cleavage assay containing radical scavengers were performed in a similar way as described above with the exception that radical scavengers such as methanol (1 mM) or ethanol (1 mM) were added to the reaction mixture before addition of cytochrome P450 reductase.

Cleavage of Supercoiled Plasmid DNA with increasing concentration of mono-*N*-oxide and di-*N*-oxide of OHP: In a typical DNA damage assay supercoiled plasmid DNA (1 μg) was incubated with increasing concentration of **6** (10-100 μM) or **5** (10-100 μM), NADPH (200 μM), cytochrome P450 reductase (0.05 U/mL), sodium phosphate buffer (50 mM, pH 7) and with SOD (100 μg/mL), catalase (100 μg/mL),

desferal (1 mM) as control reactions in a total volume 40 μL. The reactions were initiated by addition of cytochrome P450 reductase, then wrapped with aluminium foil to prevent exposure of light and incubated under aerobic condition at room temperature (24^{o}C) for 5-6 hours. After incubation, the reactions were stopped by addition of 6.6 μL of 50% glycerol loading buffer, and the resulting reaction mixture was loaded onto a 0.9% agarose gel. The gel was electrophoresed for approximately 2 h at 90 V in 1 x TAE buffer and then stained in a solution of ethidium bromide (0.3 μg/mL) for 3 hours. DNA in gel was visualized by UV-transillumination and the amount of DNA in each band was quantified using an Alpha Innotech IS-1000 digital imaging system.

Comparison of aerobic DNA damage ability between *N*-oxides of OHP with menadione and TPZ: In a typical plasmid based DNA damage assay DNA (1 μg) was incubated with **5** (100 μM) or **6** (100 μM) or **menadione** (100 μM) or **TPZ** (100 μM), NADPH (200 μM), cytochrome P450 reductase (0.05 U/mL), sodium phosphate buffer (50 mM, pH 7) and with SOD (100 μM), catalase (100 μg/mL), desferal (1 mM) as control reactions in a total volume 40 μL at room temperature (24^{o}C) under aerobic condition for 5-6 hour. The reaction mixture was wrapped by aluminium foil to prevent exposure of light. After 5-6 hours later of incubation the reaction was stopped by addition of 6.6 μL of 50% glycerol loading buffer, and the resulting reaction mixture was loaded onto a 0.9% agarose gel. The gel was electrophoresed for approximately 2 h at 90 V in 1 x TAE buffer and then stained in a solution of ethidium bromide (0.3 μg/mL) for 3 hours. DNA in gel was visualized by UV-transillumination and the amount of DNA in each band was quantified using an Alpha Innotech IS-1000 digital imaging system.

Metabolism study of *N-oxides* of 1-hydroxyphenazine in presence of NADPH:cytochrome P450 reductase system: In a typical assay a solution of 200 μL containing **5** (100 μM) and sodium phosphate buffer (50 mm, pH 7) alone or **5** (100 μM), sodium phosphate buffer (50 mM, pH 7), NADPH (500 μM) and cytochrome P450 reductase (0.05 U/mL) were incubated at room temperature (24^{o}C) under aerobic condition for 12 hours. Two control experiments were done by addition of SOD (100 μg/mL), catalase (100 μg/mL) and desferal (1mM) or without addition of **5** in the reaction mixture. In some other assay in stead of **5**, **6** (100 μM) was incubated with sodium phosphate buffer (50 mm, pH 7) alone or with sodium phosphate buffer (50 mM, pH 7), NADPH (500 μM) and cytochrome P450 reductase (0.05 U/mL) at room temperature (24^{o}C) under aerobic condition for 12 hours. Similar control experiments were done in case of **6** as described above. Following incubation, the proteins were removed by centrifugation through Amicon Micron (YM3) filters. The filtrate was extracted in 50:50 ethyl acetate:hexane mixture and then analyzed by HPLC employing a Microsorb-MV-100 NH_2 normal phase column (5 um particle size, 25 cm length, 100 A^{o} pore size and 4.6 mm i.d.) eluted with gradient solvent system starting with 40% A (0.5 % acetic acid in ethyl acetate) and 60 % B (0.5 % acetic acid in heptane) followed by linear increase to 55 % A from 0 minute to 2 minute, 70% A from 2 to 4 minute. Then 70% A was held for next 13 minutes and in next 2 minutes again A is reached to 40% and gets equilibrated for next 8 minutes. The flow rate was 0.7 mL/min and the products were monitored by UV-absorbance at 284 nm. Both *N*-oxides of OHP was identified by co-injection with authentic standard and also identified by LC/MS. LC/MS analysis was performed by using TSQ7000 triple-quadruple mass spectrometer where we used same HPLC method

as described above to detect the metabolites and used APCI (atmospheric pressure chemical ionization) positive ion mode to determine the mass (m/z = M+H) of the metabolites.

References:

1. Sadikot, R. T.; Blackwell, T. S.; Christman, J. W.; Price, A. S. *Am. J. Respir. Crit. Care. Med.* **2005**, *171*, 1209-1223.

2. J. D.; Dohrman, A. F.; Gallup, M.; Miyata, S.; Gum, J. R.; Kim, Y. S.; Nadel, J. A.; Prince, A.; Basbaum, C. B. *Proc. Natl. Acad. Sci. USA*. **1997**, *94*, 967-972.

3. Taggart, C. C.; Greene, C. M.; Smith, S. G.; Levin, R. L.; McCray, P. B. Jr.; O'Neill S.; McElvaney, N. G. *J. Immunol.* **2003**, *171*, 931-937.

4. Singh, P. K.; Jia, H. P.; Wiles, K.; Hesselberth, J.; Liu, L.; Conway, B. A.; Greenberg E. P.; Valore, E. V.; Welsh, M. J.; Ganz, T. *Proc. Natl. Acad. Sci. USA.* **1998**, *95*, 14961-14966.

5. DiMango, E.; Ratner, A. J.; Bryan, R.; Tabibi, S.; Prince, A. *J. Clin. Invest.* **1998**, *101*, 2598-2605.

6. DiMango, E.; Zar, H. J.; Bryan, R.; Prince, A. *J. Clin. Invest.* **1995**, *96*, 2204-2210.

7. Tsai, W. C.; Strieter, R. M.; Mehrad, B.; Newstead, M. W.; Zeng, X. *Infect. Immun.* **2000**, *68*, 4289-4296.

8. Loukides, S.; Bouros, D.; Papatheodorou, G.; Lachanis, S.; Panagou, P.; Siafakas, N. M. *Chest* **2002**, *121*, 81-87.

9. Jobsis, Q.; Raatgeep, H. C.; Schellekens, S. L.; Kroesbergen, A.; Hop, W. C. J.; De Jongste, J. C. *European Respiratory Journal* **2000**, *16*, 95-100.

10. Valente, E.; Assis, M. C.; Alvim, I. M. P.; Pereira, G. M. B.; Plotkowski, M. C. *Microbial Pathogenesis* **2000**, *29*, 345-356.

11. Kerr, J. *Infect. Dis. Rev.* **2000**, *2*, 184-194.

12. Laursen, J.; Nielsen, J. *Chem. Rev.* **2004**, *104*, 1663-1685.

13. Nagai, K.; Carter, J. B.; Xu, J.; Hecht, M. S. *J. Am. Chem. Soc.* **1991**, *113,* 5099-5100

14. *DNA damage by Heterocyclic N-oxides: A novel class of antitumor agents,* PhD thesis submitted by Goutam Chowdhury in **2005.**

15. Issidorides, C. H.; Atfah, M. A.; Sabounji, J. J.; Sidani, A. R.; Haddadin, M. J. *Tetrahedron*. **1978**, *34,* 217-221.

16. Mitra, K.; Kim, W.; Daniels, J. S.; Gates, K. S. *J. Am. Chem. Soc.* **1997**, *119,* 11691-11692.

17. Daniels, J. S.; Gates, K. S. *J. Am. Chem. Soc.* **1996**, *118*, 3380-3385.

18. Chowdhury, G.; Kotandeniya, D.; Daniels, J. S.; Gates, K. S. *Chem. Res. Toxicol*. **2004**, *17,* 1399-1405.

19. Forman, H. J.; Torres, M. *Am. J. Respir. Crit. Care. Med.* **2000**, *166*, S4-S8.

20. Dacheux, D.; Attree, I.; Schneider, C.; Toussaint, B. *Infection and Immunity* **1999**, *67*, 6164-6167.

21. Paget, T.; Maroulis, S.; Mitchell, A.; Edwards, M. R.; Edward, L. *Microbiology* **2004**, *150*, 1231-1236.

22. Morgan, W. A.; Kaler, B.; Bach, P. H. *Toxicology letters* **1998**, *94*, 209-215.

23. Fang, F. C. *J. Clin. Invest.* **1997**, *99*, 2818-2825.

24. Behki, R. M.; Lesley, S. M. *J. Bacteriol.* **1972**, *109*, 250-261.

25. Pretsch, E.; Buhlmann, P.; Affolter, C. *Structure Determination Of Organic Compounds.*

26. ^{1}H NMR and ^{13}C NMR of both mono-*N*-oxide and di-*N*-oxide of OHP submitted with this chapter.

27. Kirsch, M.; Groot, H. *J. Biol. Chem.* **2002**, *277*, 13379-13386.

28. Miranda, K.; Dutton, A.; Ridnour, L.; Foreman, F.; Paolocci, N.; Katori, T.; Tocchetti, C.; Mancardi, D.; Thomas, D.; Espey, M.; Houk, K.; Fukuto, J.; Wink, D. *J. Am. Chem. Soc.* **2005**, *127*, 722-731.

29. Halliwell, B.; Gutteridge, J. M. C. *Methods Enzymol.* **1990**, *186*, 1.

30. Bagley, A. C.; Krall, J.; Lynch, R. E. *Proc. Nat. Acad. Sci. U.S A.* **1986**, *83*, 9189.

31. Hassan, H. M.; Fridovich, I. *Arch. Biochem. Biophys.* **1979**, *196*, 385.

32. Sanchez Sellero, I.; Lopez-Rivadulla Lamas, M. *Recent Res. Dev. Drug Metab. Disp.* **2002**, *1*, 1163-275.

33. Finkel, T.; Holbrook, N. J. *Nature* **2000**, *408*, 239.

34. Davis, W.; Ronai, Z.; Tew, K. D. *J. Pharm. Exp. Ther.* **2001**, *296*, 1.

35. Yoshimi, Y.; Maeda, H.; Hatanaka, M.; Mizuno, K. *Tetrahedron* **2004**, *60*, 9425-9431.

36. Gates, K. S. *Pergamon: New York* **1999**, *7*, 491-552.

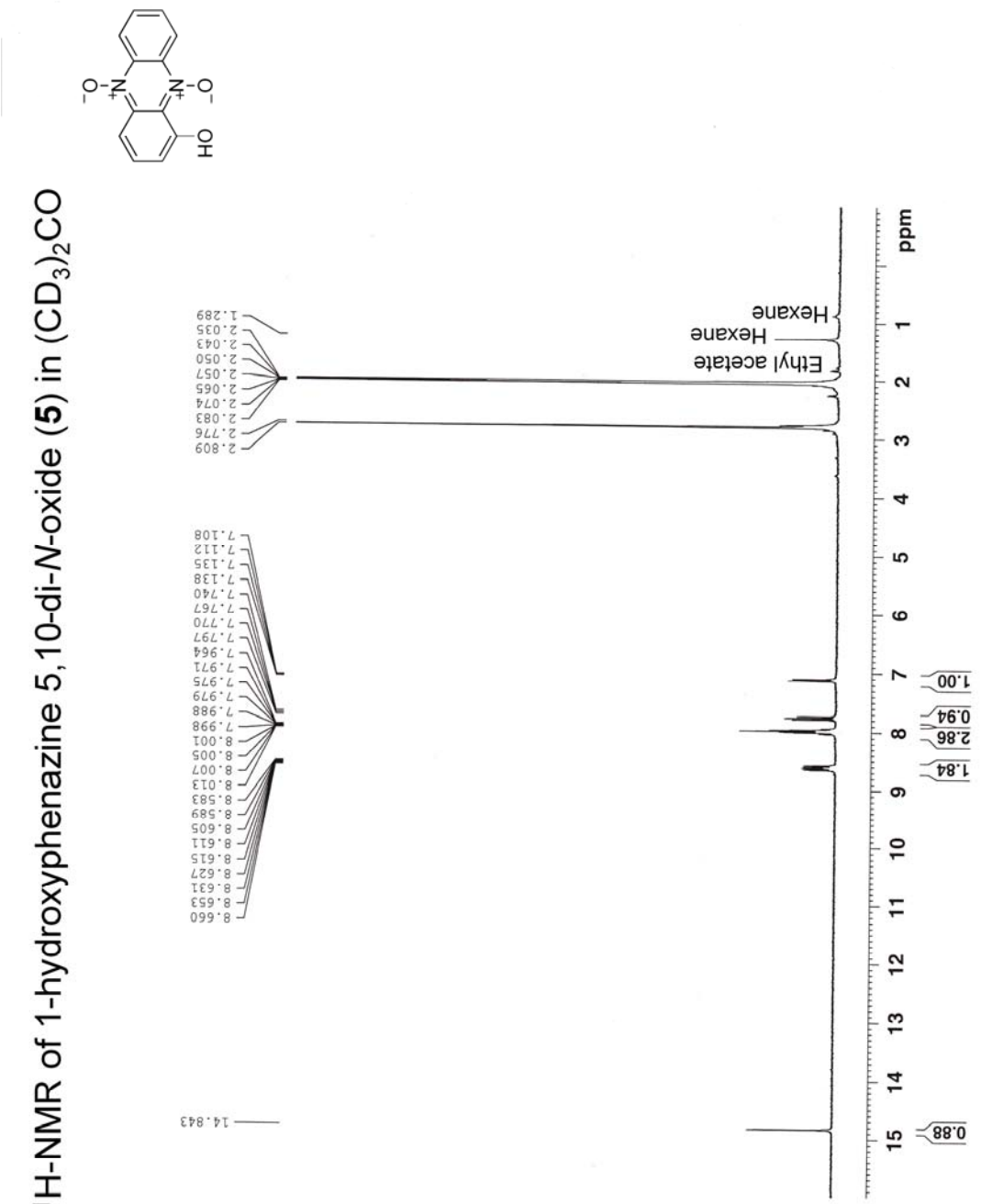
^{1}H-NMR of 1-hydroxyphenazine 5,10-di-*N*-oxide (**5**) in $(CD_3)_2CO$
Ethyl acetate
Hexane
Hexane
ppm

^{13}C-NMR of 1-hydroxyphenazine 5,10-di-*N*-oxide (**5**) in d_6-DMSO

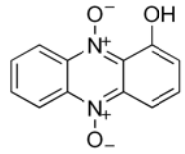

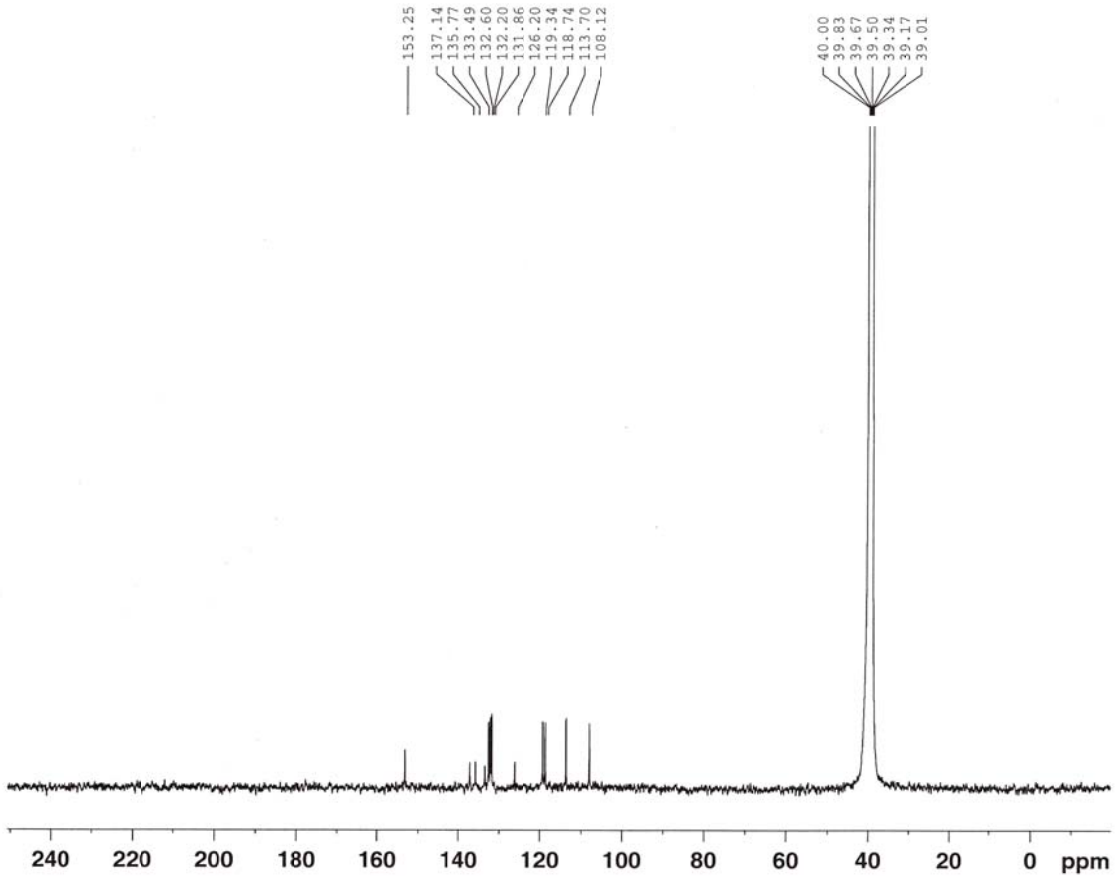

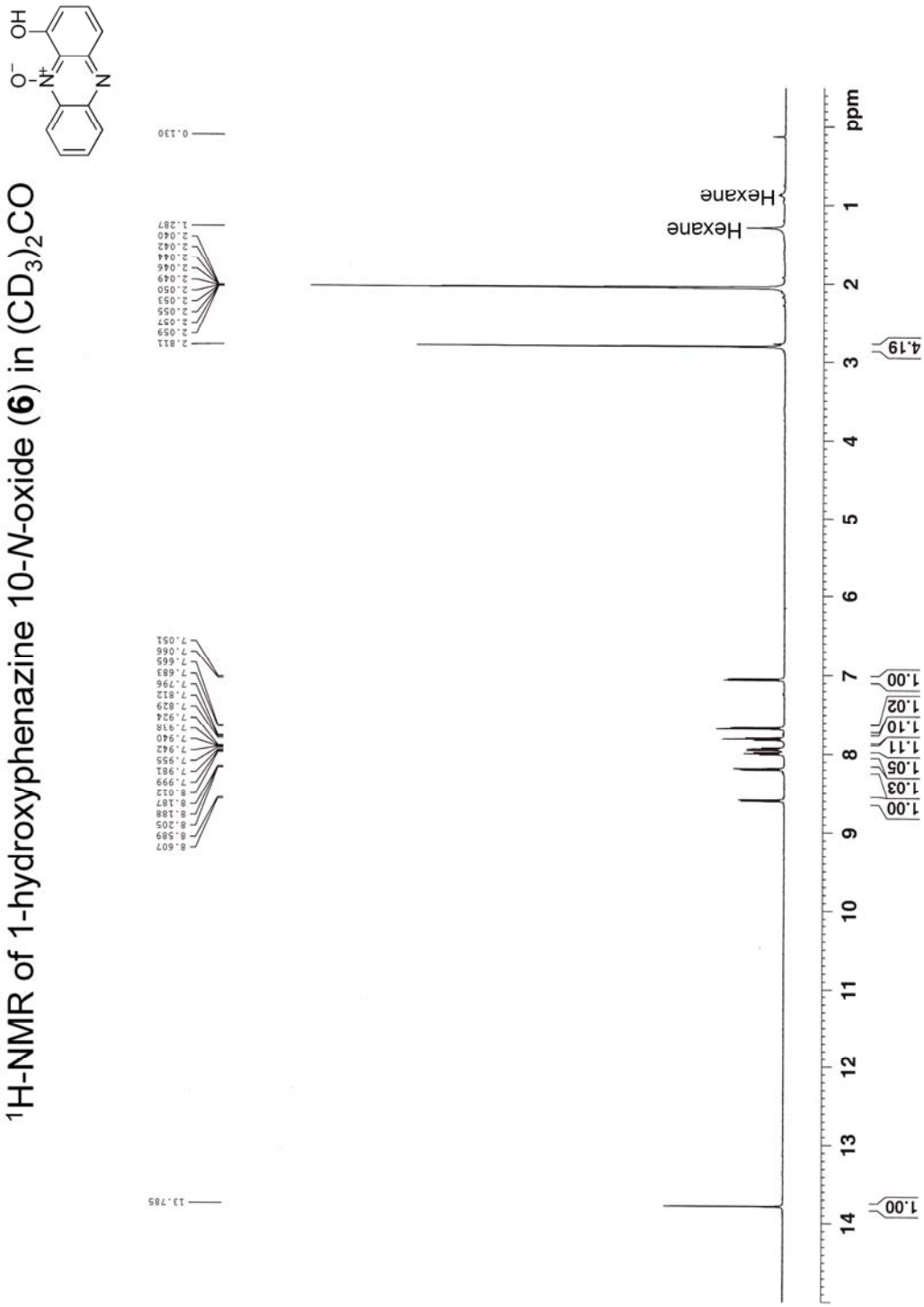
^{1}H-NMR of 1-hydroxyphenazine 10-*N*-oxide (**6**) in $(CD_3)_2CO$
OH
O⁻
N⁺
N
Hexane
Hexane
ppm

^{13}C-NMR of 1-hydroxyphenazine 10-*N*-oxide (**6**) in d_6-DMSO

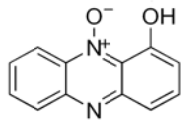

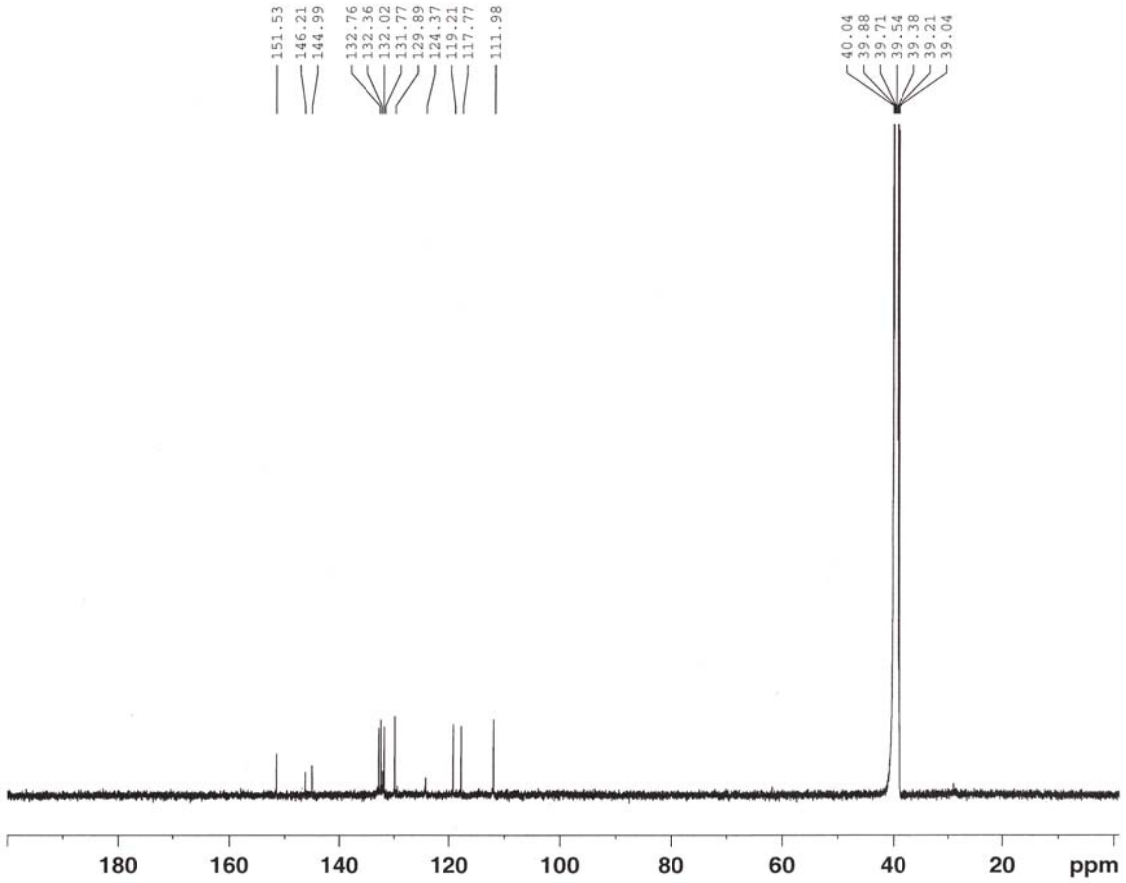

^{1}H-NMR of 10 mM1-hydroxyphenazine 10-*N*-oxide (6) in $(CD_3)_2CO$

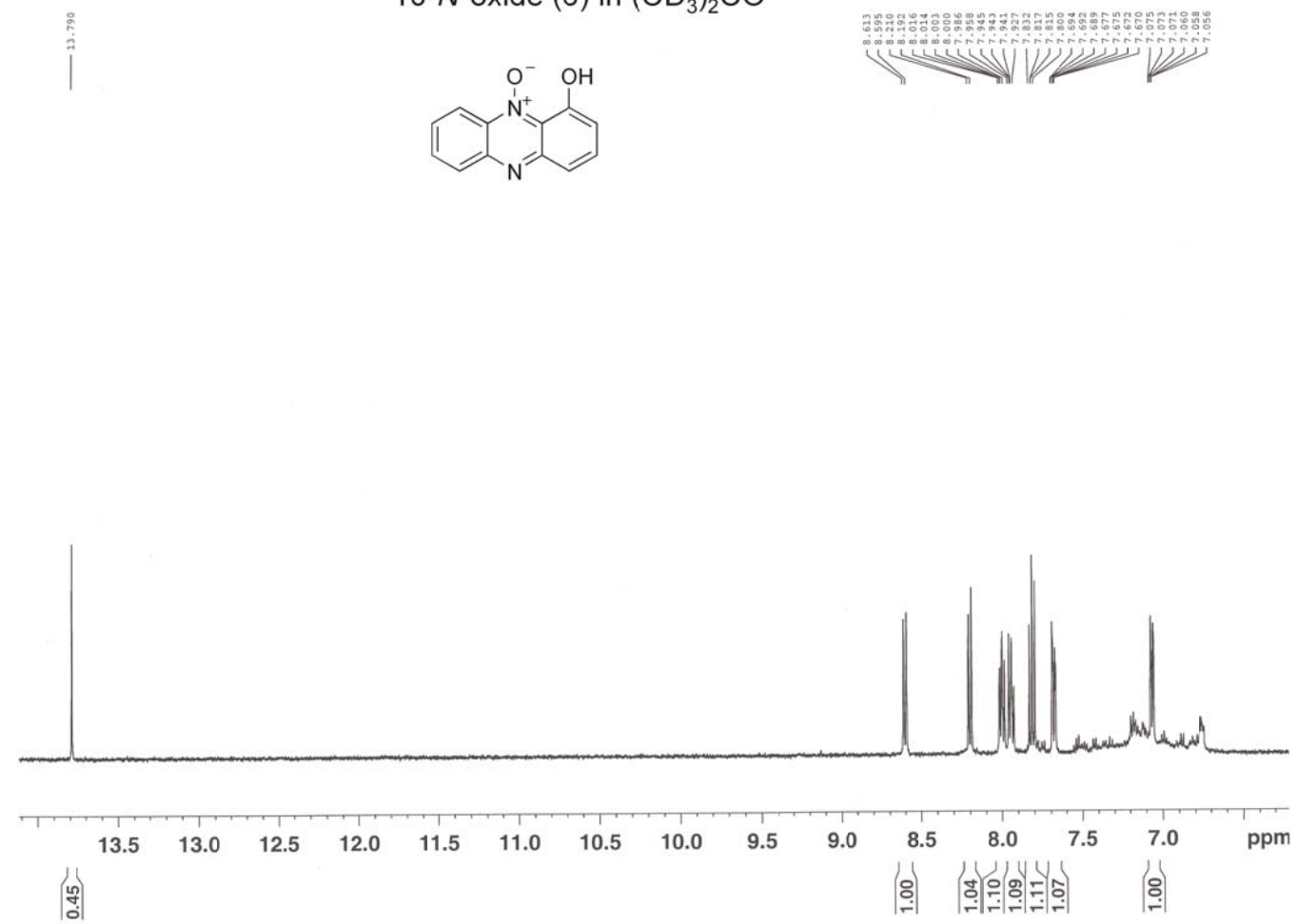

^{1}H-NMR of 1 mM1-hydroxyphenazine 10-*N*-oxide (6) in $(CD_3)_2CO$

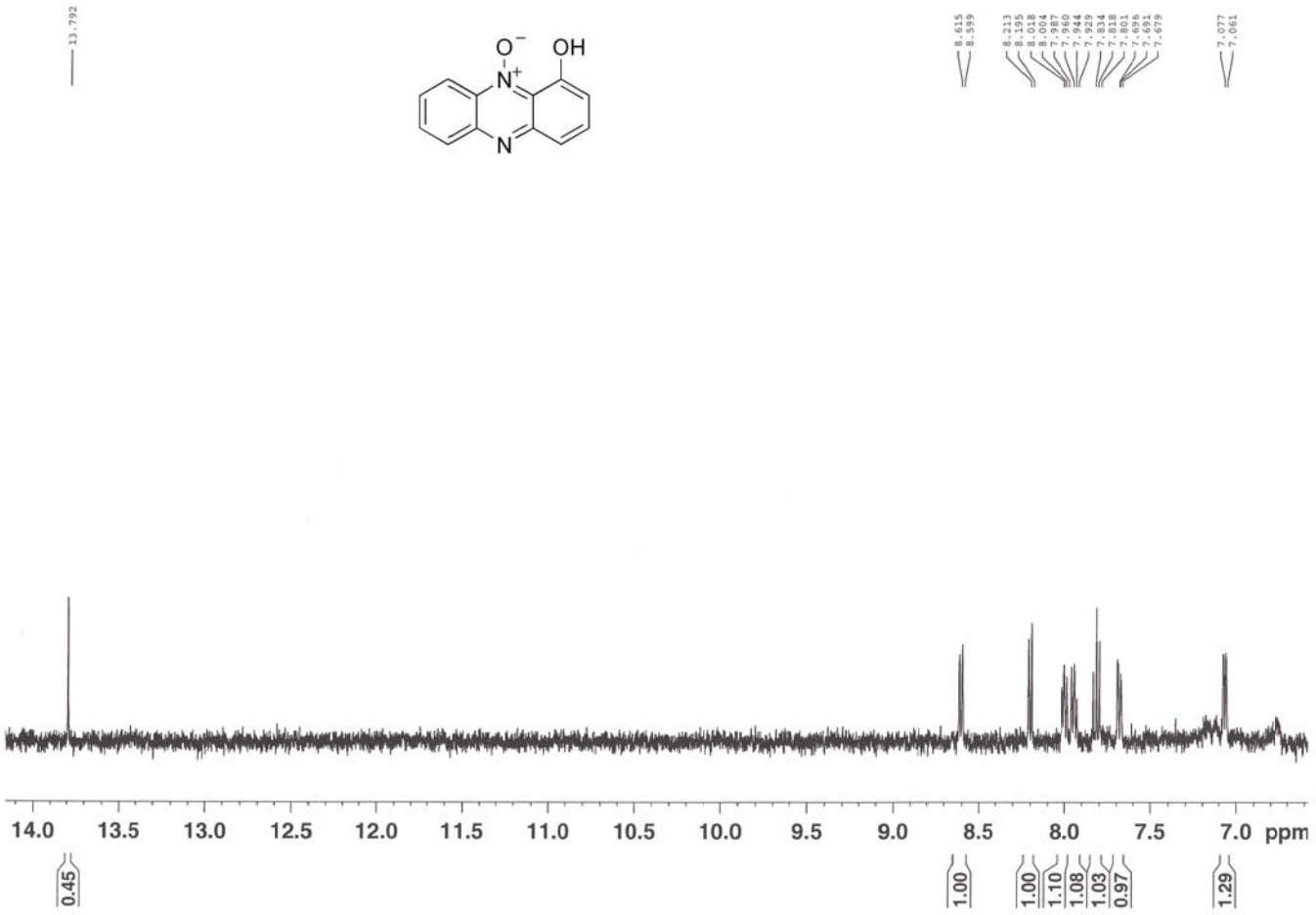

Chapter 3: DNA Strand Cleavage by the 1,2,4-benzotriazine 1,4-Dioxide Family of Antitumor Agents: Mechanistic Insight from the use of a classical hydroxyl radical scavenging agent

3.1. Introduction:

Heterocyclic aromatic *N*-oxides are promising antitumor agents that display redox-activated hypoxia-selective DNA-damaging properties.[1-4] As tumor cells are hypoxic in nature, the hypoxia selectivity of these compounds has made these heterocyclic *N*-oxides attractive candidates for anticancer chemotherapy.[5,6] Examples of heterocyclic *N*-oxides examined in preclinical studies include 3-amino-1,2,4-benzotriazine 1,4-dioxide (Tirapazamine, TPZ), quinoxaline-di-*N*-oxides and phenazine di-*N*-oxide.[7-10]

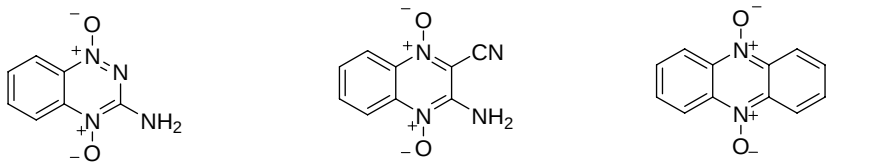

Figure 1: Example of heterocyclic *N*-oxides.

TPZ is the lead compound in this group and displays hypoxia-selective antitumor properties and currently is undergoing phage I, II, III clinical trials.[5,11] TPZ achieves its medicinal activity through its ability to damage DNA selectively in the oxygen poor or hypoxic cells inside the solid tumors.[1-6,11] TPZ undergoes one electron reductive

activation in presence of one-electron reducing system to yield a radical intermediate **(Scheme 1)**.[1,12,13,14]

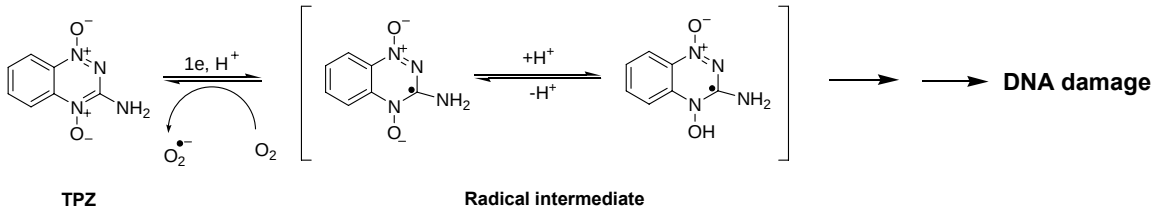

Scheme 1: One electron reductive activation of TPZ.

Under hypoxic conditions, this radical intermediate leads to oxidative DNA damage that includes oxidation of the nucleobases[15,16] and generation of DNA strand breaks by the abstraction of hydrogen atoms from the 2'-deoxyribose residues of the DNA backbone.[1,3,13,17] In normal, oxygenated cells, the radical intermediate is back-oxidized into parent compound with simultaneous production of superoxide radical (**Scheme 1**) due to redox cycling.[13,1,14] Cellular enzymes including superoxide dismutase, catalase, glutathione peroxidase and peroxiredoxines diminish the deleterious effect of superoxide radical and its decomposition products.[18,19]

The identity of the reactive intermediate of TPZ which is responsible for bioreductively-activated oxidative DNA damage under hypoxic condition remains a subject of ongoing research. Three proposals have been suggested to explain the identity of the reactive intermediate and the mechanistic pathway of DNA damage by TPZ (**Scheme 2**).

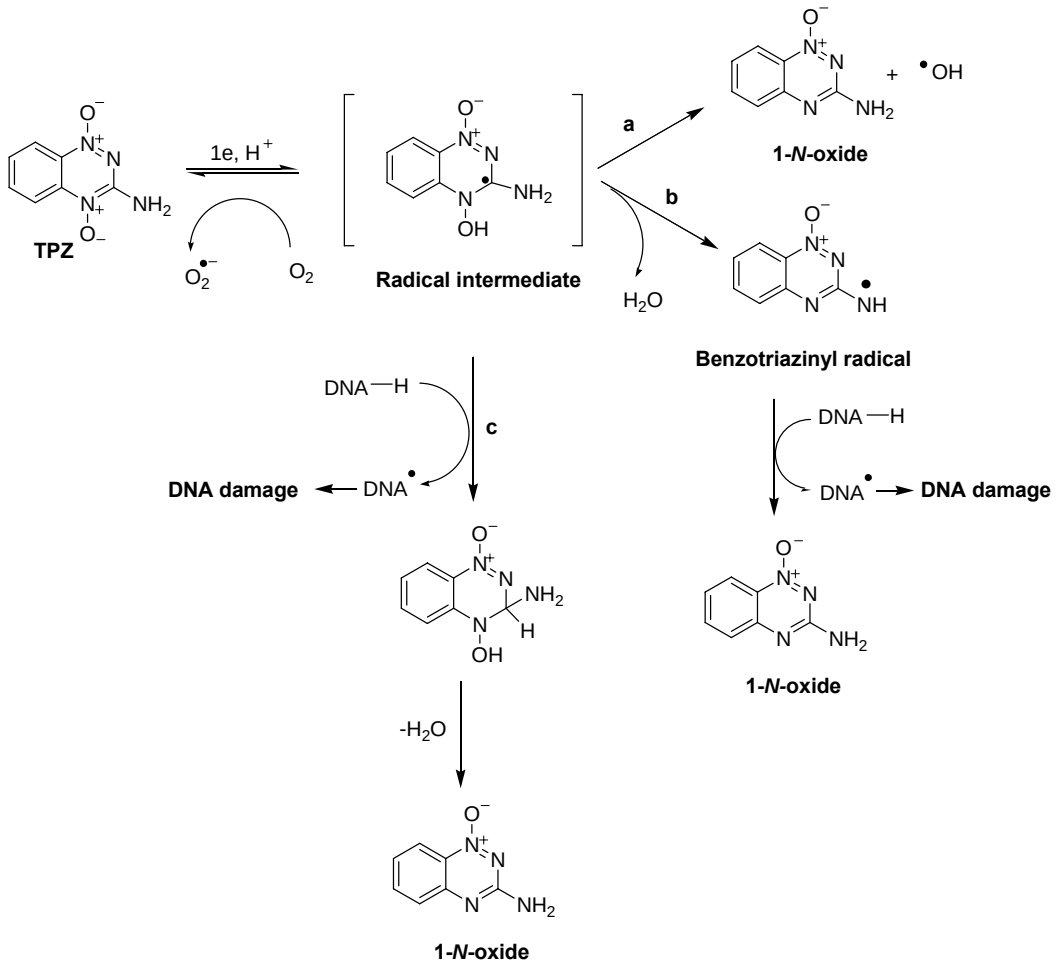

Scheme 2: Three proposed mechanism of DNA damage by TPZ.

It is known that TPZ causes DNA strand cleavage by abstraction of hydrogen atom from deoxyribose residue of duplex DNA.[1,3,13,17] Recently our group has characterized the sugar-derived products obtained from TPZ-mediated DNA strand cleavage and we found that DNA strand cleavage initiated by TPZ under hypoxic condition generates 5-methylene-2-furanone, oligonucleotide 3'-phosphoglycolates, malondialdehyde equivalents and furfural as shown in **Scheme 3**.[20]

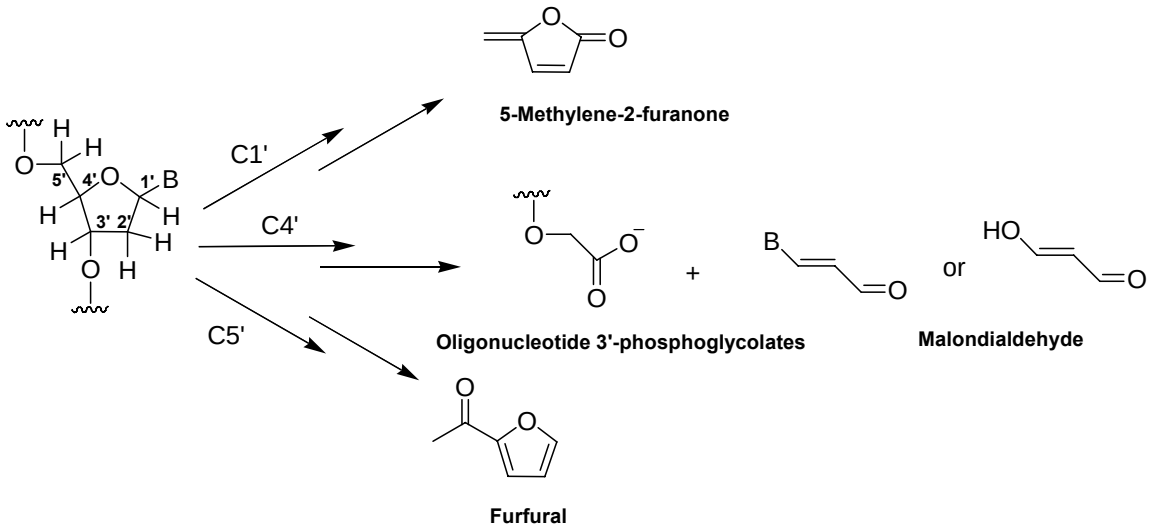

Scheme 3: End products obtained from DNA damage by abstraction of hydrogen atom from deoxyribose sugar backbone of duplex DNA.[20]

This result provide evidence that TPZ initiates DNA damage by abstracting hydrogen atom from (C1') and (C4' and C5') positions of deoxyribose sugars in the duplex DNA and the products obtained are identical to those products produced by hydroxyl radical.[20] In addition to that it has been studied by our group that one electron reducing enzyme xanthine/xanthine oxidase activates TPZ to cleave DNA and DNA damage is inhibited in presence of radical scavengers like methanol, ethanol, *tert*-butyl alcohol, mannitol and DMSO. TPZ in presence of xanthine/xanthine oxidase converts DMSO into methanesulfinic acid which is a typical product of reaction of hydroxyl radical with DMSO.[3] Moreover, activated TPZ on treatment with ^{32}P-labeled DNA results in cleavage at every base pair of DNA which is similar to the highly reactive non selective hydroxyl radical-mediated cleavage pattern.[3] Thus, on the basis of our previous results, we support a mechanism (**Scheme 2, pathway a**) in which radical intermediate undergoes homolysis of N-OH bond to produce mono-*N*-oxide as a metabolite and the known DNA damaging agent hydroxyl radical.[3,15] Alternatively it has been suggested that

radical intermediate (**Scheme 2, pathway b**) undergoes dehydration and generates benzotriazinyl radical which initiates DNA damage by abstracting hydrogen atom from the DNA backbone.[21] Moreover, it has been proposed that radical intermediate (**Scheme 2, pathway c**) itself may abstract H atom from DNA backbone finally generating the mono-*N*-oxide by eliminating water.[1] It is important to determine in which pathways TPZ is metabolized, as better understanding of the molecular mechanisms underlying the biological activities of TPZ will help to design better drugs within this new class of antitumor agents.

A large number of TPZ analogues have been synthesized and evaluated their hypoxia selective cytotoxicity.[22-28] From those we have chosen 3-alkyl-1,2,4-benzotriazine 1,4-dioxides or MeTPZ (**Figure 2**) to carry out the mechanistic study underlying the biological activities of these benzotriazine-*N*-oxides for two reasons.

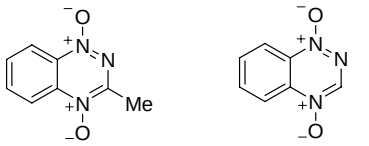

Figure 2: Examples of analogues of TPZ.

First, MeTPZ exhibits hypoxia-selective cytotoxicity similar to TPZ and consequently alkyl TPZ analogues have been suggested as potential clinical "back-ups" for TPZ.[24] In spite of their promising preclinical properties, the ability of these analogues to cause redox activated DNA damage under hypoxic condition has not been studied. Moreover the 3-alkyl functional group in these analogues might provide a mechanistic window that would determine whether benzotriazinyl radical intermediates are a key

player in oxidative DNA damage by the 1,2,4-benzotriazine 1,4-dioxide family. Specifically, if the presumed benzotriazinyl radical are generated in the deuterated solvents, the deuterium-containing mono-*N*-oxide metabolite would be produced. Moreover 1,2,4-benzotriazine 1,4-dioxide or DesTPZ, another analogue of TPZ also display hypoxia selective DNA damaging properties which leads to cytotoxicity[27] but the mechanism of DNA damage has not been investigated.

3.2. Goal: So, our goal was to examine whether TPZ and its analogues MeTPZ and DesTPZ cause DNA damage by hydroxyl radical pathway under hypoxic condition as shown in **Scheme 4**.

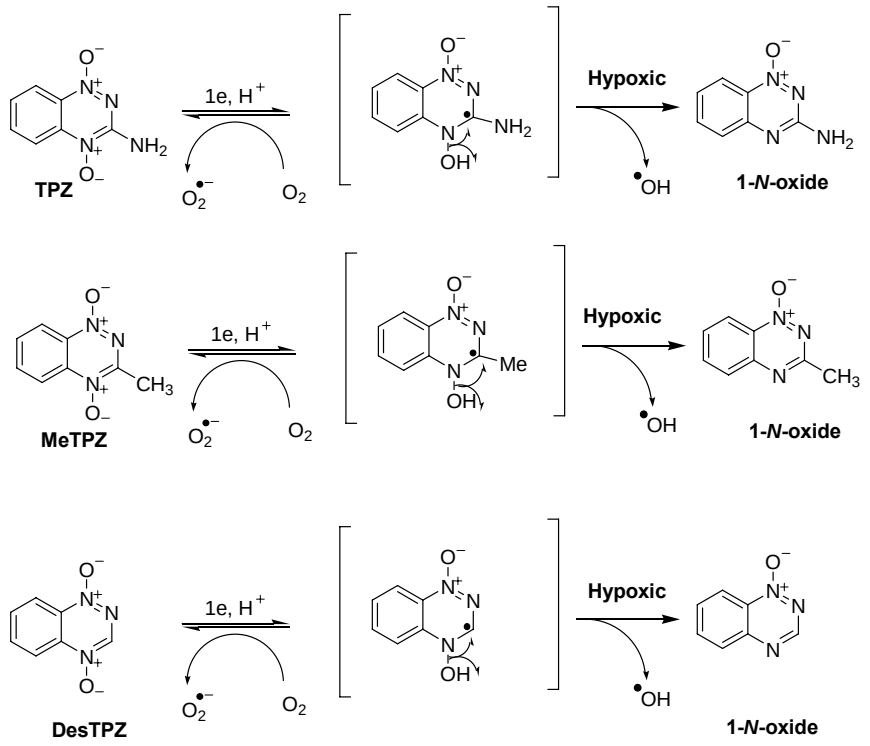

Scheme 4: Proposed mechanism of generation of hydroxyl radical from activated TPZ, MeTPZ and DesTPZ.

3.3. Hypoxia-Selective, Enzyme-Activated DNA damage by TPZ, MeTPZ and desTPZ: The hypoxia-selective cytotoxicity of MeTPZ is very similar to TPZ.[19] Moreover DesTPZ, another analogue of TPZ also display cytotoxicity under hypoxic condition.[27] Other group members in our lab showed that these compounds MeTPZ and desTPZ cause redox-activated DNA damage that mirrors TPZ.[29] In addition to that one electron reductive activation of TPZ by enzyme system such as NADPH:cytochrome P450 reductase or X/XO produces 3-amino-1,2,4-benzotriazine-1-oxide as the major metabolite (**1-*N*-oxide**) (**Scheme 5**)[13,30,31] and 3-amino-1,2,4-benzotriazine (**no-*N*-oxide**), 3-amino-1,2,3-benzotriazine 4-oxide (**4-*N*-oxide**) as minor metabolites.[13,30,31]

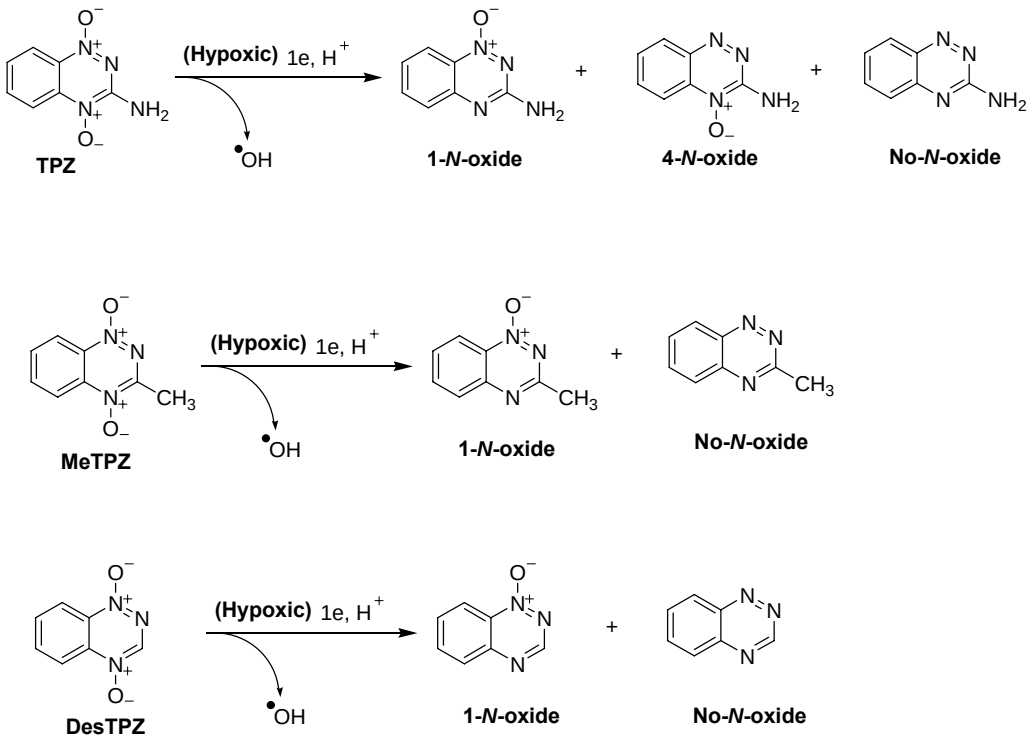

Scheme 5: Metabolites of TPZ, MeTPZ and DesTPZ produced by enzymatic metabolism of TPZ, MeTPZ and DesTPZ.

Similar to TPZ in case of both MeTPZ and desTPZ, the metabolites are 1-*N*-oxides and No-*N*-oxides (**Scheme 5**) which is determined in our lab.[29] Now, to determine whether dehydration mechanism is operative in case of MeTPZ, a isotopic labeling study was performed by other member in our lab.[29] In this work, MeTPZ was incubated with NADPH:cytochrome P450 reductase in presence of deuterated buffer containing hydrogen donor CD_3OD. The isotopic content of the 1-*N*-oxide was analyzed by mass spectroscopy (LC/ESI-MS in the positive ion mode). It was found that the resulting 3-methyl-1,2,4-benzotriazine 1-oxide consists of only 5% of the deuterated product and 95% of the protio product (**1-*N*-oxide**).

Therefore, these observations do not support that benzotriazinyl radical is the main DNA-damaging intermediate whereas it indirectly supports the alternative mechanism involving release of hydroxyl radical from activated MeTPZ.

3.4. Trapping of hydroxyl radical generated from redox activated TPZ, MeTPZ and DesTPZ:

We set at to provide evidence for the production of hydroxyl radical from activated TPZ, MeTPZ and desTPZ as shown in **Scheme 4**. Salicylic acid is a well known hydroxyl radical trapping agent.[32,33] Hydroxyl radical on treatment with salicylic acid produce 2,3-dihydroxybenzoic acid and 2,5-dihydroxybenzoic acid (**Scheme 6**).[32,33]

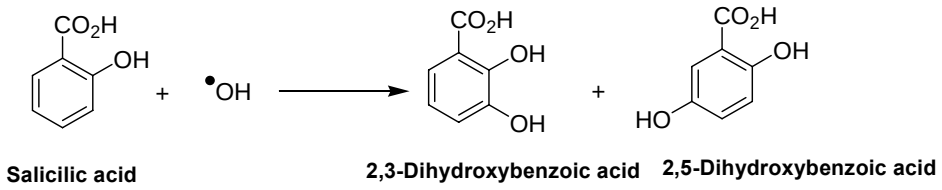

Scheme 6: Trapping of hydroxyl radical by salicylic acid.

Therefore, in our study, we used salicylic acid as a hydroxyl radical trapping agent. Excess amount (10 mM) of salicylic acid was incubated with TPZ or MeTPZ or DesTPZ in presence of NADPH:cytochrome P450 reductase system under anaerobic condition. In a typical assay, stock solutions of TPZ or MeTPZ or DesTPZ in sodium phosphate buffer, NADPH, desferal and salicylic acid were degassed by performing three cycles of freeze pump thaw to remove dissolved oxygen from the solutions and then to initiate the reaction cytochrome P450 reductase and catalase were added to the reaction mixture in argon filled glove bag and the reaction mixture was incubated for18 hours inside the glove bag. As a control experiment salicylic acid without the drug was incubated with NADPH:cytochrome P450 reductase under anaerobic condition. Catalase and desferal were added in the reaction mixture to prevent generation of hydroxyl radical due to redox cycling. Another control experiment was done by incubating TPZ or MeTPZ with excess amount of salicylic acid in presence of sodium phosphate buffer (50 mM, pH 7) at room temperature under aerobic condition for 16-18 hours. Reaction mixtures were analyzed by performing reverse phage HPLC.

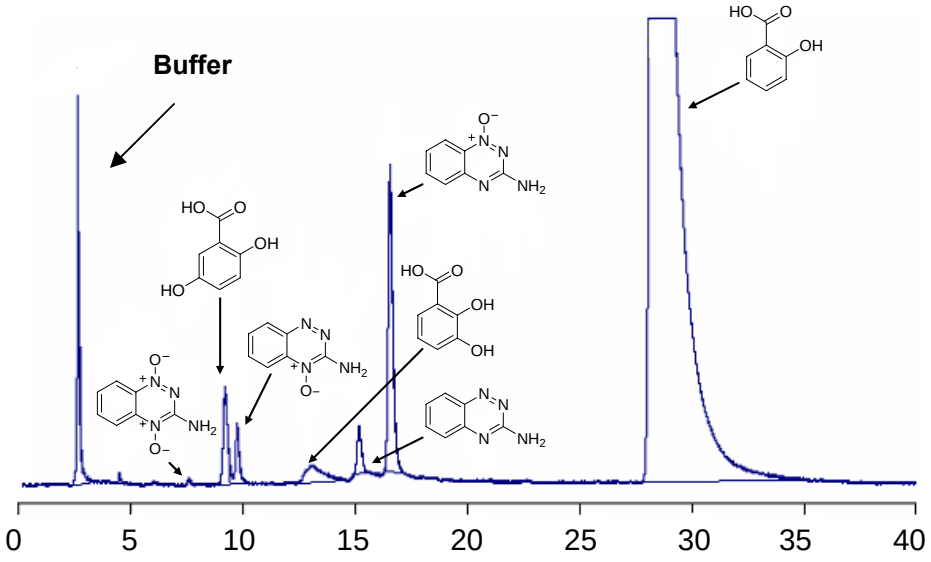

Figure 3: HPLC trace of products arising from *in vitro* anaerobic metabolism of TPZ in the presence of well known hydroxyl radical trapping agent salicylic acid. A 300 µL solution of sodium phosphate buffer (pH 7.0, 50 mM), TPZ (250 µM), catalase (50 µg/mL), desferal (1 mM) and salicylic acid (10 mM) were incubated with cytochrome P450 reductase (50 mU/mL) and NADPH (1 mM) under anaerobic conditions for 18 h.

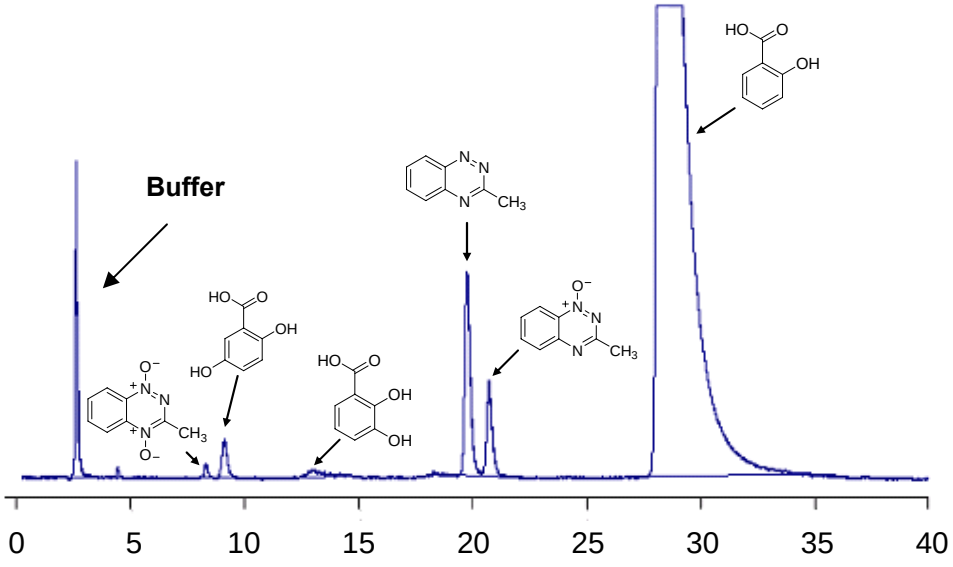

Figure 4: HPLC trace of products arising from *in vitro* anaerobic metabolism of MeTPZ in the presence of well known hydroxyl radical trapping agent salicylic acid. A 300 µL solution of sodium phosphate buffer (pH 7.0, 50 mM), MeTPZ (250 µM), catalase (50 µg/mL), desferal (1 mM) and salicylic acid (10 mM) were incubated with cytochrome P450 reductase (50 mU/mL) and NADPH (1 mM) under anaerobic conditions for 18 h.

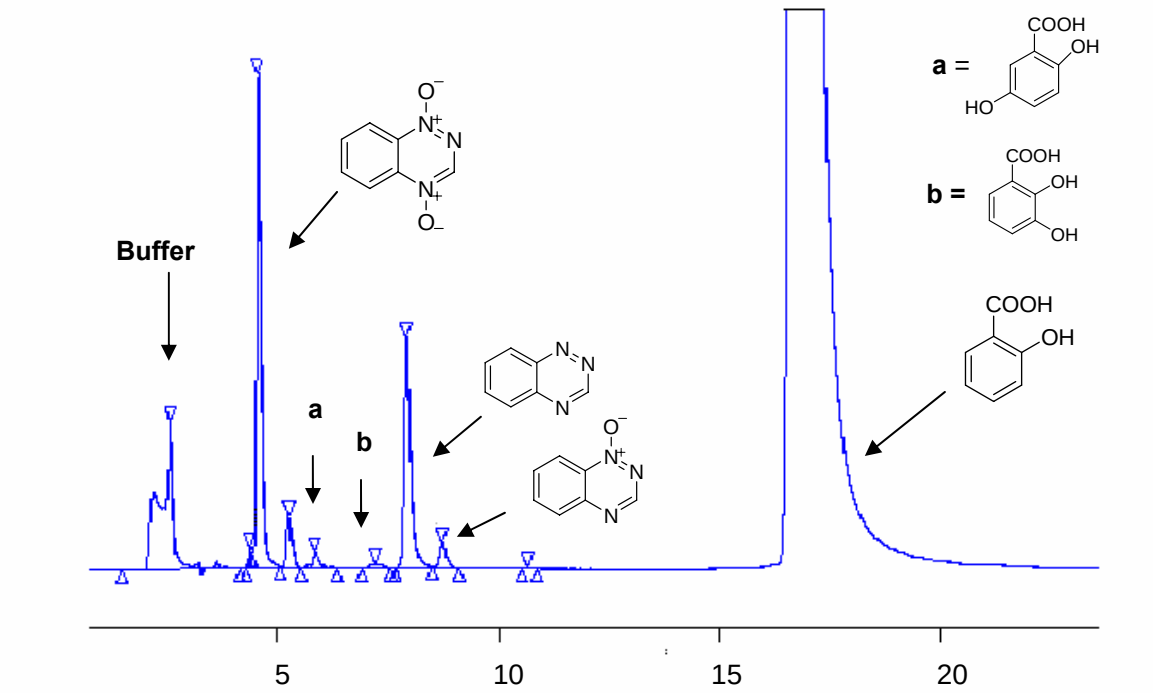

Figure 5: HPLC trace of products arising from *in vitro* anaerobic metabolism of DesTPZ in the presence of well known hydroxyl radical trapping agent salicylic acid. A 300 µL solution of sodium phosphate buffer (pH 7.0, 50 mM), DesTPZ (250 µM), catalase (50 µg/mL), desferal (1 mM) and salicylic acid (10 mM) were incubated with cytochrome P450 reductase (50 mU/mL) and NADPH (1 mM) under anaerobic conditions for 18 h.

We found that enzymatic activation of TPZ, MeTPZ and DesTPZ under hypoxic conditions in presence of salicylic acid produced the expected 2,3-dihydroxybenzoic acid and 2,5-dihydroxybenzoic acid. We calculated the concentration (and yield) of hydroxylated products generated from each compound by preparing a calibration curve (peak area versus. concentration) of both 2,3-dihydroxybenzoic (2,3-DHB) and 2,5-dihydroxybenzoic acid (2,5-DHB).

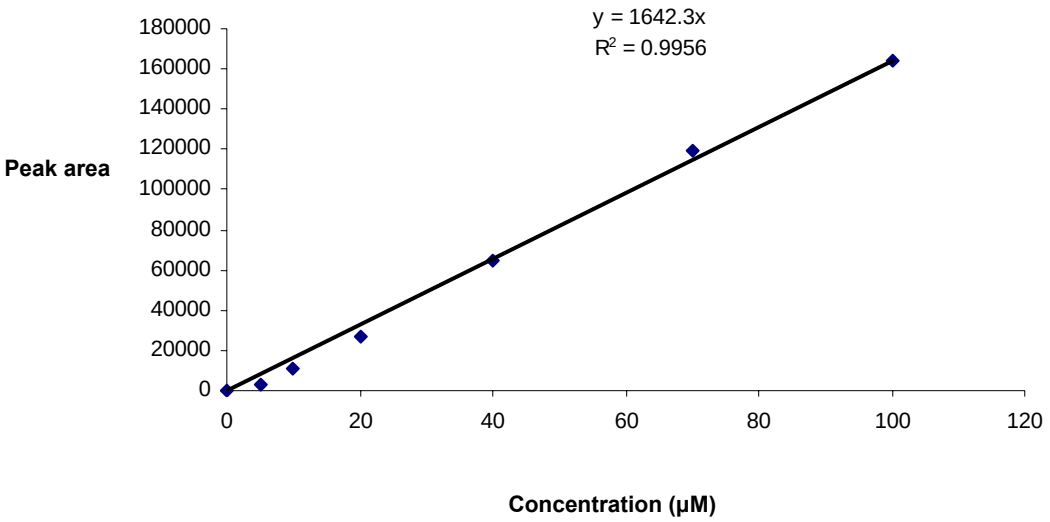

Figure 6: Calibration curve of 2,3-dihydroxybenzoic acid.

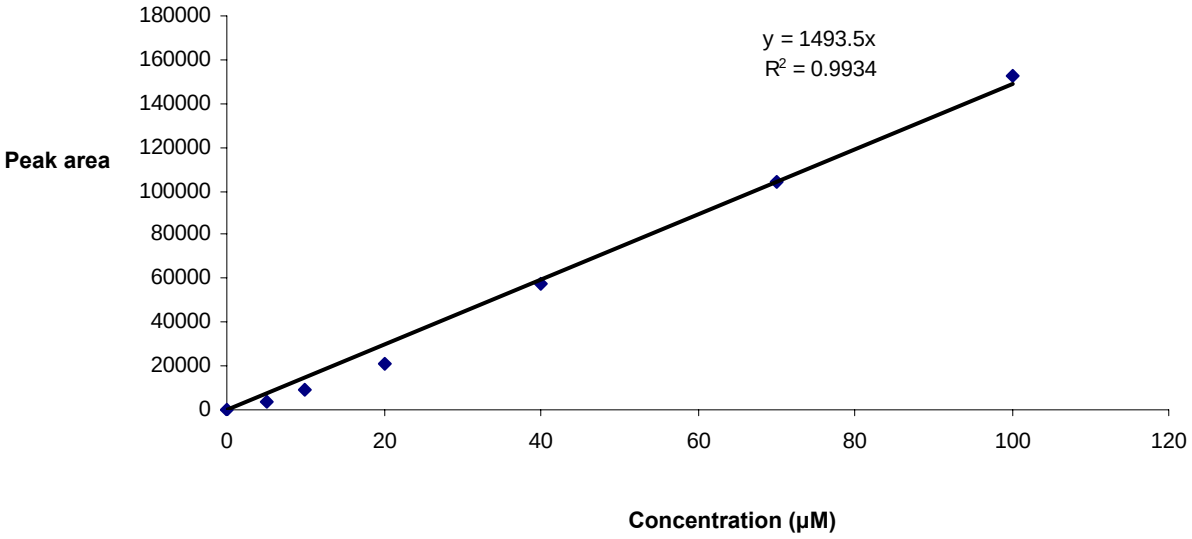

Figure 7: Calibration curve of 2,5-dihydroxybenzoic acid.

We found that DesTPZ was extensively metabolized in presence of NADPH:cytochrome P450 reductase and produced a higher amount of 2,3-dihyderoxybenzoic acid and 2,5-dihydroxybenzoic acid with14.2% yield compare to TPZ 6.12% and MeTPZ 5.40% (**Table 1**). The yield of hydroxylated products generated both from TPZ and MeTPZ is comparable as shown in **Table 1**. Control experiments showed that incubation of salicylic acid with the NADPH:cytochrome P450 reductase systems in the absence of drugs and incubation of salicylic acid with only drugs in the absence of enzyme didn't yield significant amount of these hydroxylated products.

Drug	Initial drug concentration (μM)	Consumption of drug (μM)	Concentration of 2,5 DHB (μM)	Concentration of 2,3 DHB (μM)	2,5 DHB (moles)	2,3 DHB (moles)	Moles of consumptions of drug	Total yield (moles)	% yield
DesTPZ	250	243.67	18.36	12	0.0055	0.0036	0.0091	0.010	12.46
TPZ	250	214.63	4.6	3.37	0.0014	0.0010	0.0024	0.004	3.71
MeTPZ	250	167.74	2.41	1.31	0.0007	0.0004	0.0011	0.0027	2.21

Table 1: Table for comparative study of yield of 2,3-dihydroxybenzoic acid & 2,5-dihydroxybenzoic acid obtained from TPZ, MeTPZ and DesTPZ.

The identity of hydroxylated products was confirmed by LC/ESI-MS operated in the negative ion mode (**Figure 8**).

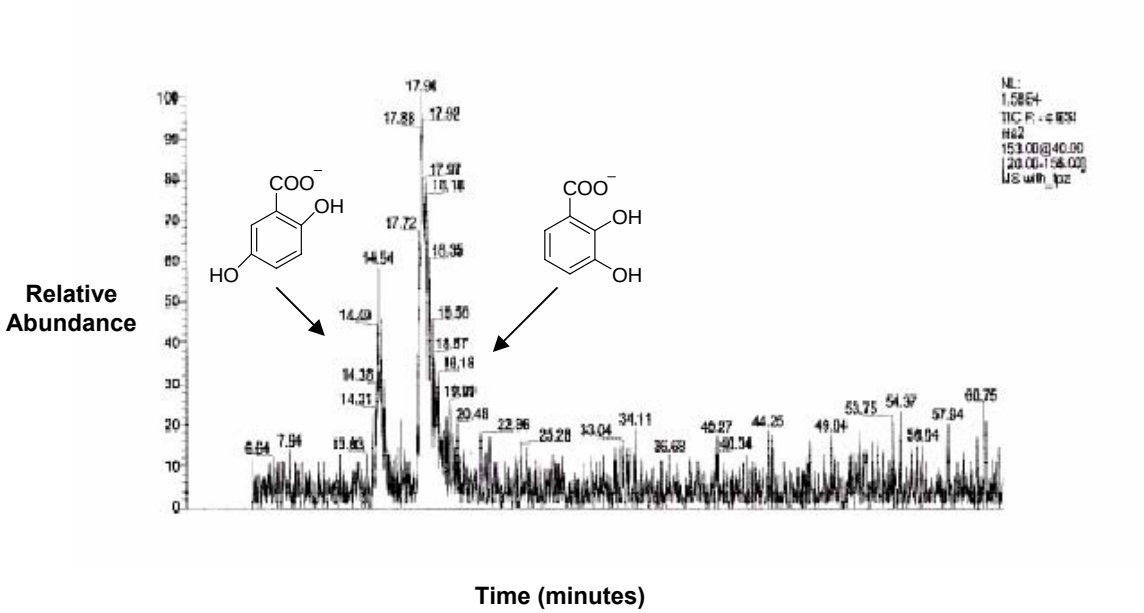

Figure 8: LC/MS analysis of products arising from *in vitro* anaerobic metabolism of TPZ in the presence of well known hydroxyl radical trapping agent salicylic acid. The hydroxylated products means 2,3-dihydroxybenzoic acid and 2,5-dihydroxybenzoic acid were detected by using reverse phase HPLC method and mass of the peaks (m/z = 153) was determined by operating ESI negative ion mode. The above selected ion chromatogram was obtained by monitoring the single ion of mass 153. A 300 µL solution of sodium phosphate buffer (pH 7.0, 50 mM), TPZ (250 µM), catalase (50 µg/mL), desferal (1 mM) and salicylic acid (10 mM) were incubated with xanthine (750 µM), XO (0.6 U/mL) under anaerobic conditions for 18 h.

We also examined the reaction of salicylic acid with hydroxyl radical generated by γ-radiolysis of N_2O-saturated solutions to produce 2,3-dehydroxybenzoic acid and 2,5-dihydroxybenzoic acid. These hydroxylated products were identified by reverse phase HPLC and LC/MS/MS analysis operating in the negative ion mode (**Figure 9** and **Figure 10**).

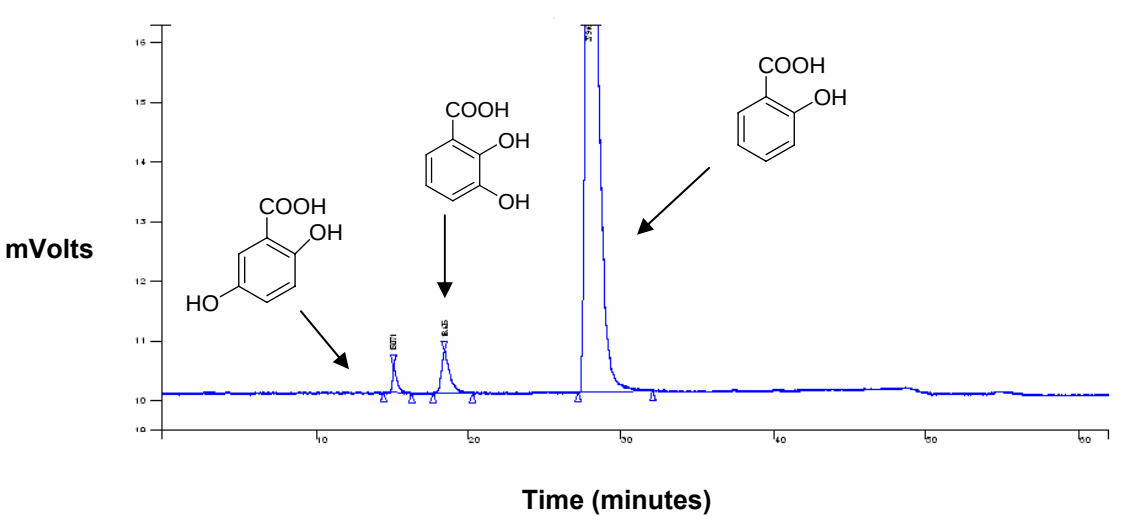

Figure 9: HPLC trace of products arising from radiolysis of N_2O-saturated water in presence of salicylic acid. A 500 µL N_2O-saturated solution of 5 mM salicylic acid in water was exposed to γ radiation for 90 h 30 min (124890 rads). Next the reaction mixture was analyzed by reverse phase HPLC.

A.

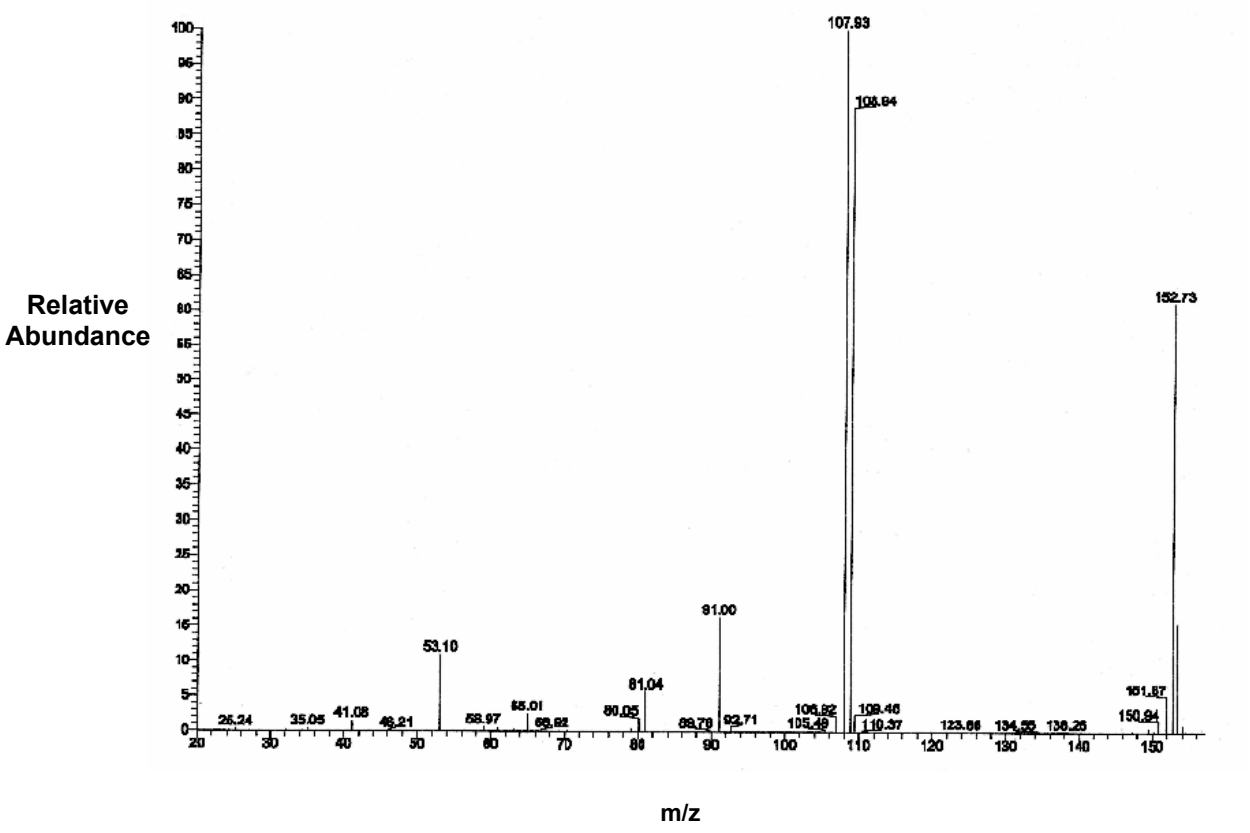

B.

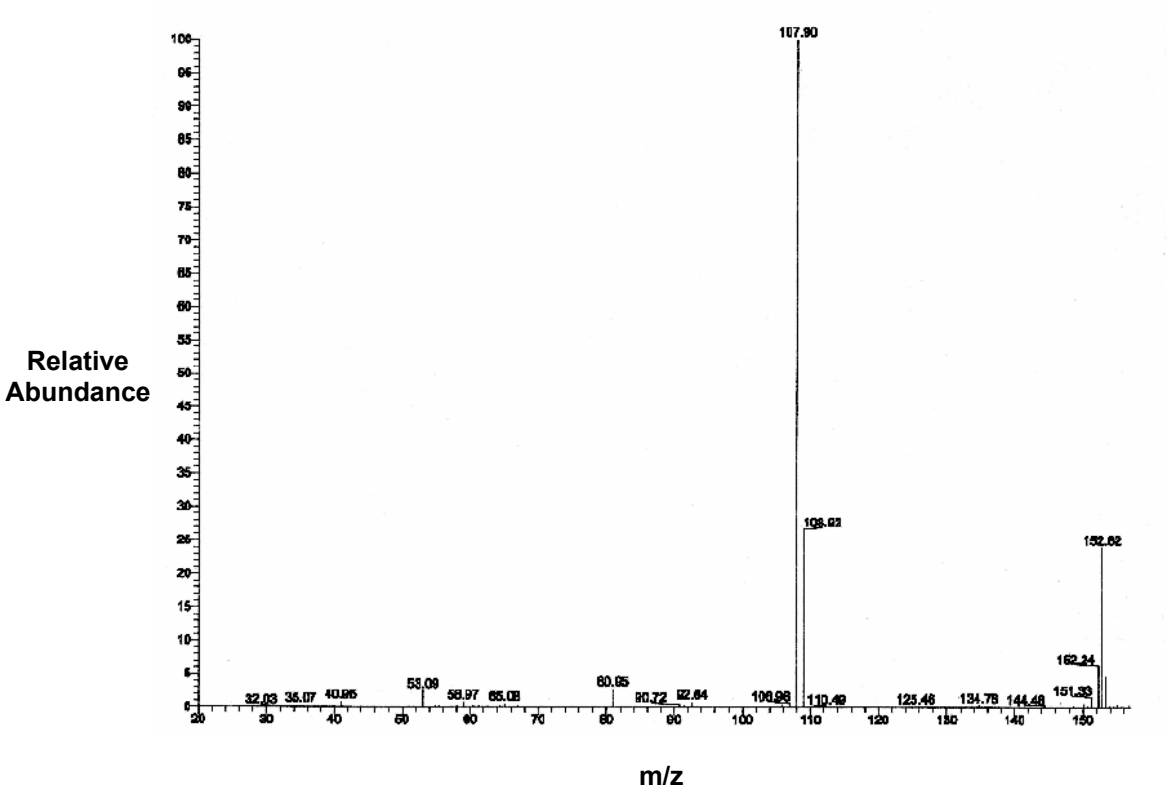

Figure 10: LC/MS/MS analysis of products arising from trapping of hydroxyl radical generated by γ-radiolysis of water by salicylic acid. A 500 μL N_2O-saturated solution of 5 mM salicylic acid in water was exposed to γ radiation for 90 h 30 min (124890 rads). Next the reaction mixture was analyzed by LC/MS/MS analysis operating in ESI negative ion mode. **A.** LC/MS/MS analysis of 2,3-dihydroxybenzoic acid obtained by reaction of hydroxyl radical with salicylic acid. **B.** LC/MS/MS analysis of 2,5-dihydroxybenzoic acid obtained by reaction of hydroxyl radical with salicylic acid.

LC/MS/MS analysis was operated in negative ion mode. In case 2,3-dihydroxybenzoic acid the parent ion peak comes at 153 m/z and another small peak comes at 152 m/z due to removal of one proton from one of the phenolic OH groups. Decarboxylation from the parent ion peak of mass 153 generates daughter ion peak at 109 m/z and one more daughter ion peak is generated at m/z 91 due to dehydration from the daughter ion peak of mass 109. In case of 2,5-dihydroxybenzoic acid the parent ion peak comes at 153 m/z. Removal of CO_2 from the parent ion peak generates daughter ion peak

at 109 m/z and another peak at 108 m/z due to removal of proton from phenolic OH group.

3.5. Conclusion:

Improved understanding of the molecular mechanisms underlying the biological activities of novel antitumor agent can facilitate to design better drugs. As TPZ exhibits promising antitumor properties and is the lead compound in a new chemical class of hypoxia selective anticancer drugs,[1,2,12] it is important to understand the chemical mechanism responsible for the medicinal properties of this class of molecules.[3,4,14,15,15,25,26] In the recent literature three mechanisms have been considered to explain the bioactivation of 3-amino 1,2,4-benzotriazine 1,4-dioxides or TPZ that initiates DNA strand cleavage under hypoxic conditions. Based upon characterization of the DNA damage products generated by TPZ we proposed a mechanism where TPZ generates radical intermediate due to one electron reductive activation and that radical intermediate release well known DNA damaging agent hydroxyl radical by homolysis of the N-OH bond and also yield mono-*N*-oxide metabolite (**Scheme 4**).[3,15,16,38,34] Early studies support that structurally-related heterocyclic nitrogen radicals lead to this type of homolytic N-O bond scission.[35,36,37] Alternatively resent literature has suggested that the radical intermediate (**Scheme 2, pathway b**) undergoes dehydration to generate benzotriazinyl radical which leads to DNA damage.[21]

As TPZ analogues both MeTPZ and DesTPZ display potent hypoxia-selectivity against cancer cell lines that is comparable to that of TPZ we felt that it might be important to

determine whether this compound also exhibit redox-activated, hypoxia-selective DNA strand cleavage analogous to TPZ.

The results presented here provide the first evidence that TPZ analogues MeTPZ and DesTPZ cause hypoxia-selective oxidative DNA strand cleavage by one-electron reductive activation and DNA damage properties of those drugs are similar to TPZ. The evidence suggests that one-electron reductive activation of MeTPZ and DesTPZ leads to generation of highly reactive, nonselective oxidizing radical that causes strand cleavage via abstraction of hydrogen atoms from the deoxyribose backbone. Our hydroxyl radical trapping experiment directly provides evidence that TPZ and its analogues generate hydroxyl radical upon one-electron reductive activation. Moreover it has been shown in our lab that bioreductive activation of MeTPZ in solvent mixtures composed of CD_3OD/D_2O generates predominantly the non-deuterated product **1-*N*-oxide** of MeTPZ (95%) with only small amounts (5%) of the deuterated metabolite. Thus, hydroxyl radical trapping experiments in conjugation with CD_3OD/D_2O isotopic labeling study indicates that benzotriazinyl radicals should not be invoked as *general* intermediates to account for hypoxia-selective, bioreductively-activated DNA strand cleavage by the 1,2,4-benzotriazine 1,4-dioxide antitumor agents, rather our results are consistent with the mechanism involving release of hydroxyl radical to explain oxidative DNA damage by this class of molecules. It remains possible that TPZ damages DNA either via hydroxyl radical pathway or via multiple mechanistic pathways. The higher acidity of the amino hydrogen in TPZ relative to methyl hydrogen in MeTPZ might facilitate formation of benzotriazinyl radical intermediate. Overall, the trapping of hydroxyl radical released from TPZ, MeTPZ and DesTPZ suggest that a single, unified mechanism involving the

release of hydroxyl radical from the drug radical intermediate may best rationalize the redox-activated, hypoxia selective DNA damaging properties of the 1,2,4-benzotriazine 1,4-dioxide family of antitumor agents.

Materials & Methods:

Materials: Materials with highest purity available were obtained from following sources. Sodium phosphate, xanthine from Aldrich Chemical Co. (Milwaukee, WI); NADPH, desferal, cytochrome P450 reductase and catalase from Sigma Chemical Co. (St. Louis, MO); xanthine oxidase from Roche Molecular Biochemicals (Indianapolis, IN); HPLC grade solvents (acetonitrile, methanol) and acetic acid from Fischer (Pittsburg, PA); salicylic acid, 2,3-dihydroxybenzoic acid and 2,5-dihydroxybenzoic acid from Sigma Chemical Co. (St. Louis, MO); TPZ was synthesized according to literature methods. [Fuchs, T.; Chowdhury, G.; Barnes, C. L.; Gates, K. S. *J. Org. Chem.* 2001, 66, 107-114].

Hydroxyl radical trapping experiments with salicylic acid: In a typical assay, TPZ, Me-TPZ or Des-TPZ (250 μM), salicylic acid (10 mM), NADPH (1 mM), sodium phosphate buffer (50 mM, pH 7), water and desferal (1 mM) were taken in separate pyrex tubes and degassed by three cycles of freeze-pump-thaw. Pyrex tubes containing degassed solutions were scored and opened in an argon filled glove bag. Reaction solution (300 μL) was prepared by using sodium phosphate buffer (50 mM, pH 7), desferal (1 mM), catalase (50 μg/mL), NADPH (1 mM), cytochrome P450 reductase (50 mU/mL) and TPZ, Me-TPZ or Des-TPZ (250 μM). Enzyme stock solutions were prepared with degassed water. Control reaction was prepared similar to the reaction mixture except adding the drug. The reaction mixtures were incubated for 16-18 h in an argon filled glove bag. Another control experiment was done by incubating TPZ or MeTPZ (250 μM) with salicylic acid (10 mM) in presence of sodium phosphate buffer

(50 mM, pH 7) at room temperature under aerobic condition for 16-18 hours. After incubation enzymes present in reactions were removed using Amicon Microcon (YM3) filters. The filtrates were analyzed by reverse phase HPLC. Products formed in TPZ or MeTPZ reactions were analyzed using C18 reverse phase Rainin Microsorb-MV column (5 μm, particle size, 100 A^o pore size, 25 cm length, 4.6 mm i.d.) eluted with gradient solvent system starting with 80% A (0.5 % acetic acid in water) and 20% B (2:1 methanol/acetonitrile) followed by linear increase to 30% B from 0 min to 20 min. Then, 30% B was held until 30 min and in next 10 min 20% B was achieved. The flow rate of 0.9 mL/min was used and the products were monitored by UV-absorbance at 310 nm. Products obtained from DesTPZ reaction were analyzed using the same gradient but with the solvent system containing 2% acetic acid in water (aqueous) and acetonitrile (organic). Hydroxylated products (2,5 dihydroxy benzoic acid & 2,3 dihydroxy benzoic acid) obtained from TPZ (250 μM) with reaction with xanthine (750 μM), XO (0.6 U/mL) instead of NADPH:cytochrome P450 reductase in presence of catalase (50 μg/mL), desferal (1mM), sodium phosphate buffer (50 mM) and salicylic acid (5mM) was identified by LC/ESI-MS analysis. LC/MS analysis was performed by using TSQ7000 triple-quadruple mass spectrometer where we used a C18 reverse phase column eluted with gradient solvent system starting with 95% A (2% acetic acid in water) and 5% B (methanol) for 2 minutes followed by gradual increase of B to 25% from 2 min to 10 min, to 40% from 10 min to 20 min, to 50% from 20 min to 30 min, to 80% from 30 min to 45 min, then 5% B is achieved with in 2 minutes and is held for next 15 minutes. The flow rate was 0.9 mL/min and the products were monitored by UV-absorbance at 310 and

278 nm. The mass of the products were determined by operating ESI-MS negative ion mode.

Hydroxyl radicals obtained from γ-radiolysis of water was also trapped by salicylic acid. In a typical radiolysis assay, 5 mM salicylic acid in water by total volume 500 μL was taken in a pyrex tube and degassed by four cycles of freeze-pump-thaw. Pyrex tube containing degassed solution was sealed, scored and opened in an argon filled glove bag. After that the degassed solution was saturated with N_2O by passing N_2O through the solution for 5-7 minutes and then N_2O saturated solution was transferred to a small, dry, N_2O saturated small pyrex tube. After that the reaction mixture was exposed to γ radiation for 90 h 30 min (124890 rads). Next the reaction mixture was analyzed by reverse phase HPLC in a similar method described above and the hydroxylated products were identified by LC/MS/MS analysis operating in ESI negative ion mode.

References:

1. Brown, J. M. *Cancer Res*. **1999**, *59*, 5863-5870.
2. Brown, J. M.; Wang, L. *Anti-Cancer Drug Design* **1998**, *13*, 529-539.
3. Daniels, J. S.; Gates, K. S. *J. Am. Chem. Soc*. **1996**, *118*, 3380-3385.
4. Denny, W. A. *The Lancet* **2000**, *1*, 25-29.
5. Brown, J. M. *Br. J. Cancer* **1993**, *67*, 1163-1170.
6. Brown, J. M.; Siim, B. G. *Seminars Rad. Oncol*. **1996**, *6*, 22-36.
7. Monge, A.; Martinez-Crespo, F. J.; de Cerain, A. L.; Palop, J. A.; Narro, S.; Senador, V.; Marin, A.; Sainz, Y.; Gonzalez, M.; Hamilton, E.; Barker, M. S. *J. Med. Chem.* **1995**, *38*, 4488-4494.
8. Monge, A.; Palop, J. A.; Cerain, A.; Senador, V.; Martinez, F. J.; Sainz, Y.; Narro, S.; Garcia, E.; Miguel, C. *J. Med. Chem.* **1995**, *38*, 1786-1792
9. Solano, B.; Junnotula, V.; Marin, A.; Villar, R.; Burguete, A.; Vicente, E.; Perez-Silanes, S.; Aldana, I.; Monge, A.; Dutta, S.; Sarkar, U.; Gates, K. S. *J. Med. Chem.* **2007**, *50*, 5485-5492.
10. Cerecetto, H.; Gonzalez, M.; Lavaggi, M. L.; Azqueta, A.; Lopez de Cerain, A.; Monge, A. *J. Med. Chem.* **2005**, *48*, 21-23.
11. Von Powel, J.; Von Roemeling , R.; Gatzemeier, U.; Boyer, M.; Elisson, L. O.; Clark, P.; Talbot, D.; Rey, A.; Butler, T. W.; Hirst, V.; Olver, I.; Bergman, B.; Ayoub, J.; Richardson, G.; Dunlop, D.; Arcenas, A.; Vescio, R.; Viallet, J.; Treat, J. *J. Clin. Oncol*. **2000**, *18*, 1351-1359.
12. Brown, J. M.; Wilson, W. R. *Nature Review* **2004**, *4*, 437-447.

13. Laderoute, K.; Wardman, P.; Routh A. M. *Biochem Pharmacol*. **1988**, *37*, 1487-1495.

14. Priyadarsini, K. I.; Tracy, M.; Wardman, P. *Free. Radic. Res.* **1996**, *25*, 393-402.

15. Kotandeniya, D.; Ganley, B.; Gates, K. S. *Bioorg. Med. Chem. Lett*. **2002**, *12*, 2325-2334.

16. Birincioglu, M.; Jaruga, P.; Chowdhury, G.; Rodriguez, H.; Dizdaroglu, M.; Gates, K. S. *J. Am. Chem. Soc*. **2003**, *125*, 11607-15.

17. Fitzsimmons, S. A.; lewis, A. D.; Riley, R. T.; Workman, P. *Carcinogenesis* **1994**, *15*, 1503-10.

18. Halliwell, B.; Gutteridge, J. M. *Arch Biochem. Biophy.* **1990**, *280*, 1-8.

19. Bagley, A. C.; Krall, J.; Lynch, R. E. *Proc. Natl. Acad. Sci. USA.* **1986**, *83*, 3189-3193.

20. Chowdhury, G.; Junnotula, V.; Daniels, J. S.; Greenberg, M. M.; Gates, K. S. *J. Am. Chem. Soc.* **2007**, *129*, 12870-12877.

21. Anderson, R. F.; Shinde, S. S.; Hay, M. P.; Gamage, S. A.; Denny, W. A. *J. Am. Chem. Soc.* **2003** *125*, 748-56.

22. Jiang, F.; Yang, B.; Fan, L.; He, Q.; Hu, Y. *Bioorg. Med. Chem. Lett.* **2006**, *16*, 4209-13.

23. Zeman, E. M.; Baker, M. A.; Lemmon, M. J.; Pearson, C. I.; Adams, J. A.; Brown, J. M.; Lee, W. W.; Tracy, M. *Int. J. Radiat. Oncol. Biol. Phys.* **1989**, *16*, 977-81.

24. Kelson, A. B.; McNamara, J. P.; Pandey, A.; Ryan, K. J.; Dorie, M. J.; McAfee, P. A.; Menke, D. R.; Brown, J. M.; Tracy, M. *Anticancer Drug Des.* **1998**, *13*, 575-92.

25. Hay, M. P.; Pruijn, F. B.; Gamage, S. A.; Liyanage, H. D.; Kovacs, M. S.; Patterson, A. V.; Wilson, W. R.; Brown, J. M.; Denny, W. A. *J. Med. Chem.* **2004** , *47*, 475-88.

26. Hay, M. P.; Gamage, S. A.; Kovacs, M. S.; Pruijn, F. B.; Anderson, R. F.; Patterson, A. V.; Wilson, W. R.; Brown, J. M.; Denny, W. A. *J. Med. Chem.* **2003**, *46*, 169-82.

27. Minchinton, A. E.; Lemmon, M. J.; Tracy, M.; Pollart, D. J.; Martinez, A. P.; Tosto, L. M.; Brown, J. M. *Int. J. Radiat. Oncol. Biol. Phys.* **1992**, *22*, 701-5.

28. Cerecetto, H.; Gonzalez, M. *Mini Rev. Med. Chem.* **2001**, *1*, 219-31.

29. Synthesis of TPZ, MeTPZ and DesTPZ, DNA damage assay, *in vitro* metabolism study and isotopic labeling study were performed by Venkatraman Junnotula in our lab.

30. Laderoute, K. R.; Routh, A. M. *Biochem. Pharmacol.* **1986**, *35*, 3417-20.

31. Fuchs, T.; Chowdhury, G.; Barnes, C. L.; Gates, K. S. *J. Org. Chem.* **2001**, *66*, 107-14.

32. Halliwell, B.; Kaur, H. *Free Radic. Res.* **1997**, *27*, 239-44.

33. Kaur, H.; Whiteman, M.; Halliwell, B. *Free Radic. Res.* **1997**, *26*, 71-82.

34. Ganley, B.; Chowdhury, G.; Bhansali, T.; Daniels, J. S.; Gates, K. S. *Bioorg. Med. Chem.* **2001**, *9*, 2395-401.

35. Nagai, K.; Carter, J. B.; Xu, J.; Hecht, M. S. *J. Am. Chem. Soc.* **1991**, *113*, 5099-5100.

36. Nagai, K.; Hecht, M. S. *J. Biol. Chem.* **1991**, *266*, 23994-24002.

37. Lorance, E. D.; Kramer, W. H.; Gould, I. R. *J. Am. Chem. Soc.* **2002**, *124*, 15225-38.

38. Chowdhury, G.; Kotandeniya, D.; Daniels, J. S.; Barnes, C. L.; Gates, K. S. *Chem. Res. Toxicol.* **2004**, *17*, 1399-405.

Chapter 4: Is the Tirapazamine radical Capable of hydrogen atom abstraction? A Preliminary Study

4.1. Introduction: Presence of hypoxia, or regions containing low oxygen concentration, in solid tumor cells was demonstrated by Thomlinson and Gray.[1] The concentration of oxygen in human tumors in terms of partial pressure is 7-12 mm Hg whereas in normal cell it is 40-51 mm Hg.[3] It is known that due to presence of low level of oxygen in the solid tumor, tumor cells are resistant by ionization radiation.[2,3,4] In case of oxygenated (normal) cell, oxygen reacts with DNA radicals which formed by ionizing radiation and leads to DNA damage. DNA damage causes cytotoxicity. In the case of hypoxic (tumor) cells, in absence of oxygen DNA radical is restored to its original undamaged form by hydrogen donation from nonprotein sulfhydryls in the cells (**Scheme 1**).[3,5] Thus, the cell-killing ability of ionizing radiation is suppressed in tumor cells due to hypoxia.

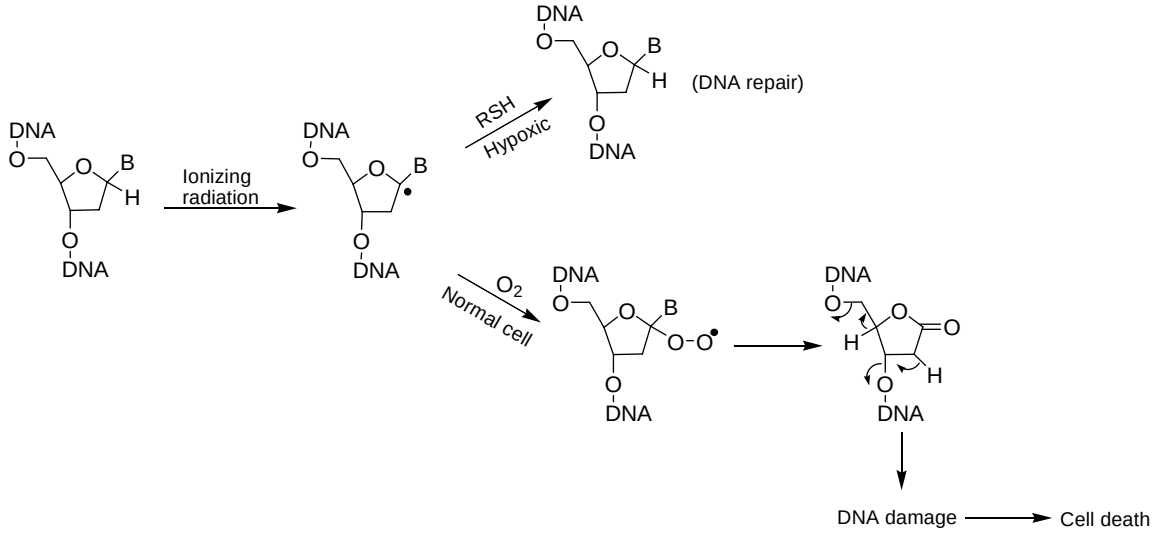

Scheme 1: Effect of ionizing radiation in both normal cell and hypoxic tumor cell.[5,22]

To resolve the problem of radiation resistance by hypoxic tumor cells, nitroimidazoles such as, etanidazole were discovered which could mimic oxygen and consequently sensitize hypoxic cells towards radiation.[3,5,14]

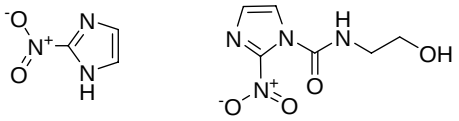

Figure 1: Example of nitroimidazole.[22]

Although clinical trials using nitroimidazoles with ionizing radiation were conducted, the outcome of these clinical trials was not successful due to dose-limiting toxicity.[3,6] In addition to radiotherapy solid tumors are also resistant to most of the anticancer drugs due to various factors.[3] One such factor is that hypoxic cells are situated far from the blood vessels and are not sufficiently exposed to some types of anticancer drugs.[3,7,8] Moreover it has been found that some anticancer agents for example, bleomycin display oxygen-dependent cytotoxicity and as a result hypoxic tumor cells are also resistant to these drugs.[3,9,10] Beside this, hypoxia up regulates genes which are involved in developing resistance against anticancer drugs.[3,11,12]

Although tumor hypoxia causes problems by generating resistance against currently available cancer therapies,[3,5] under appropriate condition tumor hypoxia can be a unique target which could be utilized to selectively kill cancer cells in solid tumors.[3,5] At first Lin *et. al.* proposed the idea that tumor hypoxia can be exploited to achieve therapeutic advantages in cancer therapy and accordingly he suggested that some compounds containing quinone moiety will be more toxic under hypoxic condition.[13]

Overall, this led to the development of hypoxia-selective cytotoxins. Hypoxia-selective cytotoxins are also known as bioreductive prodrugs which get reductively activated by chemicals or enzymes *in vivo* to produce an oxygen-sensitive activated intermediate. Under hypoxic condition the activated intermediate causes DNA damage whereas in normal condition the activated intermediate back oxidized to its parent compounds by reaction with molecular oxygen.[15,16] The natural product mitomycin C is the first clinically hypoxia selective cytotoxins.[17,18] Its hypoxia selectivity is modest as in most of the cell lines it shows only 2-fold selectivity to kill hypoxic cells compared to normal oxygenated cells.[19,20] Mitomycin C doesn't react in its quinone form but it undergoes one electron reductive activation by NADPH:cytochrome P450 reductase to form semoquinone or hydroquinone form which is activated intermediate and this activated intermediate causes DNA crosslink under anaerobic condition (**Scheme 2**).[22] In presence of molecular oxygen the activated intermediate of mitomycin C is back oxidized into the unreactive quinone form.[22]

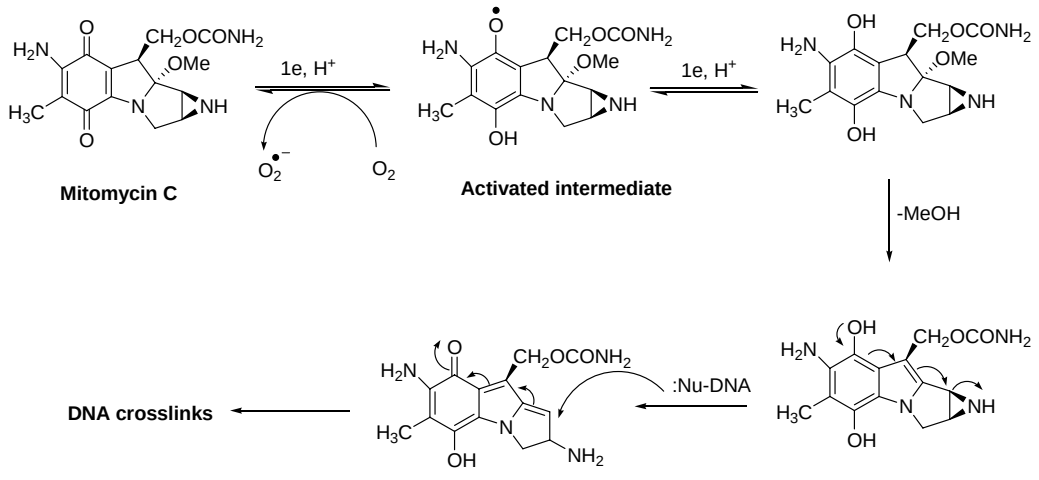

Scheme 2: Mechanism of DNA damage by mitomycin C.[22]

The other redox-activated, hypoxia selective antitumor agents of clinical interest are quinones porfiromycin, EO9, heterocyclic-*N*-oxides including tirapazamine, quinoxaline, phanazine-*N*-oxides, AQ4N (**Figure 2**) etc.[15,16,21,22,23]

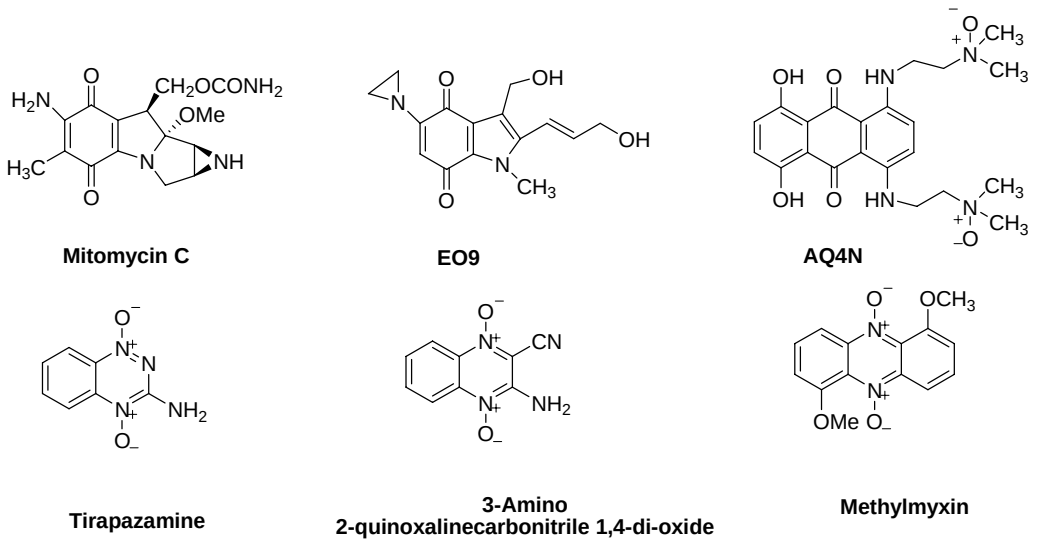

Figure 2: Examples of hypoxia-selective cytotoxins.

Tirapazamine or TPZ is a novel, hypoxia selective, redox activated antitumor agent.[3,5] The hypoxia selective toxicity of TPZ was first studied on a variety of Chinese hamster ovary, mouse, human cell lines and tumors of mouse.[24] The hypoxia cytotoxicity ratio (ratio of concentration required to produce equivalent cytotoxicity under aerobic and anaerobic condition) of TPZ is in the range 15-50 for human cell lines.[5,24,25] The HCR of mitomycin C is in between 1-5 for various cell lines[19,20] and HCR for nitroimidazoles is between 15-20.[26,27] So, far TPZ is the best hypoxia selective anticancer agent and TPZ is currently undergoing phase III clinical trials in combination with cisplatin and ionization radiation for the treatment of various cancer.[25,28-31] One hypothesis to explain the success of TPZ to kill selectively hypoxic cells in clinical trials compare to other bioreductive

prodrugs is its unusual oxygen sensitivity.[32] It has been reported by Koch that TPZ requires higher oxygen concentration for inhibition its metabolism and cytotoxicity compare to nitroimidazole alkylating agent RSU-1069.[33] Besides this, Kevin *et al.* studied the oxygen sensitivity of TPZ by examining both its cytotoxicity and bioreductive metabolism in HT29 colon carcinoma cells under a range of gas phase oxygen concentration and they determined that the oxygen concentration required to inhibit activation of TPZ by 50% (K_{O2}) is approximately 1.21 ± 0.09 μM.[32] So, according to early studies it can be suggested that higher oxygen sensitivity of TPZ makes a superior hypoxia selective cytotoxin.[3,32,33] The cytotoxicity by TPZ arises due to its ability to cause extensive oxidative DNA damage under hypoxic condition.[5,34] TPZ leads to both single strand and double stranded DNA damage.[35,36] Recent study has been demonstrated that, in addition to DNA damage, TPZ also inhibits DNA replication as it is reported that DNA replication has been decreases by 80% in presence of TPZ under hypoxic condition.[22,37] Early studies also suggest that TPZ reduces the activity of topoisomerase II under hypoxic condition.[38] We have already mentioned in our previous chapter that metabolism of TPZ requires one electron reductive activation and TPZ is metabolized into nontoxic mono-*N*-oxide.[5,35,39,40,41,42] TPZ undergoes one electron reductive activation in presence of one electron reducing system and yields radical intermediate **(Scheme 3)**[3,5,35,43] and this radical intermediate causes oxidative DNA damage under hypoxic condition.[5,35,39,40,41,42]

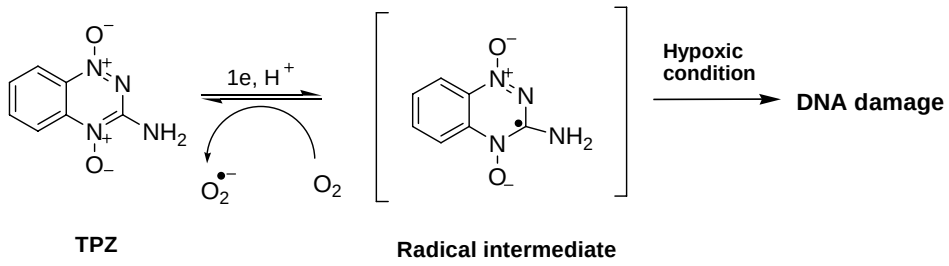

Scheme 3: One electron reductive activation of TPZ.

In normal oxygenated cells, the radical intermediate is back oxidized into parent compound with simultaneous production of superoxide radical (**Scheme 3**) due to redox cycling.[35,43] Early studies suggest that TPZ can be activated by a number of enzymes *in vitro* for example, xanthine oxidase, NADPH:cytochrome P450 reductase and these enzymes are present in cytoplasms.[35,44-48] The cellular enzymes responsible for the activation of TPZ *in vivo* are still a matter of debate. Patterson *et al.* has been identified a correlation between NADPH:cytochrome P450 reductase activity and TPZ mediated DNA damage.[49] Based on early studies it was suggested that although cytoplasm containing NADPH:cytochrome P450 reductase is responsible for the major activation (71 ± 6.7%) of TPZ in cell but it does not contribute TPZ mediated DNA cleavage and cytotoxicity.[44,47] TPZ mediated DNA damage and cytotoxicity occurs by activation of TPZ (~ 20%) in nuclei by nucleus enzymes.[44] As we described in our previous chapter that three proposals are suggested to describe the identity of the reactive intermediate and the mechanistic pathway of DNA damage by TPZ.

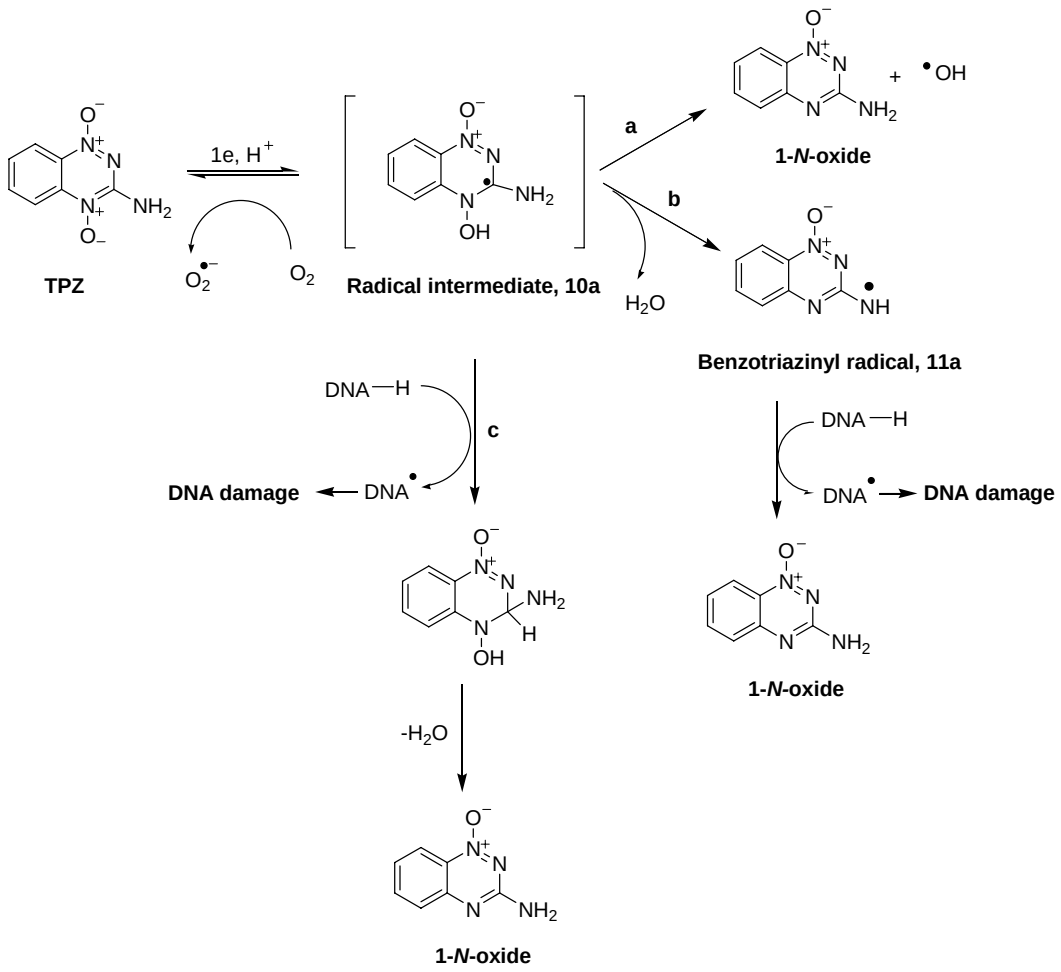

Scheme 4: Three proposed mechanism of DNA damage by TPZ.

Our work support a mechanism (**Scheme 4, pathway a**) in which radical intermediate **10a** undergoes homolysis of N-OH bond to produce 1-*N*-oxide as a metabolite and the known DNA damaging agent hydroxyl radical[39,40] and I have provided direct evidence of release of hydroxyl radical from activated TPZ by trapping hydroxyl radical by salicylic acid in the previous chapter. Alternatively it has been suggested that radical intermediate (**Scheme 4, pathway b**) undergoes dehydration and generate benzotriazinyl radical **11a** which finally initiates DNA damage by abstracting hydrogen

atom from DNA backbone.[50] According to our previous results which is already discussed in **chapter 3** we came to the conclusion that **11a** should not be invoked as general intermediates to account for hypoxia-selective, bioreductively-activated DNA strand cleavage by the 1,2,4-benzotriazine 1,4-dioxide antitumor agents, rather our results are consistent with the another mechanism involving release of hydroxyl radical to explain oxidative DNA damage by this class of molecules. The third mechanism (**Scheme 4, pathway c**) was proposed by Martin Brown and according to his hypothesis **10a** will abstract hydrogen atom directly from macromolecules including DNA (**Scheme 4, pathway c**) to produce DNA radicals which initiates both single-strand and double-strand break.[5] To date no one has examined whether the TPZ radical **10a** can directly abstract hydrogen atoms.

4.2. Goal: In this chapter, I describe whether TPZ is metabolized into1-*N*-oxide by hydrogen atom abstraction pathway where after formation of **10a** by one electron reductive activation, it directly abstracts hydrogen atom from hydrogen donor like GSH and glucose (**Scheme 4, pathway c**). As part of this worked toward a methodology to determine critical oxygen concentration which is defined as the oxygen concentration that inhibit metabolism of TPZ. We used Uv-vis spectroscopy to study oxygen sensitivity of TPZ and to determine whether the presence of hydrogen atom donors alters rate of metabolism of TPZ.

4.3. Effect of potent hydrogen donor glutathione or GSH on the rate of metabolism of TPZ:

Glutathione or GSH is a potential hydrogen atom donor towards oxidizing species and it is found at higher concentration (5-10 mM) in cells of higher animals.[51] The structure of GSH is given below.[51] The pKa of GSH is 9.2. So, at physiological pH almost 0.1% glutathiolate or GS^- is present.[51]

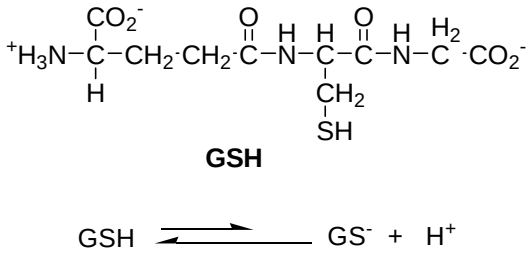

Figure 3: The equilibrium between GSH and GS^- at physiological pH.

Glutathione is mostly found in the reduced (GSH) form as the enzyme glutathione reductase always reverts back the oxidized form (GSSG) into the reduced form (GSH).[51] In the reduced state the thiol group of GSH is able to donate hydrogen atom towards unstable molecule like reactive oxygen species (ROS) and after donation of hydrogen atom it forms $GS^{\cdot}$ radical which by reacting with another molecule of $GS^{\cdot}$ produces GSSG. Glutathione reductase regenerates GSH from GSSG.[51] GSH reacts very fast with hydroxyl radical with the rate constant $(1–2) \times 10^{10}$ M^{-1} sec^{-1}.[4]

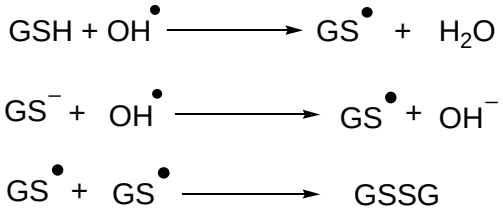

Scheme 5: Reaction of GSH with hydroxyl radical.[51]

So, GSH behaves as a potential radical scavenger by donating reducing equivalent of hydrogen atom to reactive oxygen species such as, hydroxyl radical and consequently GSH behaves as an antioxidant which protects cells against the deleterious effect of ROS.[52] Moreover, early studies have been described GSH as a defensive reagent against xenobiotics like drugs, pollutants, carcinogens etc.[52] Besides that GSH can form disulfide bonds with cysteine residues of proteins and consequently it regulates the function of proteins by the mechanism "S-glutathionylation".[52] The main role of GSH is regulation of cell life, proliferation, and death.[52] Therefore, as GSH is a potential hydrogen donor, we chose GSH to investigate whether rate of metabolism of TPZ get effected by potent hydrogen donor GSH.

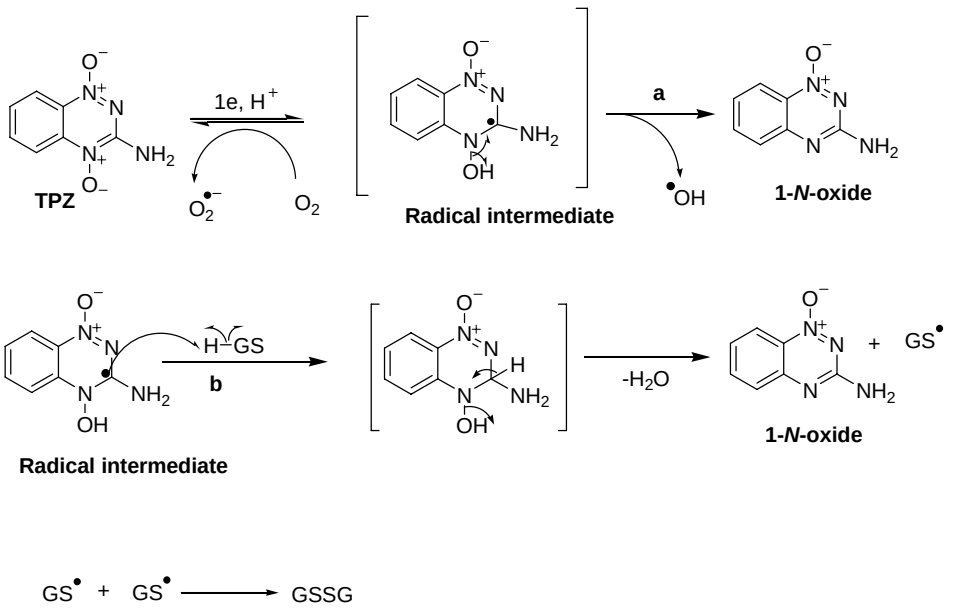

Scheme 6: Proposed mechanism of metabolism of TPZ in presence of hydrogen donor GSH.

Release of hydroxyl radical from TPZ radical or **10a** is a unimolecular reaction whereas the reaction of **10a** with hydrogen donor RH is a bimolecular reaction. If addition of hydrogen donor increases rate of TPZ disappearance this suggest that TPZ radical or **10a** abstracts H· from hydrogen donor. After hydrogen atom abstraction by **10a**, dehydration occurs which is a very fast step as it makes the system aromatic (**Scheme 6)**. Accordingly, we carried out kinetic study of metabolism of TPZ in presence of GSH by using Uv-vis spectroscopy. In this work, we used xanthine/xanthine oxidase (X/XO) as one-electron reducing system. At first we examined the rate of metabolism of TPZ in presence of X/XO by using a Uv-vis spectroscopy in which we monitored the kinetics of metabolism of TPZ or in other words change of absorbance of TPZ with time at a particular wave length 474 nm with in the time range 0 sec to 57600 seconds. After that we examined the rate of metabolism of TPZ in presence of different concentration of

GSH. In this experiment we used desferal in the reaction mixture to prevent aerial oxidation of GSH into GSSH. Moreover as the1-*N*-oxide of TPZ shows absorbance at 474 nm we subtracted the absorbance of 1-*N*-oxide of TPZ from the absorbance of TPZ which was taken at 474 nm with in the time range 0 sec to 57600 sec.

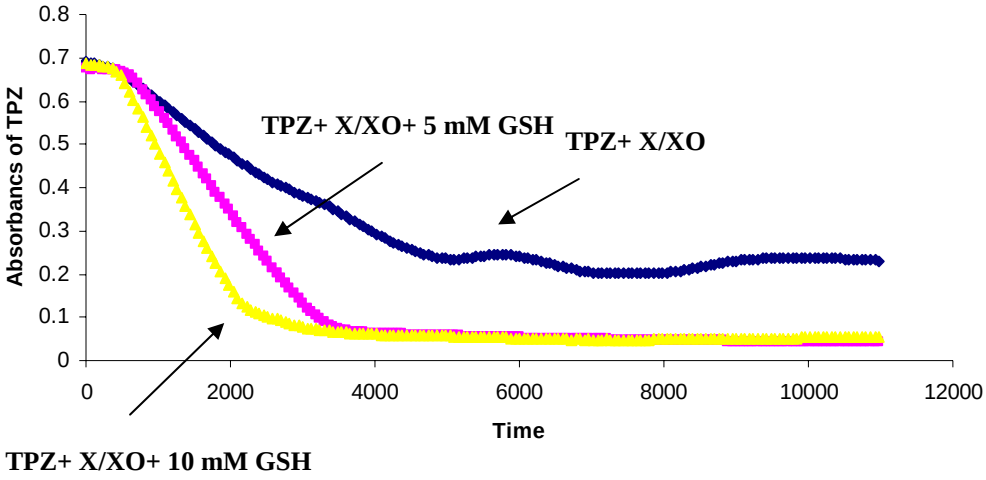

Figure 4: Higher rate of metabolism of TPZ in presence of hydrogen donor GSH. Rate of metabolism of TPZ in presence of X/XO with 5 & 10 mM concentration of GSH or without GSH was examined by performing Uv-vis kinetics at 474 nm with in the time range 0 sec-57600 sec.

Our preliminary data demonstrated that rate of metabolism of TPZ was increased with increasing concentration of GSH. We know that GSH is a reducing agent[52] so; we also checked whether TPZ is metabolized only in presence of GSH or GSH and xanthine oxidase as control experiments.

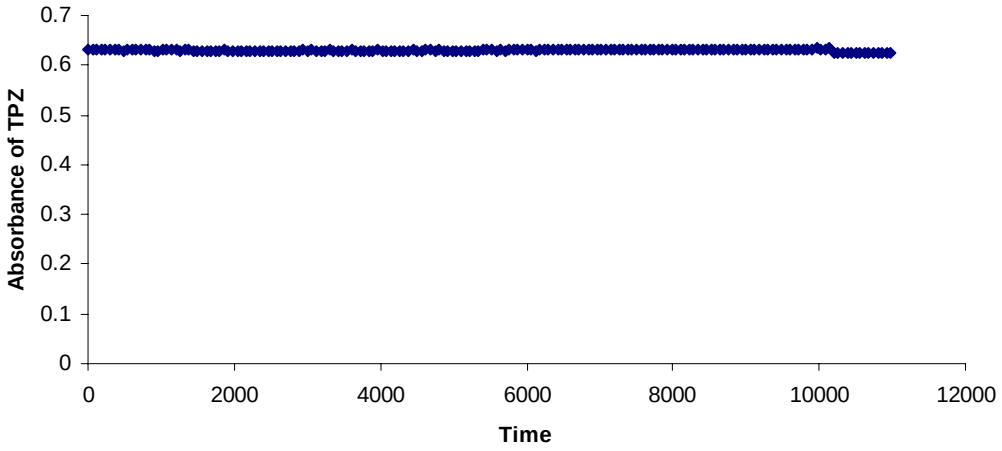

Figure 5: TPZ is not metabolized in presence of GSH and xanthine oxidase. Rate of metabolism of TPZ in presence of 5 mM GSH and xanthine oxidase was examined by performing Uv-vis kinetics at 474 nm with in the time range 0 sec-57600 sec.

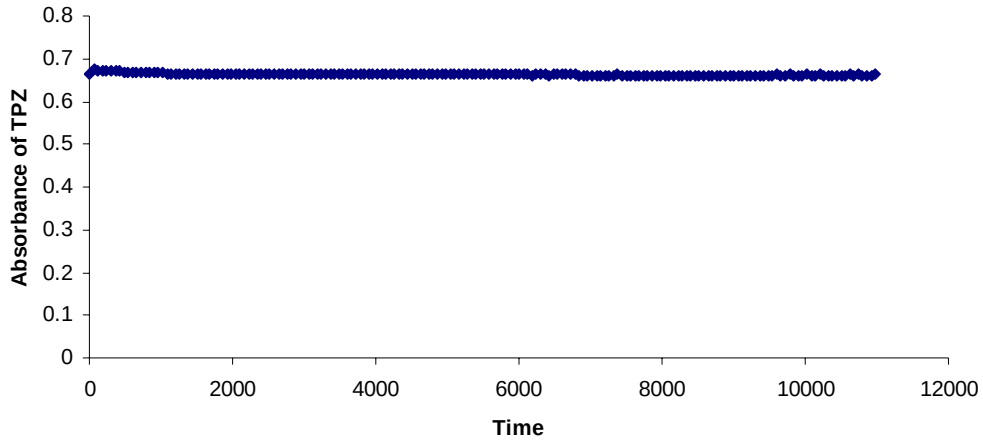

Figure 6: TPZ is not metabolized in presence of only GSH (no enzyme). Rate of metabolism of TPZ in presence of 5 mM GSH was examined by performing Uv-vis kinetics at 474 nm with in the time range 0 sec-57600 sec.

We found that TPZ was not metabolized in the presence of only GSH or GSH and xanthine oxidase which indicate that although GSH is a reducing agent.[52] it cannot

activate TPZ either alone or in presence of xanthine oxidase. TPZ requires one-electron reductive activation by one electron reducing system like xanthine/xanthine oxidase to form activated TPZ which under hypoxic condition (**Scheme 7**) gets metabolized into its 1-*N*-oxide.

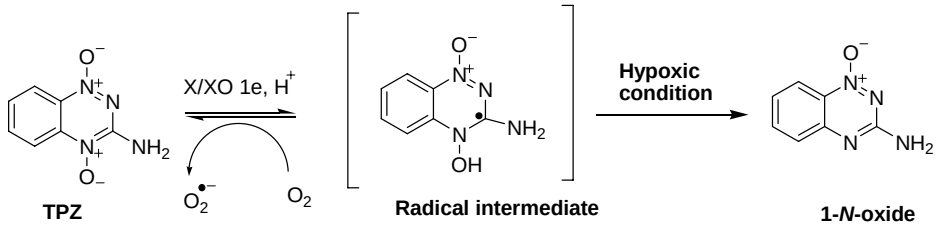

Scheme 7: Activation of TPZ by one electron reducing system X/XO.

We also did another control experiment to check whether GSH can change the activity of xanthine oxidase. In this work we monitored the generation of uric acid with time in presence of GSH.

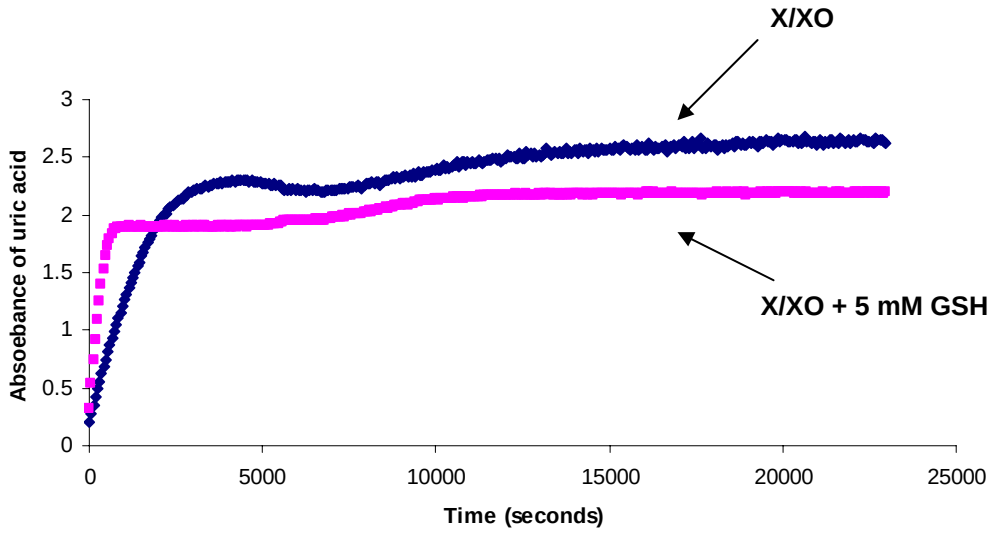

Figure 7: Rate of formation of uric acid in absence and presence of GSH was examined by performing Uv-vis kinetics at 300 nm with in the time range 0 sec-40000 sec.

We found that activity of xanthine oxidase is increased to some extend in presence of GSH and as a result the rate of generation of uric acid is higher in presence of GSH. Therefore, based on this preliminary data it can be suggested that in addition to behave as a potential H donor, GSH also can increase the metabolism of TPZ by increasing the activity of enzyme.

4.4. Effect of hydrogen donor glucose on the rate of metabolism of TPZ:

It is interesting to consider whether TPZ radical, **10a** can abstract H· from sugars such as those found in DNA. The mono-saccharide glucose can serve as a model for deoxyribose of DNA.

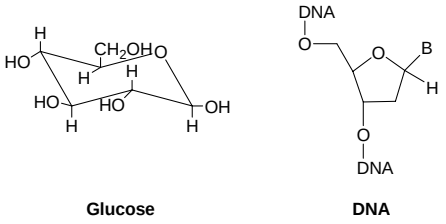

Figure 8: Structure of DNA and glucose.

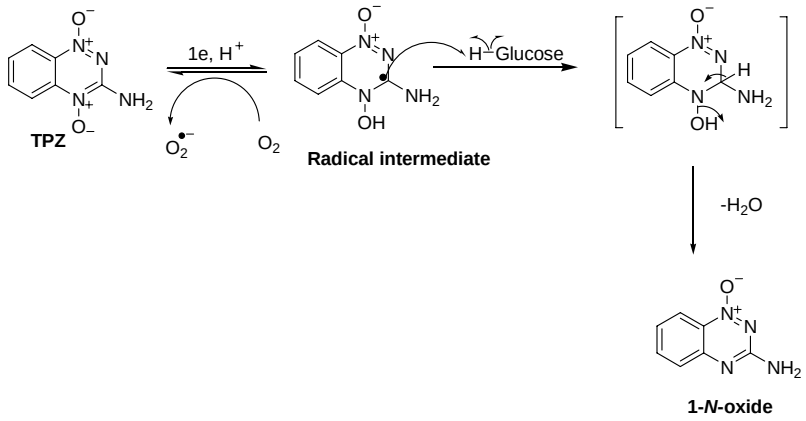

Scheme 8: Proposed mechanism of hydrogen atom abstraction by radical intermediate of TPZ from hydrogen donor glucose.

Thus, we examined rate of metabolism of TPZ in presence of various concentrations of glucose. In a typical assay, we monitored the rate of metabolism of TPZ in presence of 5 and 10 mM of glucose by performing Uv-vis kinetics at 474 nm within the time range 0-57600 seconds (**Figure 9**). As control experiments, we examined whether TPZ get metabolized in presence glucose and xanthine oxidase (**Figure 10**) and also we subtracted the absorbance of 1-*N*-oxide of TPZ from the absorbance of TPZ which was acquired at 474 nm.

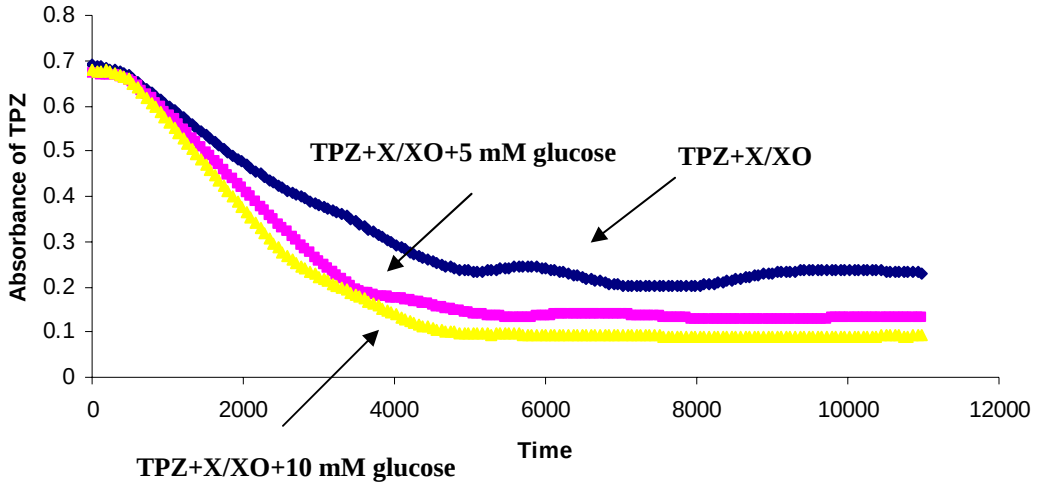

Figure 9: Higher rate of metabolism of TPZ in the presence of H-donor glucose. Rate of metabolism of TPZ in presence of X/XO with 5 and 10 mM concentration of glucose or without glucose was examined by performing a Uv-vis kinetics at 474 nm with in the time range 0-57600 sec.

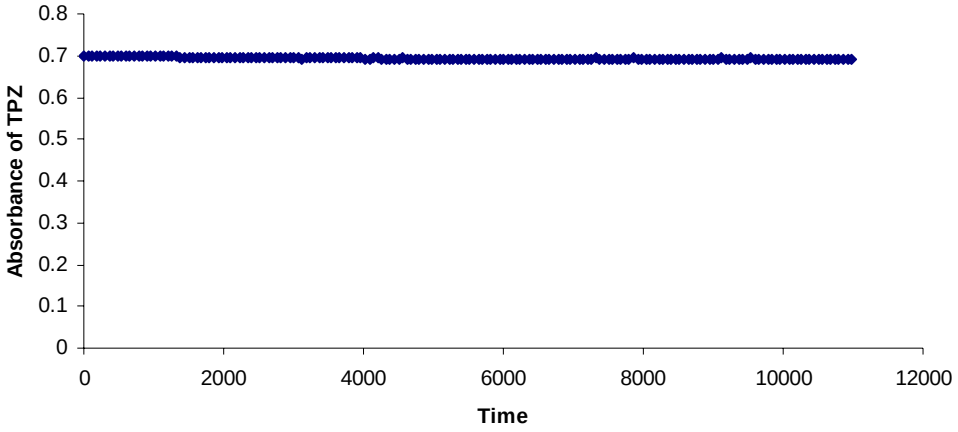

Figure 10: TPZ is not metabolized in presence of glucose and xanthine oxidase. Rate of metabolism of TPZ in presence of 10 mM glucose and xanthine oxidase was examined by performing a Uv-vis kinetics at 474 nm with in the time range 0-57600 sec.

So, we found that TPZ metabolized faster in presence of glucose and rate of metabolism of TPZ increases with increasing concentration of glucose. The control experiment showed that TPZ is not metabolize in presence of glucose and xanthine oxidase which suggest that TPZ required one electron reductive activation by xanthine/xanthine oxidase to form radical intermediate under hypoxic condition that is metabolized into its 1-*N*-oxide. We also did another control experiment to check whether glucose can change the activity of xanthine oxidase. In this work we monitored the generation of uric acid with time in presence of glucose (**Figure 11**).

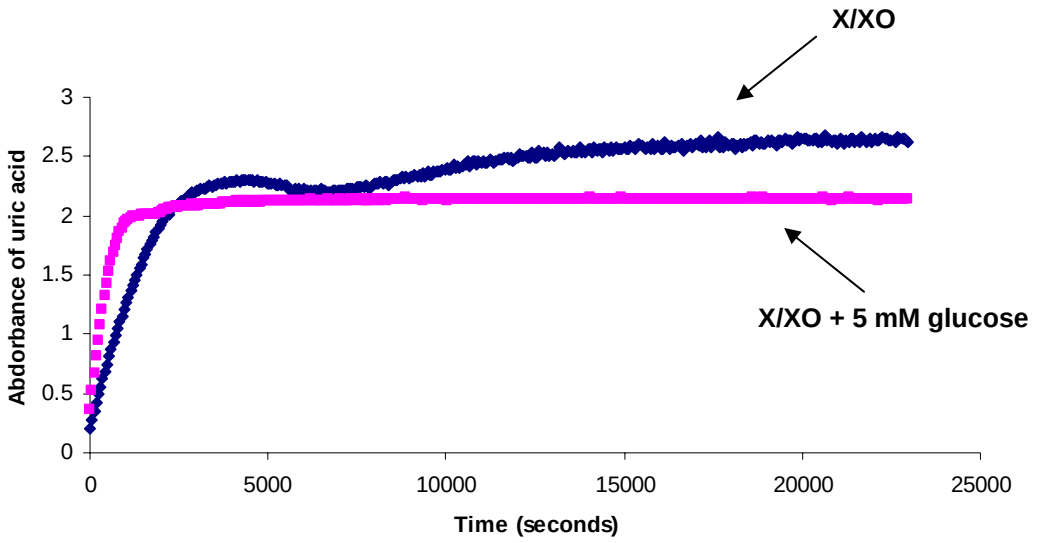

Figure 11: Rate of formation of uric acid in absence and presence of glucose was examined by performing Uv-vis kinetics at 300 nm with in the time range 0 sec-40000 sec.

We found that activity of xanthine oxidase is increased to some extend in presence of glucose and as a result the rate of generation of uric acid is higher in presence of glucose. Therefore, based on this preliminary data it can be suggested that in addition to behave as a potential H donor, glucose also can increase the metabolism of TPZ by increasing the activity of enzyme. We also compared the hydrogen donor ability of glucose with GSH (**Figure 12**).

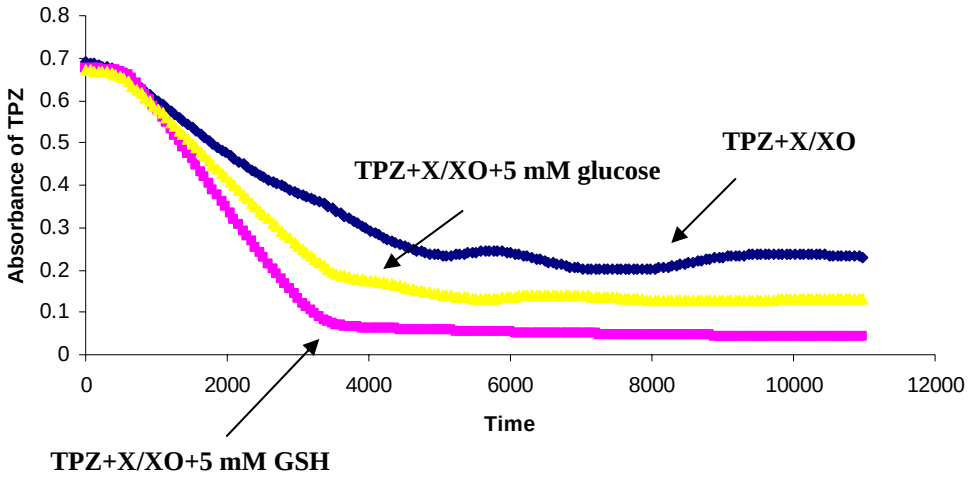

Figure 12: Rate of metabolism of TPZ is higher in presence of GSH compare to glucose. Rate of metabolism of TPZ in presence of hydrogen donor glucose or GSH or without hydrogen donors were examined by performing Uv-vis kinetics at 474 nm with in the time range 0 sec-57600 sec

We noticed that rate of metabolism of TPZ is higher in presence of GSH compared to glucose. We note that GSH is a superior hydrogen atom donor. Therefore, according to our preliminary results we came to this conclusion that as activated TPZ or **10a** abstract hydrogen-atom from the hydrogen-donor GSH and glucose it may have the potential to abstract hydrogen atom from DNA backbone (**Scheme 4, pathway C & Scheme 9**) as DNA contains sugar moiety similar to glucose.

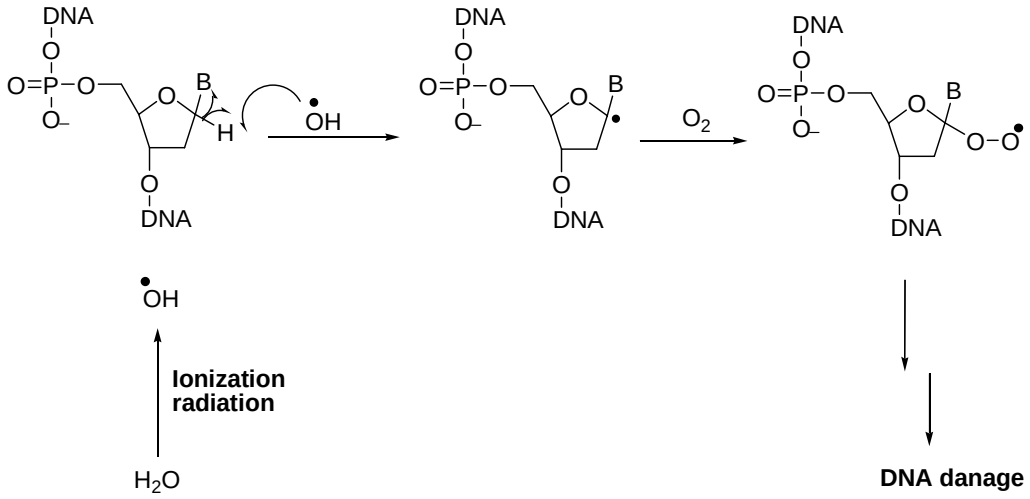

Scheme 9: Proposed mechanism of H-1'abstraction pathway for DNA strand cleavage.[53,54]

Overall this preliminary study suggests that TPZ radical **10a** in addition to release of hydroxyl radical, also abstract hydrogen atom from hydrogen-donor like GSH, glucose and metabolized into 1-*N*-oxide by dehydration.

4.5. Oxygen sensitivity of TPZ: Early studies showed that TPZ is a novel hypoxia selective, bioreductive anticancer drug.[35,43,55] Hypoxia selective means TPZ doesn't show cytotoxicity in normal oxygenated cells as it undergoes redox cycling by formation of superoxide radicals.[35,43,55] Cellular enzymes like SOD, catalase glutathione peroxidase diminish the deleterious effect of superoxide radical and its decomposition products.[57,58] Under hypoxic conditions, TPZ damage DNA which leads to cytotoxicity and get metabolized into the 1-*N*-oxide (**Scheme 10**).[35,43,55]

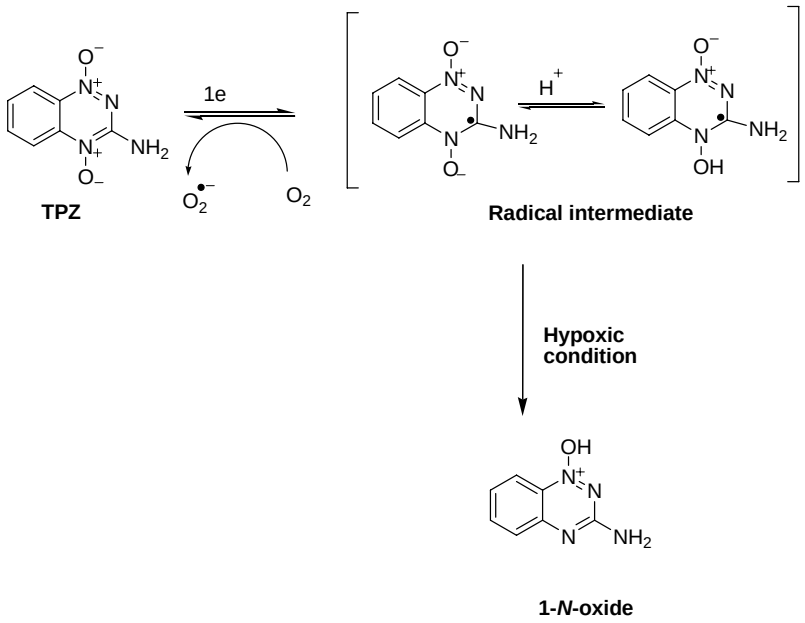

Scheme 10: Oxygen sensitivity and metabolism of TPZ under anaerobic condition.

The oxygen sensitivity or hypoxia selectivity and activation of bioreductive drugs by cellular enzymes depend on their one electron reduction potential.[22,43,55,56] For example, TPZ having one electron reduction potential -0.45 V can be easily reduced by NADPH:cytochrome P450 reductase as the redox potential of TPZ falls within the range of the substrates of NADPH:cytochrome P450 reductase.[43,55] The one electron reduction potential of oxygen is -0.18 V.[22,55] So, compounds having reduction potential lower than -0.18 V can easily transfer electron to molecular oxygen after activation and exhibit hypoxia selectivity. On the other hand, compounds having reduction potential above -0.18 V cannot transfer electron towards molecular oxygen and are not hypoxia selective.[22,55] Therefore, by considering both the minimum reduction potential required for activation of bioreductive drugs by common flavoproteins and the maximum redox potential to protect reduction by molecular oxygen, it has been suggested that reduction

potential required for most types of hypoxia selective bioreductive drugs is in the range of -0.5 V to -0.1 V at pH 7.[55] TPZ is an oxygen sensitive, hypoxia selective, bioreductive drug as its one electron reduction potential is within this range.[3,32,33] The oxygen concentration required to inhibit activation of TPZ by 50% (K_{O2}) is approximately 1-3 μM.[32,33] This oxygen concentration was determined by using HT29 colon carcinoma cells under a wide range of different gas phase oxygen concentration.[32] We have worked toward a quick and easy kinetic method to determine this critical oxygen concentration by using Uv-vis spectroscopy. Critical oxygen concentration is defined as the particular oxygen concentration at which TPZ will metabolize; above this oxygen concentration TPZ wouldn't get metabolized. In this Uv-vis kinetics method we monitored the rate of metabolism of TPZ in presence of one-electron reducing system NADPH:cytochrome P450 reductase under aerobic condition. The kinetics of metabolism of TPZ was monitored at the wavelength 474 nm with in the time range 0-40000 s.

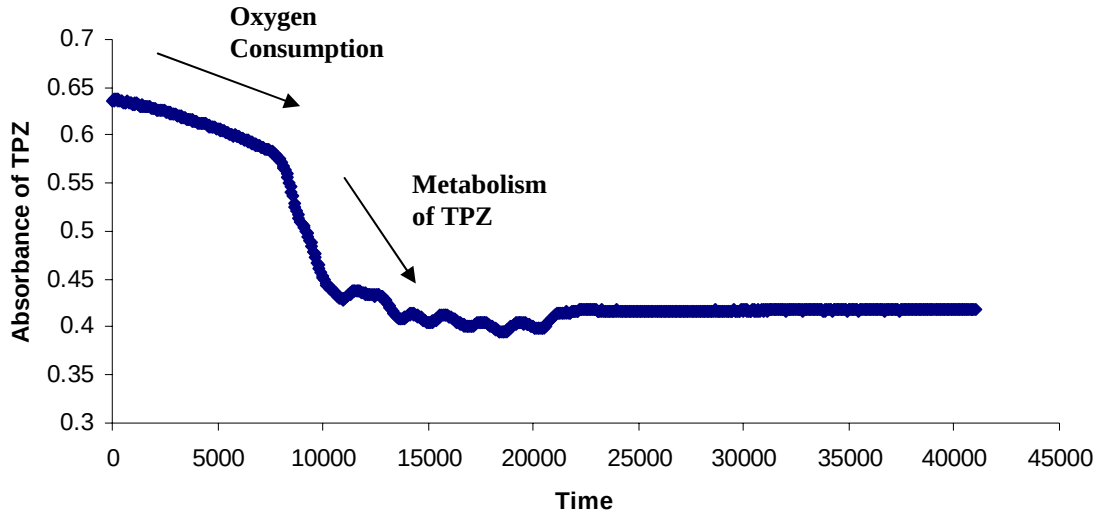

Figure 13: Oxygen sensitivity of TPZ in presence of NADPH:cytochrome P450 reductase system was acquired by performing Uv-vis kinetic method at 474 nm within the time range 0 sec-40000 sec.

The above data shows that at the beginning of the reaction within the time duration 0 sec to 8281.9 seconds the absorbance of TPZ at 474 nm didn't change much which reflects the fact that with in this time period TPZ was not consumed much. But after crossing this certain period of time (8289.1 sec) the absorbance of TPZ decreased sharply which indicates that concentration of TPZ was decreasing with time as TPZ was consuming faster by NADPH:cytochrome P450 reductase. So, this preliminary data indicates that in present of oxygen TPZ undergoes redox cycling (**Scheme 10**) with formation of superoxide radical and doesn't get metabolized until most of the dissolved oxygen get consumed by NADPH:cytochrome P450 reductase and as a result we didn't see much decrease of absorbance of TPZ during the consumption of oxygen (with in 0 sec to 8281.9 sec). After that when most of the oxygen gets consumed by NADPH:cytochrome P450 reductase enzyme then TPZ started metabolized by NADPH:cytochrome P450 reductase system which reflects decrease of absorbance of TPZ with time (**Scheme 10)**. So, overall this preliminary Uv-vis kinetics method represents the oxygen sensitivity of TPZ. In some portion of absorption vs. time graph as shown in **Figure 13** with in the time range 10000-20000 s we observed wiggles due to instrumental error.

4.6. Conclusion:

Overall the study suggests that the Uv-vis spectroscopy could be used to examine the oxygen sensitivity of various bioreductive drugs *in vitro*. TPZ is a novel hypoxia selective anticancer drug and the oxygen sensitivity of TPZ has been examined successfully by using this Uv-vis kinetics method. With further development this assay

could be used to determine or at least compare the critical oxygen concentration for various bioreductive drugs.

Moreover, in this chapter, we described that addition of additives like the hydrogen donors GSH and glucose increased the rate of metabolism of TPZ and on the basis of our preliminary results it can be suggested that in addition to hydroxyl radical producing mechanism, TPZ radical **10a** (**Scheme 4, pathway C, Scheme 6 and 8**) may be able to abstract hydrogen atom from biological substances and then undergoes dehydration to yield the well known the 1-*N*-oxide metabolite of TPZ (**Scheme 4, pathway C, Scheme 6 and 8**).

Material & Methods:

Materials: Materials with highest purity available were obtained from following sources. Sodium phosphate, xanthine from Aldrich Chemical Co. (Milwaukee, WI); NADPH, desferal, cytochrome P450 reductase, GSH, glucose from Sigma Chemical Co. (St. Louis, MO); xanthine oxidase from Roche Molecular Biochemicals (Indianapolis, IN); Cuvet QS 1.000 from Fisher Scientific (Pittsburg, PA); TPZ and 1-*N*-oxide of TPZ were synthesized according to literature methods. [Fuchs, T.; Chowdhury, G.; Barnes, C. L.; Gates, K. S. *J. Org. Chem.* 2001, 66, 107-114]. UV-vis kinetics was performed by using Uv-vis spectroscopy.

Kinetic method to monitor rate of metabolism of TPZ in presence of GSH and glucose: In a typical assay, first the blank solution was prepared by 50 mM sodium phosphate buffer in a total volume 800 μL and the reaction mixture was prepared with 100 μM TPZ, 500 μM xanthine and 50 mM sodium phosphate buffer in a total volume 800 μL. Next we took the reading of blank and after that we transferred the reaction mixture in the cuvet to take the absorbance. After that, the Uv-vis kinetic method was set at the wave length 474 nm, cycle time 60 seconds and total runtime 57600 seconds. Next we added xanthine oxidase (60 mU) to the reaction mixture to initiate the reaction. The cuvet was covered by septum. After that the acquisition was taken at the wavelength 474 nm for the time periods 0-57600 s to examine the rate of metabolism of TPZ. The rate of metabolism of TPZ in presence of various concentrations of GSH (5 mM and 10 mM) was measured in the similar way as we described above only the exception that 1 mM

desferal was added both in the blank and the reaction mixture. For control experiments, we monitored the rate of metabolism of TPZ (100 μM) in presence of GSH (5 mM) and GSH (5 mM), xanthine oxidase (60 mU) by using the same Uv-vis kinetics method as described above. For another controls, we also monitored the rate of formation of uric acid in presence xanthine (500 μM), XO (75 mU/mL) or in presence of xanthine (500 μM), XO (75 mU/mL) and GSH (5 mM) in a total volume 1.5 mL by using the same kinetics method as described above only the exception that the formation of uric acid was monitored at 300 nm within the time range 0-40000 seconds. The rate of metabolism of TPZ in presence of various concentrations of glucose (5 mM and 10 mM) and the control experiments were performed in the similar way as described above.

Kinetic method to examine oxygen sensitivity of TPZ: In this work, we also used the same Uv-vis kinetic method that described above. At first, we took the reading of blank containing sodium phosphate buffer (50 mM) by using cuvet and next we took the absorbance of reaction mixture containing TPZ (100 μM), NADPH (500 μM) and sodium phosphate buffer (50 mM). Now, we covered the cuvet by septum and then we purged N_2 gas through the septum over the empty place of the cuvet for 2-3 minutes to remove oxygen from the empty place of the cuvet. After that we initiated the reaction by injecting 242 mU/mL cytochrome P450 reductase through the septum. The acquisition was taken at 474 nm for the time periods 0-40000 s to examine the rate of metabolism of TPZ.

References:

1. Thomlinson, R. H.; Gray, L. H. *Br. J. Cancer.* **1955**, *9*, 539-549.
2. Gray, L. H.; Conger, A. D.; Ebert, M.; Homsey, S.; Scott, O. C. *Br. J. Radiol.* **1953**, *26*, 638-648.
3. Brown, J. M.; Wilson, W. R. *Nature Rev.* **2004**, *4*, 437-447.
4. Crabtree, H. G.; Cramer, W. *Proc. R. Soc. Ser. B.* **1933**, *113*, 238-250.
5. Brown, J. M. *Cancer Research* **1999**, *59*, 5863-5870.
6. Brown, J. M. *Int. J. Radiat. Oncol. Biol. Phys.* **1984**, *10*, 425-429.
7. Tannock, I. F. *Lancet.* **1998**, *351*, 9-16.
8. Durand, R. E. *In vivo.* **1994**, *8*, 691-702.
9. Teicher, B. A.; Lazo, J. S.; Sartorelli, A. C. *Cancer Res.* **1981**, *41*, 73-81.
10. Batchelder, R. M.; Wilson, W. R.; Hay, M. P.; Denny, W. A. *Br. J. Cancer Suppl.* **1996**, *27*, S52-S56.
11. Comerford, K. M.; Wallace, T. J.; Karhausen, J.; Louis, N. A.; Montalto, M. C.; Colgan, S. P. *Cancer Res.* **2002**, *62*, 3387-3394.
12. Wartenberg, M.; Ling, F. C.; Muschen, M.; Klein, F.; Acker, M.Gassmann, H.; Petrat, K.; Putz, V.; Hescheler, J.; Sauer, H. *Faseb. J.* **2003**, *17*, 497-499.
13. Lin, A. J.; Cosby, L. A.; Shansky, C. W.; Sartorelli, A. C. *J. Med. Chem.* **1972**, *15*, 1247-1252.
14. Sheldon, P. W.; Foster, J. L.; Fowler, J. F. *Br. J. Cancer.* **1974**, *30*, 560-565.
15. Brown, J. M.; Siim, B. G. *Seminars Rad. Oncol.* **1996**, *6*, 22-36.
16. Denny, W. A. *The Lancet* **2000**, *1*, 25-29.

17. Tomasz, M. *Chem. Biol.* **1995**, *2*, 575-579.

18. Adams, G. E. *Radiat. Res.* **1992**, *132*, 129-139.

19. Rauth, A. M.; Mohindra, J. K.; Tannock, I. F. *Cancer Res.* **1983**, *43*, 4154-4158.

20. Fracasso, P. M.; Sartorelli, A. C. *Cancer Res.* **1986**, *46*, 3939-3944.

21. Patterson, L. H. *Drug Metab. Rev.* **2002**, *34*, 581-592.

22. *DNA damage by Heterocyclic N-oxides: A novel class of antitumor agents,* PhD thesis submitted by Goutam Chowdhury in **2005.**

23. Ganley, B.; Chowdhury, G.; Bhansali, J.; Daniels, J. S.; Gates, K. S. *Bioorg. Med. Chem.* **2001**, *9*, 2395-2401.

24. Zeman, E. M.; Brown, J. M.; Lemmon, M. J.; Hirst, V. K.; Lee, W. W. *Radiation Oncology Biiol. Phys.* **1986**, *12*, 1239-1242.

25. Brown, J. M.; Wang, L. *Anti-Cancer Drug Design* **1998**, *13*, 529-539.

26. Taylor, Y. C.; Rauth, A. M. *Cancer Res.* **1978**, *38*, 2745-2752.

27. Mohindra, J. K.; Rauth, A. M. *Cancer Res.* **1976**, *36*, 930-936.

28. Craighead, P. S.; Pearcey, R.; Stuart, G. *Int. J. Radiat. Oncology Biol. Phys.* **2000**, *48*, 791-795.

29. Gatzemeier, U.; Rodriguez, G.; Treat, J.; Miller, V.; von Roemeling, R.; Viallet, J.; Rey, A. *Br. J. Cancer* **1998**, *77*, 15-17.

30. Kovacs, M. S.; Hocking, D. J.; Evans, J. W.; Siim, B. G.; Wouters, B. G.; Brown, J. M. *Br. J. Cancer* **1999**, *80*, 1245-1251.

31. von Pawel, J.; von Roemeling, R.; Gatzemeier, U.; Boyer, M.; Elisson, L. O.; Clark, P.; Talbot, D.; Rey, A.; Butler, T. W.; Hirst, V.; Olver, I.; Bergman, B.;

Ayoub, J.; Richardson, G.; Dunlop, D.; Arcenas, A.; Vescio, R.; Viallet, J.; Treat, J. *J. Clin. Oncol.* **2000**, *18*, 1351-1359.

32. Hicks, K. O.; Siim, B. G.; Pruijn, F. B.; Wilson, W. R. *Radiation Research* **2004**, *161*, 656-666.
33. Koch, C. J. *Cancer Res.* **1993**, *53*, 3992-3997.
34. Brown, J. M. *Br. J. Cancer* **1993**, *67*, 1163-1170.
35. Laderoute, K.; Wardman, P.; Rauth, A. M. *Biochem. Pharmacol.* **1988**, *37*, 1487-1495.
36. Zeman, E. M.; Brown, J. M. *Int. J. Radiat. Oncol. Biol. Phys.* **1989**, *16*, 967-971.
37. Peters, K. B.; Wang, H.; Brown, J. M.; Iliakis, G. *Cancer Res.* **2001**, *61*, 5425-5431.
38. Peters, K. B. *Cancer Res.* **2002**, *62*, 5248-5253.
39. Daniels, J. S.; Gates, K. S. *J. Am. Chem. Soc*. **1996**, *118*, 3380-3385.
40. Kotandeniya, D.; Ganley, B.; Gates, K. S. *Bioorg. Med. Chem. Lett*. **2002**, *12*, 2325-2334.
41. Birincioglu, M.; Jaruga, P.; Chowdhury, G.; Rodriguez, H.; Dizdaroglu, M.; Gates, K. S. *J. Am. Chem. Soc*. **2003**, *125*, 11607-15.
42. Fitzsimmons, S. A.; lewis, A. D.; Riley, R. T.; Workman, P. *Carcinogenesis*, **1994**, *15*, 1503-10.
43. Priyadarsini, K. I.; Tracy, M.; Wardman, P. *Free. Radic. Res.* **1996**, *25*, 393-402.
44. Delahoussaye, Y. M.; Evans, J. W.; Brown, J. M. *Biochemical Pharmacology* **2001**, *62*, 1201-1209.

45. Wang, J.; Biedermann, K. A.; Wolf, C. R.; Brown, J. M. *Br. J. Cancer* **1993**, *67*, 321-5.

46. Patterson, A. V.; Robertson, N.; Houlbrook, S.; Stephens, M. A.; Adams, G. E.; Harris, A. L.; Stratford, I. J.; Carmichael, J. *Int. J. Radiat. Oncol. Biol. Phys.* **1994**, *29*, 369-72.

47. Patterson, A. V.; Barham, H. M.; Chinje, E. C.; Adams, G. E.; Harris, A. L.; Stratford, I. J. *Br. J. Cancer* **1995**, *72*, 1144-50.

48. Patterson, A. V.; Saunders, M. P.; Chinje, E. C.; Patterson, L. H.; Stratford, I. J. *Anticancer Drug Des.* **1998**, *13*, 541-73.

49. Patterson, A. V.; Saunders, M. P.; Chinje, E. C.; Adams, G. E.; Talbot, D. C.; Harris, A. L.; Stratford, I. J. *Br. J. Cancer* **1997**, *72*, 1144-50.

50. Anderson, R. F.; Shinde, S. S.; Hay, M. P.; Gamage, S. A.; Denny, W. A. *J. Am. Chem. Soc.* **2003** *125*, 748-56.

51. Zhao, R.; Lind, J.; Merényi, G.; and Eriksen, T. E. *J. Chem. Soc. Perkin. Trans.* **1997**, *2*, 569-574.

52. Pompella, A.; Visvikis, A.; Paolicchi, A.; Tata, V. D.; Casini, A. F. *Biochemical Pharmacology* **2003**, *66*, 1499-1503.

53. Pogozelski, W. K.; Tullius, T. D. *Chem. Rev.* **1998**, *98*, 1089-1107.

54. Kent S. Gates. *Reviews of Reactive Intermediate Chemistry* Chapter 8.

55. Wardman, P. *Current Medicinal Chemistry* **2001**, *8*, 739-761.

56. Wardman, P.; Dennis, M. F.; Everett, S. A.; Patel, K. B.; Stratford, M. R. I.; Tracy, M. Eds. *Portland Press:* London **1995**, *61*.

57. Halliwell, B.; Gutteridge, J. M. *Arch Biochem. Biophy.* **1990**, *280*, 1-8.

58. Bagley, A. C.; Krall, J.; Lynch, R. E. *Proc. Natl. Acad. Sci. USA.* **1986**, *83*, 3189-3193.

Chapter 5: 1- Hydroxyphenazine 5,10-di-*N*-oxide: A Potent Redox-Activated Hypoxia Selective DNA Damaging Agent

5.1. Introduction:

Recent literature has revealed that several heterocyclic aromatic *N*-oxides have appeared as promising antitumor agents which display redox-activated hypoxia selective DNA damaging properties.[1-4] As tumor cells are hypoxic in nature the hypoxia selective DNA damaging properties of these heterocyclic *N*-oxides has made them very attractive candidates for anticancer chemotherapy.[5,6] TPZ is the lead compound in this group which displays hypoxia selective promising antitumor properties and currently is undergoing phage III clinical trials.[5,7] TPZ achieves its medicinal activity through its ability to damage DNA selectively in the oxygen poor or hypoxic cells inside the solid tumors.[1-7] Quinoxaline 1,4-di-*N*-oxide and 3-amino 2-quinoxaline 1,4-di-*N*-oxide have also shown redox-activated, hypoxia selective DNA damaging properties and cytotoxicity similar to TPZ.[8]

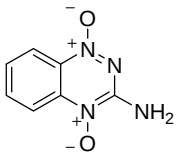

TPZ

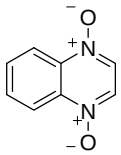

Quinoxaline 1,4-di-*N*-oxide

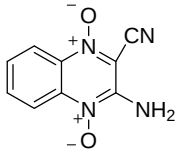

3-Amino-2-quinoxalinecarbonitrile 1,4-di-*N*-oxide

Figure 1: Example of heterocyclic *N*-oxides.

Phenazine-*N*-oxides are another example of heterocyclic *N*-oxides. Only a few naturally-occurring phenazine-*N*-oxides are known.[9] The examples of naturally occurring phenazine-*N*-oxides are 1-hydroxy-6-methoxyphenazine 5,10-di-*N*-oxide, known as

myxin,[10,11] 1,6-dihydroxyphenazine 5,10-di-*N*-oxide or iodinin[12] and 1,6-dihydroxyphenazine 5-*N*-oxide.[13] Methylmyxin or 1,6-dimethoxyphenazine 5,10-di-*N*-oxide[14] and 1-hydroxyphenazine 5,10-di-*N*-oxide are synthetic analogues of myxin.[14]

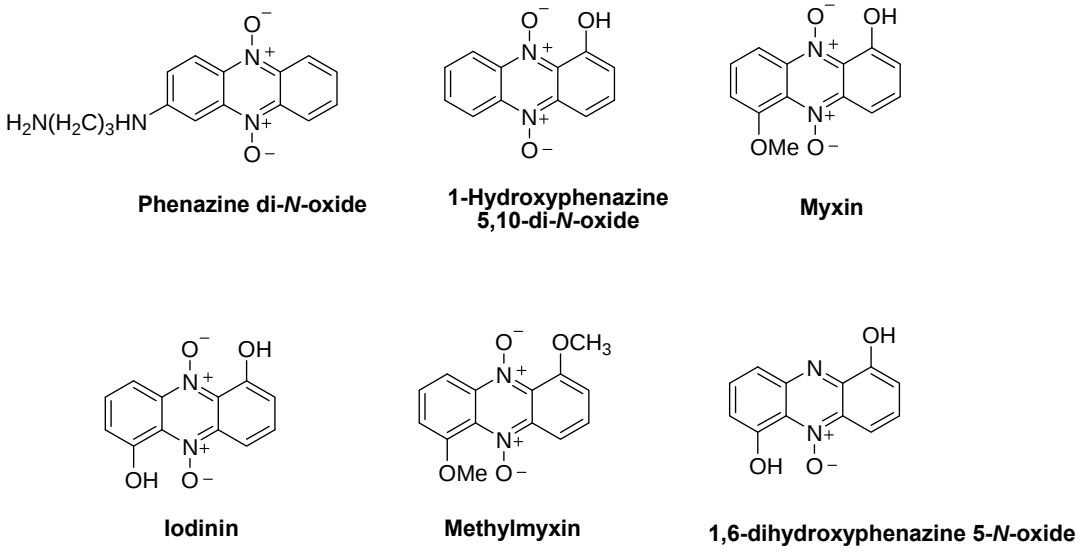

Figure 2: Examples of phenazine-*N*-oxides.

According to early literature it has been suggested that di-*N*-oxide functional group of these heterocyclic aromatic *N*-oxides is the key structural characteristic to display their DNA damaging ability under anaerobic condition.[3,8,15,16] It has been studied that both 1-*N*-oxide and no-*N*-oxide of these heterocyclic *N*-oxides do not damage DNA under anaerobic condition[3,15,16] which supports the importance of di-*N*-oxide functionality as the structural feature in the heterocyclic *N*-oxides to display DNA damaging ability under hypoxic condition.[3,8,15,16] Therefore, according to early studies about heterocyclic *N*-oxides it can be suggested that phenazine di-*N*-oxides might display DNA damaging properties under hypoxic condition as they contain di-*N*-oxide functional group.

Consistent with this idea, Hecht and his coworkers have proposed that phenazine di-*N*-oxide undergoes one electron reductive activation in presence of DTT or NADPH to produce activated radical intermediate which leads to DNA damage through generation of the hydroxyl radical under anaerobic condition. In normal oxygenated condition the radical intermediate back oxidized into parent compound via redox cycling with production of superoxide radical. (**Scheme 1**).[17,18]

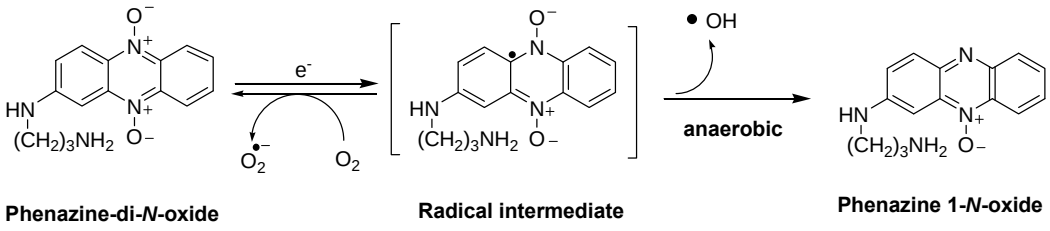

Scheme 1: Proposed mechanism for the reductive activation of phenazine-di-*N*-oxide as described by Katsuyuki *et al*.[17,18]

Moreover it has been shown by Goutam Chowdhury in our lab that phenazine-*N*-oxides myxin and methylmyxin both exhibit DNA damaging properties.[14] In this study he showed that myxin causes redox-activated, radical mediated oxidative DNA damage under both aerobic and anaerobic condition. According to his study, myxin undergoes one electron reductive activation by X/XO or NADPH:cytochrome P450 reductase system to produce activated radical intermediate (**Scheme 2)** which release putative hydroxyl radical by homolysis of N-OH bond both in aerobic and anaerobic condition and hydroxyl radical leads to oxidative DNA damage by abstraction of hydrogen atom from DNA backbone.[14]

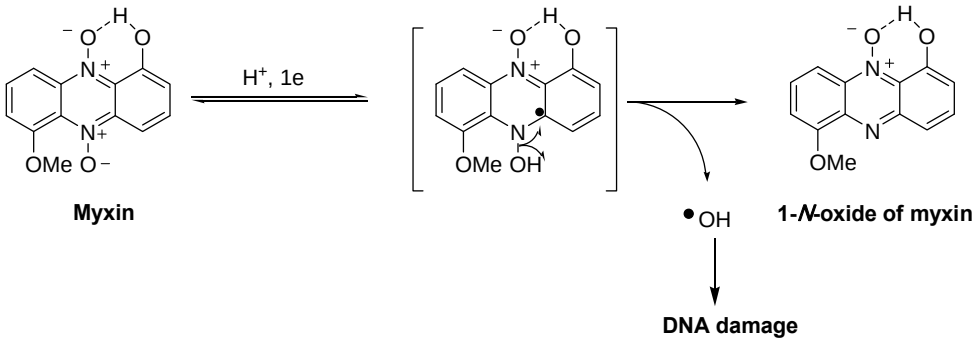

Scheme 2: Proposed mechanism of DNA damage by myxin under both anaerobic and aerobic condition.[14]

In case of methylmyxin (**Scheme 3**), it causes redox-activated, oxidative DNA damage though presumed hydroxyl radical-mediated pathway under hypoxic condition whereas under aerobic condition methylmyxin is back oxidized into parent compound via redox cycling mechanism with production of superoxide radical.[14]

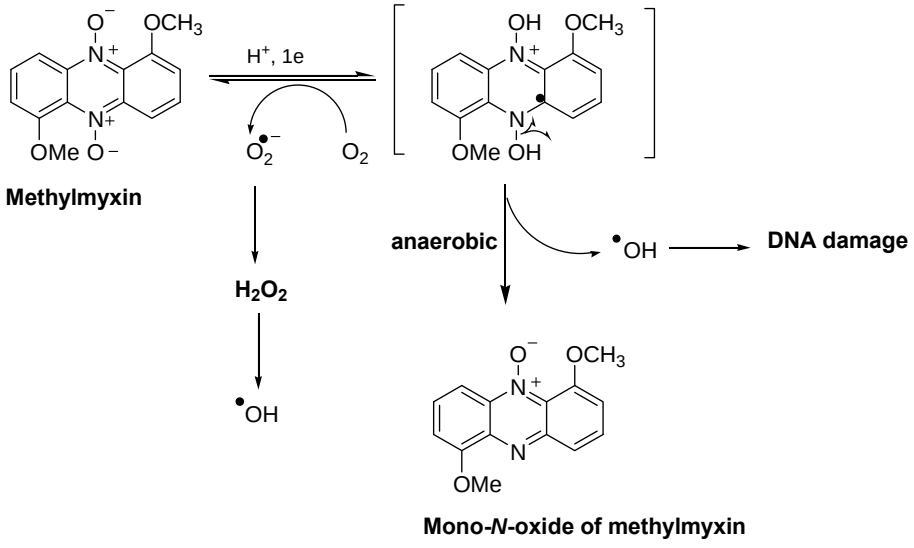

Scheme 3: Proposed mechanism of DNA damage by methylmyxin under anaerobic condition.[14]

Recently it has been found that phenazine di-*N*-oxide derivatives exhibit toxicity selectively towards hypoxic cells.[27] Thus, DNA damaging ability of phenazine di-*N*-oxide under hypoxic condition might be one of the causes of phenazine-mediated cytotoxicity selectively in hypoxic cells.

Therefore, based on early studies we thought that like other phenazine di-*N*-oxides, 1-hydroxyphenazine 5,10-di-*N*-oxide might display DNA damaging ability under hypoxic condition.

5.2. Goal: So, our primary goal was to investigate whether 1-hydroxyphenazine 5,10-di-*N*-oxide can damage DNA under anaerobic condition in presence of one electron reducing system and then to investigate the mechanism underlying the DNA damage. We hypothesized that 1-hydroxyphenazine 5,10-di-*N*-oxide might undergo one electron reductive activation in presence of one electron reducing system which under anaerobic condition causes oxidative DNA damage by generation of hydroxyl radical whereas under aerobic condition activated radical intermediate is back oxidized into parent compound via redox cycling with production of superoxide radical (**Scheme 4**). The one electron reduced metabolite of 1-hydroxyphenazine 5,10-di-*N*-oxide might be 1-*N*-oxides **6** and **7 (Scheme 4)**.

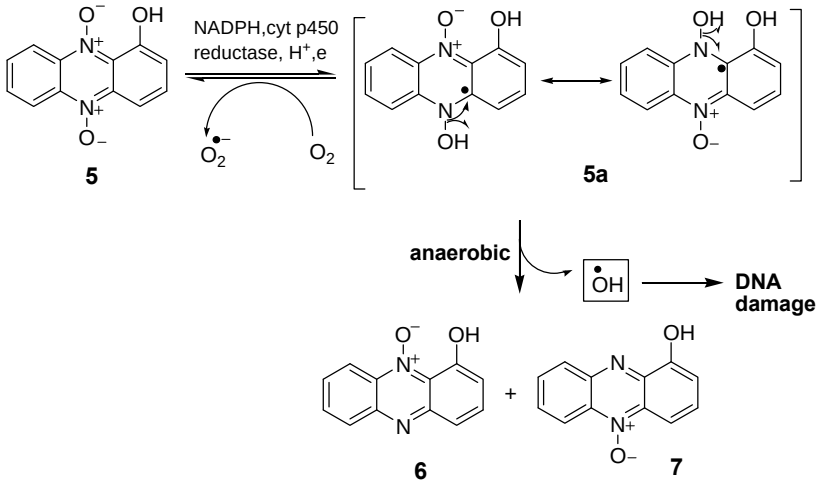

Scheme 4: Proposed mechanism of DNA damage by 1-hydroxyphenazine 5,10-di-*N*-oxide under anaerobic condition.

5.3. Hypoxia selective DNA cleavage efficiency of 1-hydroxyphenazine 5,10-di-*N*-oxide: We first investigated DNA cleavage efficiency of 1-hydroxyphenazine 5,10-di-*N*-oxide under anaerobic condition in presence of one electron reducing enzyme NADPH:cytochrome P450 reductase.[19,20] In this work, we carried out plasmid-based DNA cleavage assays with different concentrations of **5** under anaerobic condition. To create the anaerobic condition we degassed the solutions that were used in the assays by performing three cycles of freeze-pump-thaw to remove dissolved oxygen and then the assays were assembled and incubated in an inert argon filled glove bag. Superoxide dismutase (SOD), catalase and desferal were used in the reaction mixture to prevent DNA cleavage from Fenton chemistry which results from the trace amount of oxygen that might be present in the reaction mixture (**Scheme 5**). The reaction mixture was incubated in the glove bag for 12 hours and was covered by aluminum foil to prevent any photocleavage of DNA.[21,22]

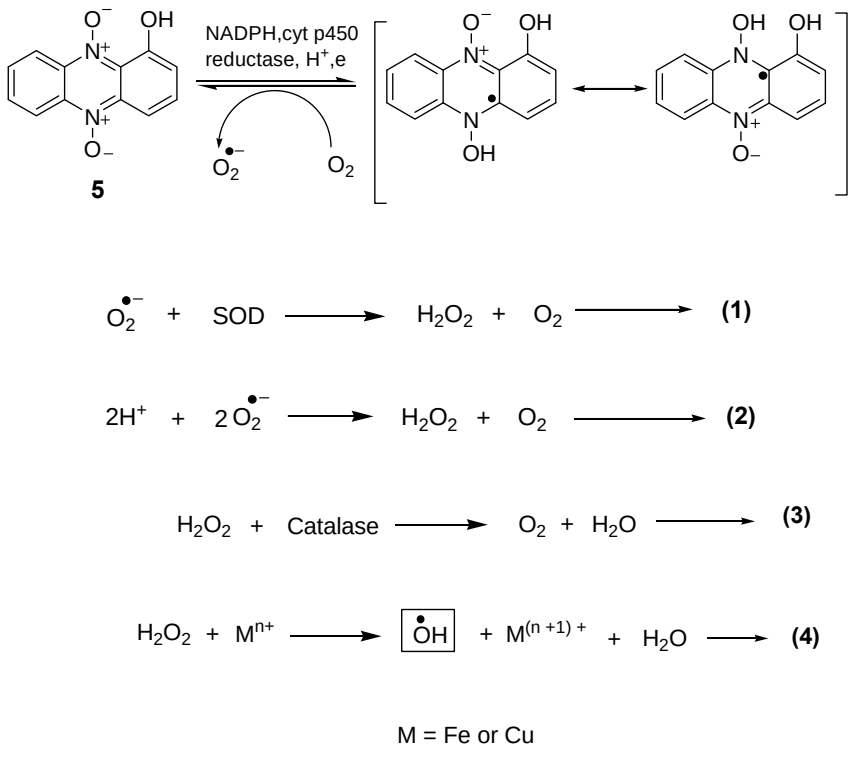

Scheme 5: Generation of hydroxyl radicals from Fenton chemistry.

DNA cleavage efficiency of **5** was determined by measuring the number of strand breaks per plasmid molecule (S value) at various concentrations of **5**. To elucidate the potential of 1-hydroxyphenazine 5,10-di-*N*-oxide, **5** as a hypoxia selective antitumor agent we compared DNA cleavage efficiency of **5** with the well known hypoxia-selective anticancer agent **TPZ**.[3,5,7]

A.

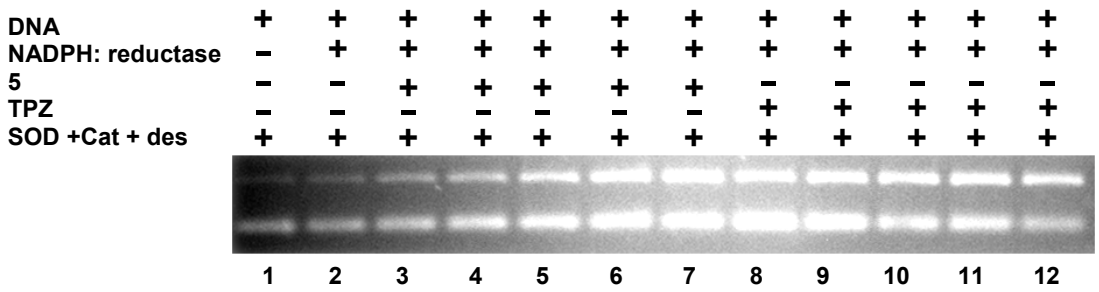

B

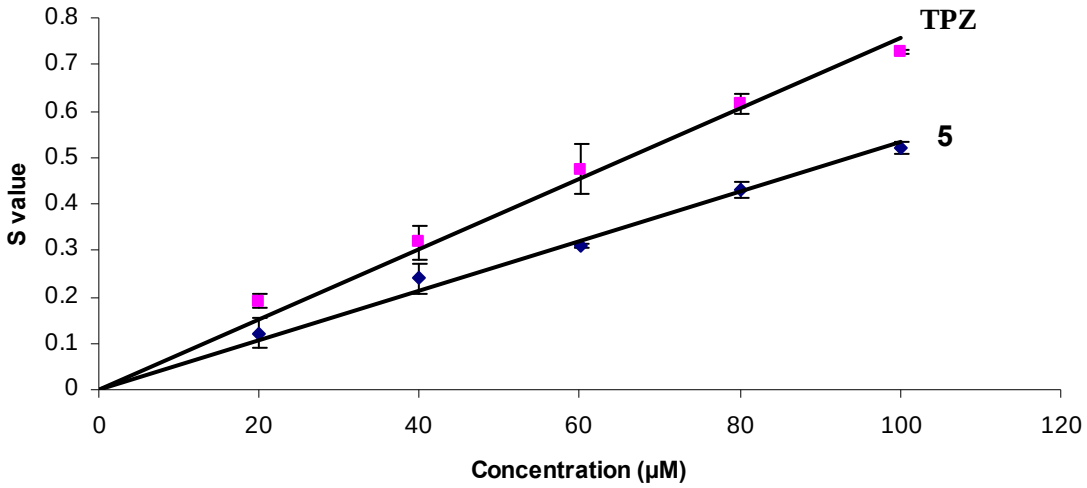

Figure 3: Efficiency of DNA cleavage of 1-hydroxyphenazine 5,10-di-*N*-oxide, **5** and **TPZ** under anaerobic condition in presence of NADPH:cytochromo P450 reductase. Supercoiled plasmid DNA (1μg) was incubated with **5** (20-100 μM) or **TPZ** (20-100 μM) in presence of NADPH (500 μM), cytochrome P450 reductase (50 mU/mL), SOD (100 μg/mL), catalase (100 μg/mL), desferal (1 mM) and sodium phosphate buffer (50 mM, pH 7) under anaerobic condition at room temperature for 12 hours. After that the reaction mixture was analyzed by agarose gel electrophoresis. **A.** Agarose gel: In all lanes SOD (100 μg/mL), catalase (100 μg/mL) and desferal (1 mM) were used. lane 1, DNA alone; lane 2, NADPH (500 μM) + reductase (0.05 U/mL); (lane 3, 4, 5, 6,7), **5** (20-100 μM)+ NADPH (500 μM) + reductase (0.05 U/mL); lane 3 (20 μM **5**, S = 0.12 ± 0.03); lane 4 (40 μM **5**, S = 0.24 ± 0.03); lane 5 (60 μM **5,** S = 0.31 ± 0.003); lane 6 (80 μM **5,** S = 0.43 ± 0.02); lane 7 (100 μM **5,** S = 0.52 ± 0.01); (lane 8,9,10,11,12), **TPZ** (20-100 μM) + NADPH (500 μM) + reductase (0.05 U/mL); lane 8 (20 μM **TPZ**, S = 0.19 ± 0.01); lane 9 (40 μM **TPZ**, S = 0.32 ± 0.04); lane 10 (60 μM **TPZ,** S = 0.47 ± 0.05); lane 11 (80 μM **TPZ,** S = 0.61 ± 0.02); lane 12 (100 μM **TPZ,** S = 0.73 ± 0.004). **B.** Plot of S value vs. various concentrations of both **5** and **TPZ**. The values, S, represent the mean number of strand breaks per plasmid molecule and were calculated using the equation S = -ln f_1 where f_1 is the fraction of plasmid present as in the supercoiled form I. S values of different concentrations of **5** and **TPZ** were obtained by subtracting background cleavage.

We found that 1-hydroxyphenazine 5,10-di-*N*-oxide, **5** causes redox-activated DNA damage under anaerobic condition in presence of one electron reducing system NADPH:cytochrome P450 reductase and DNA cleavage efficiency of **5** is comparable with **TPZ**. Moreover, we observed that in aerobic condition similar to TPZ, **5** undergoes redox cycling (**Scheme 5**) in presence of NADPH:cytochrome P450 reductase and produces ROS like superoxide radical, H_2O_2, hydroxyl radical as discussed in our **chapter 2**. As this result clearly demonstrates that 1-hydroxyphenazine 5,10-di-*N*-oxide **5** exhibits comparable DNA cleavage efficiency with TPZ under anaerobic condition and in aerobic condition similar to TPZ, **5** does redox cycling by reaction with molecular oxygen, so, we suggest that 1-hydroxyphenazine 5,10-di-*N*-oxide **5** could behave as a potent hypoxia selective antitumor agent like TPZ.

5.4. Mechanism of DNA cleavage by 1-hydroxyphenazine 5,10-di-*N*-oxide:

Our previous experiments provide direct evidence that 1-hydroxyphenazine 5,10-di-*N*-oxide, **5** induces DNA cleavage under hypoxic condition in presence of one electron reducing system. So, to understand the mechanism of DNA cleavage by **5** we performed a plasmid based DNA cleavage assay under anaerobic condition in the similar way as discussed above only with the exception that DNA cleavage assay was performed in the presence of various radical scavengers.

A.

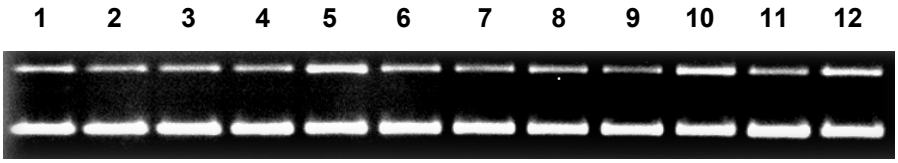

B.

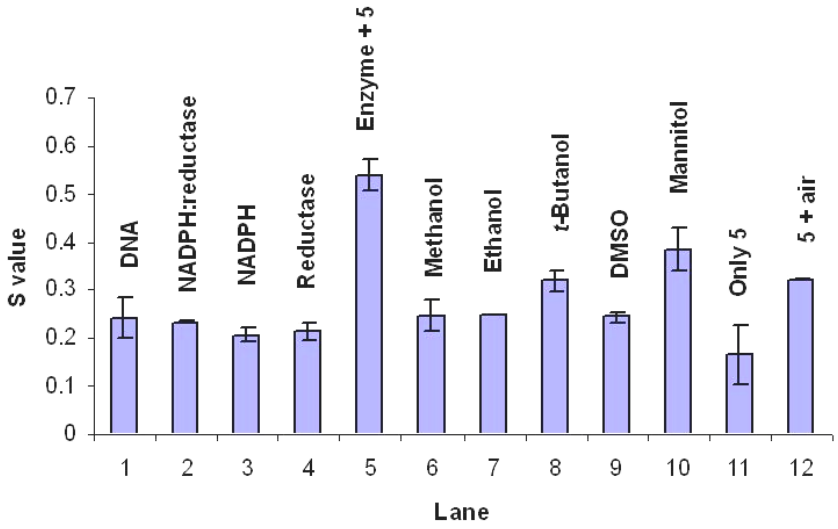

Figure 4: Mechanism of DNA damage by 1-hydroxyphenazine 5,10-di-*N*-oxide, **5.** In a typical assay plasmid DNA (1 μg) was incubated with **5** (80 μM) alone or in presence of NADPH (500 μM), cytochrome P450 reductase (50 mU/mL), SOD (100 μg/mL), catalase (100 μg/mL), desferal (1 mM), sodium phosphate buffer (50 mM, pH 7) and in some cases **5** was incubated with radical scavengers like methanol (1 M), ethanol (1 M), mannitol (1 M), DMSO (1 M) and *tert*-butanol (1 M) at room temperature under anaerobic condition for 12 hours, followed by agarose gel electrophoresis. **A.** Agarose gel: In all lanes SOD (100 μg/mL), catalase (100 μg/mL) and desferal (1 mM) were used. lane 1, DNA alone (S = 0.24 ± 0.04); lane 2, NADPH (500 μM) + reductase (0.05 U/mL) (S = 0.23 ± 0.002); lane 3, **5** (80 μM)+ NADPH (500 μM) (S = 0.21 ± 0.02); lane 4, **5** (80 μM) + reductase (0.05 U/mL) (S = 0.21 ± 0.02); lane 5, **5** (80 μM) + NADPH (500 μM) + reductase (0.05 U/mL) (S = 0.54 ± 0.03); lane 6, **5** (80 μM) + NADPH (500 μM) + reductase (0.05 U/mL) + methanol (1 M) (S = 0.25 ± 0.03); lane 7, **5** (80 μM) + NADPH (500 μM) + reductase (0.05 U/mL) + ethanol (1 M) (S = 0.25 ± 0.0); lane 8, **5** (80 μM) + NADPH (500 μM) + reductase (0.05 U/mL) + *tert*-butanol (1 M) (S = 0.32 ± 0.02); lane 9, **5** (80 μM) + NADPH (500 μM) + reductase (0.05 U/mL) + DMSO (1 M) (S = 0.24 ± 0.01); lane 10, **5** (80 μM) + NADPH (500 μM) + reductase (0.05 U/mL) + mannitol (1 M) (S = 0.39 ± 0.04); lane 11, **5** (80 μM) alone (S = 0.17 ± 0.06); lane 12, **5** (80 μM) + NADPH (500 μM) + reductase (0.05 U/mL) + air (S = 0.32 ± 0.0). **B.** Bar graph of S-values of all reaction lanes. The values, S, represent the mean number of strand breaks per plasmid molecule and were calculated using the equation S = -ln f_1 where f_1 is the fraction of plasmid present as in the supercoiled form I.

We found that 1-hydroxyphenazine 5,10-di-*N*-oxide, **5** neither induced DNA cleavage alone (lane 11) nor in presence of either only NADPH (lane 3) or cytochrome P450 reductase (lane 4). It only lead to DNA damage in presence of one-electron reducing enzyme like NADPH:cytochrome P450 reductase (lane 5) which clearly indicates that 1-hydroxyphenazine 5,10-di-*N*-oxide, **5** requires one-electron reductive activation by the enzyme to induce DNA damage under hypoxic condition. Moreover, the data clearly showed that the yield of DNA damage was significantly reduced when 1-hydroxyphenazine 5,10-di-*N*-oxide, **5** was incubated with radical scavengers (lane 6-10). Therefore, overall this study indicates that DNA cleavage by 1-hydroxyphenazine 5,10-di-*N*-oxide, **5** is redox-activated and radical mediated under hypoxic condition.

We also studied whether 1-hydroxyphenazine 10-*N*-oxide **6**, the reduced metabolite of **5** could induce DNA damage under anaerobic condition. It was found that **6** were unable to cause any detectable amount of DNA damage in presence of NADPH:cytochrome P450 reductase under hypoxic condition.

Therefore, we see that 1-hydroxyphenazine 5,10-di-*N*-oxide, **5** caused DNA damage under anaerobic condition and one-electron reductive activation was required to initiate DNA damage. The one-electron reduced metabolite **6** didn't cause any significant amount of DNA damage. So, this study clearly supports the notion that one-electron reduced species or activated radical intermediate **5a** is the key intermediate in the DNA-damaging process. Moreover as DNA damage by **5** was radical mediated it can be suggested that like other heterocyclic *N*-oxides **5** causes DNA strand cleavage through hydroxyl radical mediated pathway (**Scheme 4**).

5.5. Metabolism study of 1-hydroxyphenazine 5,10-di-*N*-oxide in presence of NADPH:cytochrome P450 reductase under hypoxic condition:

In order to identify the metabolites resulting from the anaerobic metabolism of 1-hydroxyphenazine 5,10-di-*N*-oxide, **5** in presence of NADPH:cytochrome P450 reductase we carried out an *in vitro* metabolism study of 1-hydroxyphenazine 5,10-di-*N*-oxide, **5** under anaerobic condition. In this work, **5** were incubated with NADPH:cytochrome P450 reductase in presence of sodium phosphate buffer at pH 7 under anaerobic conditions for 4 h. We also did two controls, one containing only **5** (200 μM) in sodium phosphate buffer and another containing sodium phosphate buffer, NADPH (1mM) and cytochrome P450 reductase (50 mU/mL). The controls were also incubated for 4 h in the argon filled glove bag. After that the reaction mixture was analyzed by both normal phase HPLC and LC/MS. LC/MS analysis was performed by using TSQ7000 triple-quadruple mass spectrometer where we used same normal phase HPLC method which was used in case of HPLC analysis to detect the metabolites and used APCI-MS (atmospheric pressure chemical ionization) operating in positive ion mode to determine the mass (m/z = M+H) of metabolites.

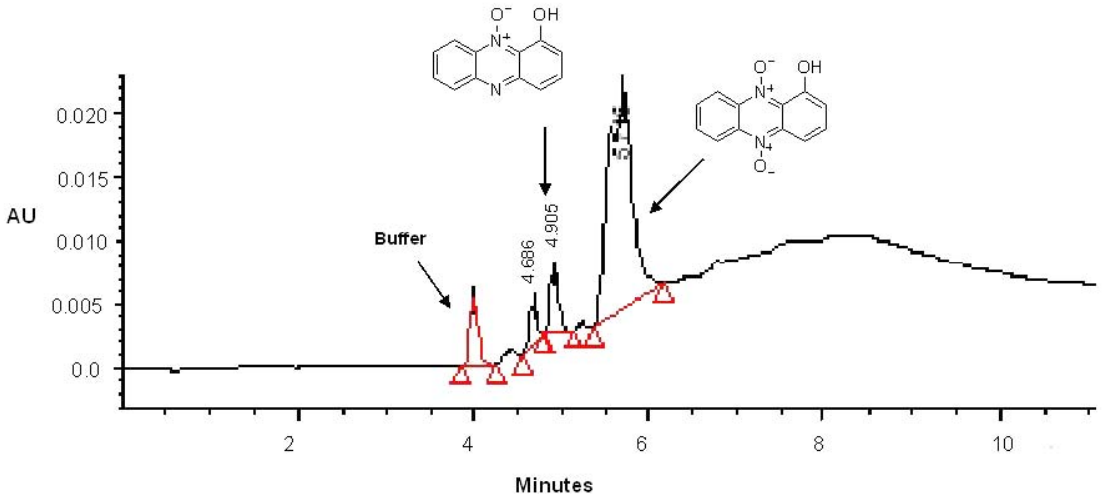

Figure 5: *In vitro* metabolism of **5** by NADPH:cytochrome P450 reductase at pH 7 buffer under anaerobic condition results in **6**. In a typical assay **5** (200 μM) in sodium phosphate buffer (50 mM, pH 7) was incubated with NADPH (1 mM) and cytochrome P450 reductase (50 mU/mL) at room temperature in argon filled glove bag for 4 hours. After that the reaction mixture was analyzed by normal phase HPLC.

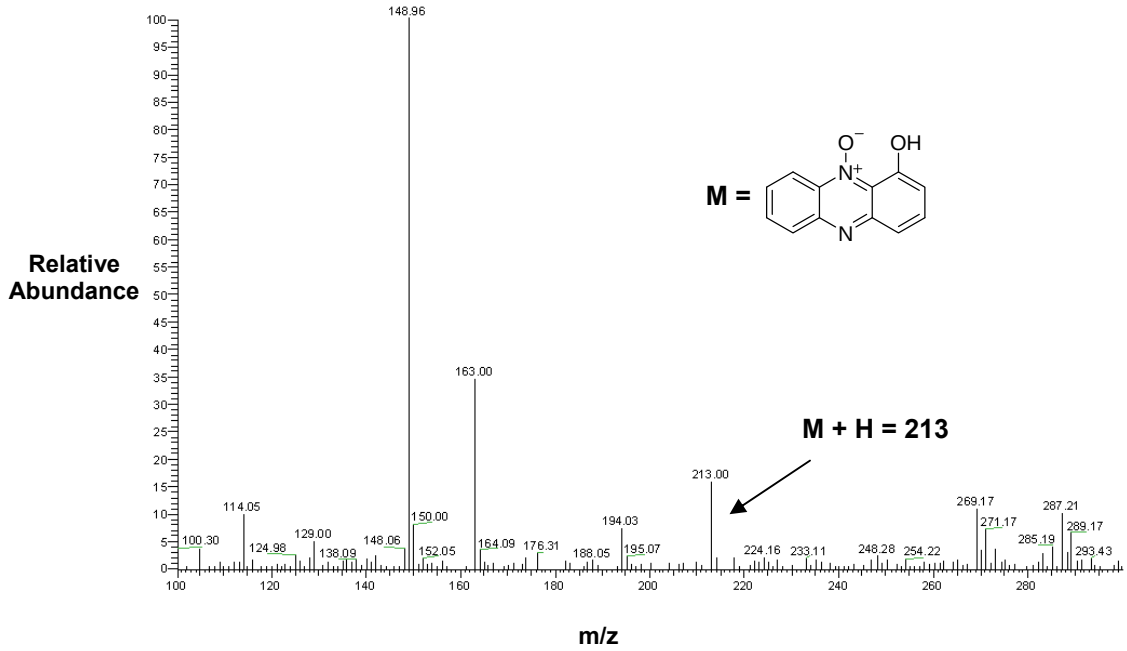

Figure 6: *In vitro* anaerobic metabolism of **5** by NADPH:cytochrome P450 reductase at pH 7 buffer results in **6.** The mass spectrum shows M+H ion of **6** at m/z 213 obtained using LC-APCI/MS operating in the positive ion mode.

HPLC analysis detected **6** as the one-electron-reduced metabolite with retention time 4.905 resulting from the anaerobic metabolism of 1-hydroxyphenazine 5,10-di-*N*-oxide by NADPH:cytochrome P450 reductase. The peak of retention time 4.906 was also identified by LCMS analysis which gave molecular ion peak of m/z 213 ($M+H^+$; APCI positive ion mode) that corresponds to **6**. Another peak with retention time 4.686 minutes was obtained but its structure was not determined yet. It could be 1-hydroxyphenazine 5-*N*-oxide **7**. Control experiments containing only **5** didn't detect any other peak except **5** and another control containing only NADPH:cytochrome P450 reductase didn't reveal any peaks. We also performed *in vitro* metabolism study of 1-hydroxyphenazine 5,10-di-*N*-oxide in presence of NADPH:cytochrome P450 reductase system under aerobic condition by using both HPLC and LC/MS as we discussed in our **chapter 2**. Both HPLC and LC/MS analysis revealed that 1-hydroxyphenazine 5,10-di-*N*-oxide **5** didn't degrade extensively and didn't produce any deoxygenated products **6**, **7** and 1-hydroxyphenazine **1** under aerobic condition. Thus, our *in vitro* metabolism study of 1-hydroxyphenazine 5,10-di-*N*-oxide supports redox cycling mechanism of **5** in presence of one electron reducing enzyme under aerobic condition (**Scheme 4**) as discussed in **chapter 2**.

Overall, our *in vitro* metabolism study supports our hypothesis that 1-hydroxyphenazine 5,10-di-*N*-oxide, **5** undergoes one electron reductive activation in presence of one electron reducing enzyme to produce activated radical intermediate **5a** as shown in **Scheme 4** which under hypoxic condition produces reduced metabolized **6** by releasing DNA damaging agent hydroxyl radical but under aerobic condition activated radical intermediate **5a** is back oxidized into parent compound with production of superoxide radical (**Scheme 4 and 5**) via redox cycling mechanism.

5.6. Conclusion: We have provided first evidence in this chapter that 1-hydroxyphenazine 5,10-di-*N*-oxide **5** causes DNA single strand breaks under hypoxic condition in presence of the one-electron reducing system NADPH:cytochrome P450 reductase. DNA damage by 1-hydroxyphenazine 5,10-di-*N*-oxide is redox activated as it requires one electron reductive activation to induce hypoxia selective DNA damage. Enzymatic metabolism of 1-hydroxyphenazine 5,10-di-*N*-oxide yields the one-electron-reduced metabolite **6** which doesn't induce detectable amounts of DNA cleavage. This result supports our hypothesis that an activated radical intermediate is the key intermediate on the pathway to DNA damage. Moreover DNA cleavage is inhibited in the presence of radical scavengers. Together the results indicate that DNA damage by 1-hydroxyphenazine 5,10-di-*N*-oxide involves a small diffusible radical which abstracts hydrogen atoms from the DNA backbone. On the basis of our previous work with TPZ[23] (discussed in **chapter 3**) we suggest a mechanism involving release of hydroxyl radical through homolytic cleavage of N-OH bond (**Scheme 4**) from the activated radical intermediate **5a**. Thus, based on this study it can be demonstrated that 1-hydroxyphenazine 5,10-di-*N*-oxide causes redox-activated hypoxia selective DNA damage and the mechanism of DNA damage is similar to TPZ. As the DNA damage efficiency of 1-hydroxyphenazine 5,10-di-*N*-oxide is comparable with TPZ, 1-hydroxyphenazine 5,10-di-*N*-oxide could be categorized as a potent redox-activated hypoxia selective antitumor agent similar to TPZ. Besides this, resent literature has revealed that attaching an intercalator with TPZ increases its potency as intercalator makes TPZ targeting better towards DNA through binding with DNA.[24] It is known that phenazines bind to both double strand DNA and RNA though intercalation with a binding

constant 10^4-10^6 range.[25] So, this study suggests that 1-hydroxyphenazine 5,10-di-*N*-oxide in addition to exhibiting hypoxia selective DNA damaging properties like TPZ and quinoxaline di-*N*-oxides, could also be used as an intercalator which could be attached with TPZ to increase its potency. Therefore, based on this study it can be demonstrated that 1-hydroxyphenazine 5,10-di-*N*-oxide could be an attractive antitumor agent for cancer chemotherapy in future.

Materials and Methods:

Materials: Materials with highest purity were bought from the following suppliers. Benzofuroxan, sodium phosphate, triethylamine, methanol, ethanol, *tert*-butanol, DMSO, mannitol and TLC plates from Aldrich Chemical Co. (Milwaukee, WI); 1,2 cyclohexanedione, 98% from Acros Organics (Pittsburgh, PA); NADPH, acetonitrile, desferal, cytochrome P450 reductase, catalase and SOD from Sigma Chemical Co. (St. Louis, MO); agarose from Seakem; HPLC grade solvents (methanol, ethanol, ethyl acetate, heptane), ethyl acetate, hexane, NaOH, HCl and acetic acid from Fisher Scientific (Pittsburg, PA); ethidium bromide from Roche Molecular Biochemicals (Indianapolis, IN); Silica gel (0.04-0.063 mm pore size) for column chromatography from Merck; The plasmid DNA pGL2BASIC was prepared using the standards protocols. [Sambrook, J.; Fritsch, E. F.; Maniatis, T. (1989) *Molecular Cloning: A Lab Manual,* Cold Spring Harbor Press, Cold Spring Harbor. NY]. 1-hydroxyphenazine 5,10-di-*N*-oxide was synthesized by following the literature methods and the synthesis was discussed in 2nd chapter.[26] High resolution mass spectroscopy was performed at the University of Illinois Urbana-Champaign Mass Spectroscopy facility and low resolution mass spectroscopy and LCMS study were performed at University of Missouri-Columbia Mass Spectroscopy facility. NMR spectra were taken using Bruker DRX 300 MHz instruments at the University of Missouri-Columbia.

In all assays **5** was used as 10-20% acetonitril in water by volume.

Cleavage of supercoiled plasmid DNA by 1-hydroxyphenazine 5,10-di-*N*-oxide: In a typical plasmid based assay, supercoiled plasmid DNA (1μg) was incubated with **5** (20-100 μM) or **TPZ** (20-100 μM) in presence SOD (100 μg/mL), catalase (100 μg/mL), desferal (1mM) and sodium phosphate buffer (50 mM, pH 7) in a total volume 30 μL. In these assays NADPH (500 μM), cytochrome P450 reductase (50 mU/mL) were used as one electron reducing system. All components used in DNA damaging assays except DNA, NADPH and enzymes were taken in the pyrex tubes and were degassed by three cycles of freeze-pump-thaw to remove dissolved oxygen. After degassing the solutions, the pyrex tubes were torched sealed under vacuum. Next the sealed tubes containing degassed solutions were scored, broken in the argon filled glove bag and the degassed solutions were used to prepare individual reactions. NADPH and enzymes were diluted by degassed water inside the glove bag to prepare stock solutions that were used in the assays. The reactions were initiated by adding NADPH and cytochrome P450 reductase and after that the reaction mixtures were covered with aluminum foil to prevent any photo cleavage of DNA. The reaction mixtures were incubated in the argon filled glove bag for 12 hours at room temperature (24^{o}C). After incubation, the reactions were stopped by addition of 6.6 μL of 50% glycerol loading buffer, and the resulting reaction mixture was loaded onto a 0.9% agarose gel. The gel was electrophoresed for approximately 2 h at 90 V in 1 x TAE buffer and then stained in a solution of ethidium bromide (0.3 μg/mL) for 3 hours. DNA in gel was visualized by UV-transillumination and the amount of DNA in each band was quantified using an Alpha Innotech IS-1000 digital imaging system. DNA-cleavage assay containing radical scavengers were performed in a similar way as described above with the exception that radical scavengers

methanol, ethanol, t-butanol, DMSO or mannitol (1 M) were added to the reaction mixture before addition of cytochrome P450 reductase.

Enzymatic metabolism of 1-hydroxyphenazine 5,10-di-*N*-oxide under anaerobic condition: In a typical assay, a solution containing **5** (200 μM) in sodium phosphate buffer (50 mM, pH 7) in a total volume 600 μL and other containing only sodium phosphate buffer (50 mM, pH 7) in a total volume 300 μL were degassed by using three cycles of freeze-pump-thaw and then the tubes were torched sealed under vacuum. Next the sealed tubes containing degassed solutions were scored, broken in the argon filled glove bag. After that NADPH (1mM), cytochrome P450 reductase (50 mU/mL) were added to the reaction mixtures one contained **5** in buffer in a total volume 300 μL and another contained only buffer in a total volume 300 μL. Another control contained only degassed solution of **5** in buffer in a total volume 300 μL. The reaction mixture and the two controls were incubated in the argon filled glove bag for 4 hours at room temperature (24^{o}C). Following incubation, the enzymes and proteins were removed by centrifugation through Amicon Microcon (YM3) filters. The filtrate was extracted in 100% ethyl acetate and then analyzed by normal phage HPLC employing a Microsorb-MV-100 NH_2 normal phase column (5 μm particle size, 25 cm length, 100 A^{o} pore size and 4.6 mm i.d.) eluted with gradient solvent system starting with 40% A (0.5 % acetic acid in ethyl acetate) and 60 % B (0.5 % acetic acid in heptane) followed by linear increase to 55 % A from 0 minute to 2 minute, 70% A from 2 to 4 minute. Then 70% A was held for next 13 minutes and in next 2 minutes again A is reached to 40% and gets equilibrated for next 8 minutes. The flow rate was 0.7 mL/min and the products were

monitored by UV-absorbance at 284 nm. The metabolite was identified by co-injection with authentic standard and also by performing LCMS. LC/MS analysis was performed by using TSQ7000 triple-quadruple mass spectrometer where we used same HPLC method as described above to detect the metabolites and used APCI-MS (atmospheric pressure chemical ionization) operating in positive ion mode to determine the mass (m/z = M+H) of metabolite.

References:

1. Brown, J. M. *Cancer Res.* **1999**, *59*, 5863-5870.
2. Brown, J. M.; Wang, L. *Anti-Cancer Drug Design* **1998**, *13*, 529-539.
3. Daniels, J. S.; Gates, K. S. *J. Am. Chem. Soc.* **1996**, *118*, 3380-3385.
4. Denny, W. A. *The Lancet* **2000**, *1*, 25-29.
5. Brown, J. M. *Br. J. Cancer* **1993**, *67*, 1163-1170.
6. Brown, J. M.; Siim, B. G. *Seminars Rad. Oncol*. **1996**, *6*, 22-36.
7. Von Powel, J.; Von Roemeling , R.; Gatzemeier, U.; Boyer, M.; Elisson, L. O.; Clark, P.; Talbot, D.; Rey, A.; Butler, T. W.; Hirst, V.; Olver, I.; Bergman, B.; Ayoub, J.; Richardson, G.; Dunlop, D.; Arcenas, A.; Vescio, R.; Viallet, J.; Treat, J. *J. Clin. Oncol*. **2000**, *18*, 1351-1359.
8. Monge, A.; Martinez-Crespo, F. J.; de Cerain, A. L.; Palop, J. A.; Narro, S.; Senador, V.; Marin, A.; Sainz, Y.; Gonzalez, M.; Hamilton, E.; Barker, M. S. *J. Med. Chem.* **1995**, *38*, 4488-4494.
9. Lausen, J. B.; Nielsen, J. *Chem. Rev.* **2004**, *104*, 1663-1685.
10. Peterson, E. A.; Gillespie, D. C.; Cook, F. D. *Can. J. Microbiol*. **1966**, *12*, 221-230.
11. Weigele, M.; Leimgruber, W. *Tetrahedron Lett*. **1967**, *8*, 715-718.
12. Mcllwain, H. J. *J. Chem. Soc*. **1943**, 322-325.
13. Gerber, N. N.; Lechevalier, M. P. *Biochemistry* **1965**, *4*, 176-180.
14. *DNA damage by Heterocyclic N-oxides: A novel class of antitumor agents,* PhD thesis submitted by Goutam Chowdhury in **2005.**

15. Baker, M. S.; Zeman, E. M.; Hirst, V. K.; Brown, J. M. *Cancer Res*. **1998**, *48*, 5947-5952.

16. Fuchs, T.; Chowdhury, G.; Barnes, C. L.; Gates, K. S. *J. Org. Chem*. **2001**, *66*, 107-114.

17. Nagai, K.; Hecht, M. S. *J. Biol. Chem.* **1991**, *266,* 23994-24002.

18. Nagai, K.; Carter, J. B.; Xu, J.; Hecht, M. S. *J. Am. Chem. Soc.* **1991**, *113,* 5099-5100.

19. Chowdhury, C.; Junnotula, V.; Daniels, J. S.; Greenberg, M. M.; Gates, K. S. *J. Am. Chem. Soc.* **2007**, *129*, 12870-12877.

20. Chowdhury, G.; Kotandeniya, D.; Daniels, J. S.; Barnes, C. L.; Zang, H.; Gates, K. S. *Chem. Res. Toxicol.* **2004**, *17*, 1399-1405.

21. Daniels, J. S.; Chatterji, T.; MacGillivray, L. R.; Gates, K. S. *J. Org. Chem.* **1998**, *63*, 10027-10030.

22. Fuchs, T.; Gates, K. S.; Hwang, J. T.; Greenberg, M. M. *Chem. Res. Toxicol.* **1999**, *12*, 1190-1194.

23. Daniels, J. S.; Gates, K. S. *J. Am. Chem. Soc.* **1996**, *118*, 3380-3385.

24. Delahoussaye, Y. M.; Hay, M. P.; Pruijn, F. B.; Denny, W. A.; Brown, J. M. *Biochem. Pharmacol*. **2003**, *65*, 1807-1815.

25. Hollstein, U.; Gemert, R. J. V. *Biochemistry* **1971**, *10*, 497-504.

26. Issidorides, C. H.; Atfah, M. A.; Sabounji, J. J.; Sidani, A. R.; Haddadin, M. J. *Tetrahedron*. **1978**, *34,* 217-221.

27. Cerecetto, H.; Gonzalez, M.; Lavaggi, M. L.; Azqueta, A.; Lopez de Cerain, A.; Monge, A. *J. Med. Chem.* **2005**, *48*, 21-23.

Vita

Sarmistha Sinha was born in 1975 in Calcutta, India. Her father's name is Mr. Jnan Bikash Sinha and mother's name is Mrs. Mira Sinha. Her sister's name is Miss Sharmila Sinha. She went to Banipith Girls' H. S. School situated in Ashokenagar, India to complete her 10^{th} and 12^{th} grade in 1992 and 1994 respectively. After that she went to Gurudas College (Gurudas College is under Calcutta University) in 1995 to complete her under graduation study in chemistry. She completed her B. Sc. Degree in chemistry from Calcutta University, India in 1999. She completed her M. Sc. in chemistry from Indian Institute of Technology, Kharagpur, India in 2002. After that in 2003 she came to University of Missouri-Columbia (UMC), USA to complete her PhD and she completed her PhD in 2008. She gets married with Dr. Kaushik Deb.